NASA Technical Memorandum 83235

RAXJET: A Computer Program for Predicting Transonic, Axisymmetric Flow Over Nozzle Afterbodies With Supersonic Jet Exhausts

Richard G. Wilmoth
Langley Research Center
Hampton, Virginia

National Aeronautics
and Space Administration

Scientific and Technical Information Branch

1982

INTRODUCTION

The nozzle afterbody is one of the main drag-producing components of an aircraft propulsion system. Thus, considerable effort has been devoted to developing techniques for predicting the afterbody flow field and drag. Using methods ranging from empirical techniques based on experimental data (ref. 1) to solutions of the Navier-Stokes equations with turbulence closure (refs. 2 and 3), investigators have had some success for isolated axisymmetric nozzles. Patched viscous-inviscid interaction methods (refs. 4 to 6, for example) have had considerable success. The patched methods require considerably less computational time than the Navier-Stokes solutions and generally yield results of comparable (and in some cases greater) accuracy.

The present paper describes a viscous-inviscid method that has evolved over a number of years through the efforts of several researchers. Reubush and Putnam (ref. 4) combined a conventional integral boundary-layer technique (ref. 7) with a linearized potential flow computation to account for the boundary-layer displacement effect. For separated flows, they employed the discriminating streamline concept of Presz (ref. 8) to separate the reverse flow region from the outer flow. Wilmoth (ref. 5) extended the method to transonic speeds by replacing the linearized inviscid method with the relaxation procedure of South and Jameson (ref. 9) for solving the exact nonlinear potential flow equation. Abeyounis (ref. 10) conducted oil-flow studies to determine the separation location on a series of circular-arc boattails and used the results to evaluate several prediction techniques including the Presz model. Presz et al. (ref. 11) developed an improved analytical model of the separated region which accounts for axial pressure gradients, surface skin friction, and jet entrainment. Putnam (ref. 6) incorporated this improved model together with a simple one-dimensional model of the inviscid jet plume blockage into the linearized method. Wilmoth and Dash (ref. 12) developed a jet entrainment model that uses the overlaid mixing analysis of Dash and Pergament (ref. 13) to calculate a jet plume displacement. This entrainment model was incorporated into the transonic method by Wilmoth (ref. 14) together with the shock-capturing—shock-fitting inviscid plume model of Dash and Thorpe (ref. 15). The work described above has provided the basis for the present viscous-inviscid model.

The present model iteratively combines the South-Jameson relaxation procedure, the Reshotko-Tucker boundary-layer solution, the Presz separation model, the Dash-Pergament mixing model, and the Dash-Thorpe inviscid plume model. These computational models are combined into a single computer program called RAXJET. RAXJET predicts transonic axisymmetric flow over nozzle afterbodies with supersonic jet exhausts and accounts for boundary-layer displacement, separation, jet entrainment, and inviscid jet plume blockage. This paper describes the various components of the computational model, illustrates its capabilities by comparison with experimental data, and provides a user's guide to the computer program. The computer program may be obtained as program LAR-12957 from

COSMIC
Suite 112, Barrow Hall
University of Georgia
Athens, GA 30602

SYMBOLS

The symbols used in the computer printouts are given in the second column.

A		cross-sectional area of body of revolution
A_{ref}	SREF	reference area for drag coefficients
	BL	boundary layer
	CDF,AFT	afterbody friction drag coefficient, $\frac{1}{A_{ref}} \int_{S(x_A)}^{S(x_M)} C_f \, dS$
	CDF,BOD	body-of-revolution friction drag coefficient, $\frac{1}{A_{ref}} \int_{0}^{S(x_M)} C_f \, dS$
$C_{D,B}$	CDP,AFT	afterbody pressure drag coefficient, $\frac{1}{A_{ref}} \int_{A(x_A)}^{A(x_M)} C_p \, dA$
	CDP,BOD	body-of-revolution pressure drag coefficient, $\frac{1}{A_{ref}} \int_{0}^{A(x_M)} C_p \, dA$
	CDT,AFT	afterbody total drag coefficient, CDP,AFT + CDF,AFT
	CDT,BOD	body-of-revolution total drag coefficient, CDP,BOD + CDF,BOD
C_f	CF	skin-friction coefficient, τ_w/q_∞
C_p	CP	pressure coefficient, $\frac{p - p_\infty}{q_\infty}$
D_b		nozzle base diameter
D		nozzle maximum diameter
	GAMMA	ratio of specific heats of gas mixture
	H	boundary-layer shape factor, δ^*/θ
	I	longitudinal grid index
kε2		two-equation turbulence model
l		length of afterbody

L	L or REFL	reference length
M	M	Mach number
	ML	local surface Mach number
M_∞	MO	free-stream Mach number
NPR		nozzle pressure ratio, ratio of jet total pressure to free-stream static pressure
p	P	static pressure
p_∞	PINF	free-stream static pressure
$p_{t,2}$	PT	total pressure measured by pitot tube; total pressure downstream of normal shock if M > 1
$p_{t,\infty}$	PTINF	free-stream total pressure
q_∞		free-stream dynamic pressure
r	R	radial coordinate of cylindrical coordinate system with origin at nose of body of revolution
r_j		radius of jet at nozzle exit
	RDS	body radius corrected for discriminating streamline and inviscid plume boundary
	REFF	effective body radius used in inviscid external flow calculation
	RPAVG	average residual in relaxation solution of potential equation
	RPMAX	maximum residual in relaxation solution of potential equation
	RVI	radius at outer edge of boundary layer or mixing layer
S		surface area
T	T	temperature
	TINF	free-stream temperature
u	U	axial velocity
	UINF	free-stream velocity
v	V	radial velocity
x	X	axial coordinate of cylindrical coordinate system with origin at nose of body of revolution
x_A		axial location of start of afterbody

x_M	XM	axial length of body of revolution
x_{sep}		axial location of separation
X,Y		computational coordinates of body-fitted grid used in inviscid external flow solution
α	ALF	radial grid stretching parameter used in external flow solution
δ		boundary-layer or mixing-layer thickness
δ^*	DEL*	boundary-layer or mixing-layer displacement thickness
Δ		incremental value
θ	THETA	boundary-layer momentum thickness
ξ,η		body-fitted grid coordinates
τ_w		boundary-layer shear stress at body surface

DESCRIPTION OF METHOD

The viscous-inviscid interaction model is constructed by dividing the afterbody flow field shown in figure 1 into six separate computational regions (see fig. 2). The viscous interaction is taken into account by displacing the body-plume shape with an appropriate displacement thickness to yield an effective body geometry for the inviscid external flow calculation. The inviscid external flow solution and inviscid jet exhaust solution provide the necessary flow conditions to calculate conditions in the viscous regions by parabolized marching procedures. The viscous and inviscid flow fields are then iteratively solved.

Inviscid External Flow Solution

The inviscid external flow solution is based on the relaxation procedure of South and Jameson (ref. 9) for solving the exact nonlinear potential flow equation in nonconservative form. This technique is valid for subsonic, transonic, and supersonic irrotational flow over bodies of revolution. RAXJET uses the computer program RAXBOD developed by Keller and South (ref. 16) to implement this technique. RAXBOD uses a body-normal coordinate system from the nose up to the first horizontal tangent and a body-fitted sheared coordinate system aft of this point. The computational grid is stretched to infinity in both the normal and downstream axial directions to facilitate handling of the far-field boundary conditions. Since RAXBOD requires that a complete body of revolution be specified, special procedures have been incorporated into RAXJET to determine grid stretching parameters that provide optimal grid point distribution over the afterbody.

Inviscid Jet Exhaust Solution

RAXJET uses the computer program SCIPAC (ref. 17) to solve the flow field in the inviscid jet region. SCIPAC solves the flow field by explicit spatial marching of the conservative finite-difference form of the inviscid flow equations for a uniform

composition gas mixture. The nozzle exit flow is assumed to be supersonic, and the calculation is initiated at the exit with exhaust properties prescribed. A uniform distribution of grid points is used between the axis and the inviscid plume boundary. As the calculation proceeds downstream, oblique shocks are numerically captured while the triple point that occurs because of the formation of a Mach disk in an underexpanded jet is treated by a shock-fitting procedure. The Mach disk location is determined by the iterative procedure of Abbett (ref. 18) which treats the subsonic region downstream of the Mach disk as a one-dimensional isentropic streamtube. Generally, for mildly underexpanded jets (low nozzle pressure ratios), the Mach disk diameter is small, and the subsonic region is approximated by a constant area streamtube.

For low Mach number (near unity) jets, the supersonic marching procedure becomes inefficient since the marching step size of the explicit scheme approaches zero as the Mach number approaches one. Also, under such conditions, the shock-fitting procedure may yield poor results since shocks are weak and difficult to define from the numerical results. Thus, RAXJET includes a low Mach number solution procedure in which the flow properties are calculated based on an isentropic expansion to the local inviscid external pressure (refs. 15 and 17). This isentropic procedure may also be applied to the flow downstream of a Mach disk. The computer program provides tests based on exit pressure and Mach number to determine whether the low-Mach-number procedure should be applied.

Boundary-Layer Solution

The properties in the attached boundary-layer region are solved by a modified version of the Pashotko-Tucker integral method for turbulent flows (ref. 7). The computer algorithm is described in references 11 and 19. The integral solution is obtained by conventional boundary-layer marching procedures to yield the displacement-thickness distribution $\delta^*(x)$ over the body.

Knowledge of the internal boundary-layer thickness is needed only to initialize the jet wake and mixing analysis. Since the nozzle internal boundary layer is generally quite thin compared to the afterbody external boundary layer, an exit boundary-layer thickness is estimated from flat-plate theory.

Separated Flow Solution

The analysis of the separated region consists of predicting the separation location and calculating the discriminating streamline shape. The discriminating streamline analysis is further divided into two regions: the separation region from the separation point to the end of the body and the jet wake region from the end of the body to the reattachment point (see fig. 2).

Separation location prediction.- The location of separation on the afterbody is calculated by the control volume technique developed by Presz (ref. 8). The technique determines the separation point based on a calculated pressure rise to separation from the minimum pressure on the afterbody. Abeyounis (ref. 10) compared the results of the Presz model and several other prediction techniques with the results of oil-flow studies on a series of circular-arc boattail nozzles. While none of the methods examined was able to successfully reproduce the experimental results over all test conditions, the Presz method seemed to yield the most accurate predictions. The largest error in most cases occurred at transonic speeds where shock-induced separa-

tion was encountered. In view of the difficulty in making accurate separation location predictions, RAXJET allows the separation location to be specified by the user as an option.

Discriminating streamline for separation region.- The discriminating streamline concept is used to separate the reverse flow region from the outer boundary-layer flow. The streamline shape is calculated by the discrete control volume analysis developed by Presz et al. (ref. 11). The method solves integral forms of the continuity and streamwise momentum equations to account for streamwise pressure gradients and surface skin friction. An error-function-type velocity profile modified to allow reverse velocities is assumed. The solution is marched downstream from the separation point to the end of the afterbody.

Discriminating streamline for jet wake region.- Two methods are provided for calculating the discriminating streamline shape in the jet wake region shown in figure 2. The first is an integral method that accounts for entrainment effects based on the turbulent mixing analysis of Peters and Phares (ref. 20). The integral method assumes a three-parameter polynomial form for the velocity profile which is matched to the error-function profile of Presz at the end of the afterbody. Integral forms of the continuity, axial-momentum, and turbulent kinetic energy equations are solved by a marching technique from the end of the afterbody to the reattachment point (at which the reverse velocity vanishes). The turbulent kinetic energy profile is related to the velocity profile by a mixing-length model for the eddy viscosity as in reference 13.

The second method for treating the jet wake region is a simple extrapolation model. In this model, the slope of the discriminating streamline at the end of the afterbody (as calculated by the Presz method) is linearly extrapolated to intersect the inviscid plume boundary. While this model is ad hoc, its results do approximate the results of the original conical discriminating streamline model used in earlier work by Presz (ref. 8).

Mixing-Layer Solution

The displacement-thickness distribution arising from entrainment into the jet mixing layer is calculated by the overlaid mixing model of reference 13 and computer program BOATAC (ref. 17). BOATAC solves the parabolic mixing equations by a finite-difference marching procedure in cylindrical streamline coordinates. Turbulence is modeled by either a mixing-length or a two-equation ($k\varepsilon 2$) transport model. A laminar viscosity option is also included. The calculation is initialized at the nozzle exit for attached flows or at the reattachment location for separated flows. A fixed number of grid points, evenly spaced in the stream function coordinate, span the mixing layer. This computational grid is overlaid onto the inviscid external and jet flow fields (also mapped into streamline coordinates) from which edge conditions and pressure gradients are determined. The solution is marched downstream a user-specified distance that is sufficient to account for the near-field interaction (typically 10 to 15 exit radii). An effective plume boundary which accounts for mass entrainment into the mixing layer and inviscid plume blockage is calculated as described in reference 14. Then the inviscid plume boundary is subtracted from this effective boundary to define a displacement thickness related only to entrainment. This displacement-thickness distribution is treated like an extension of the boundary-layer displacement distribution and is added to the inviscid plume boundary by underrelaxation in the iteration procedure described in the next section.

Viscous-Inviscid Iteration Procedure

The component solutions are combined into the following iterative procedure (presented in fig. 3):

1. Calculate the inviscid external flow field over the effective body of revolution.

2. Calculate the inviscid jet exhaust boundary and flow field. If the flow is separated, the inviscid jet exhaust solution is frozen after 10 iterations.

3. Calculate the boundary-layer displacement thickness.

4. Calculate the separation location if required. The predicted separation location may be frozen after a user-specified number of iterations.

5. Calculate the shape of the discriminating streamline if required. Note that this calculation is repeated for every iteration if separation occurs, even if the separation location is frozen.

6. Calculate the mixing-layer displacement thickness.

7. Correct the effective body geometry by adding the displacement thickness and discriminating streamline to the original body and inviscid plume boundary. The relaxation procedure given in reference 14 is used to add these corrections.

8. Repeat steps (1) to (7) for the desired number of iterations.

At the end of step (8), the user must manually check the solution for convergence (usually by monitoring surface pressure and displacement distributions). Note that the order of calculation above is different from that in reference 14, although a single iterative loop is still used.

COMPARISONS BETWEEN PREDICTIONS AND EXPERIMENT

Predictions of program RAXJET are compared in figures 4 to 6 with experimental afterbody pressures from references 21, 22, and 23. All predictions were made with 77 by 39 grid points in the inviscid external region, 41 grid points in the mixing layer, and 41 grid points in the inviscid jet exhaust. The two-equation turbulence model was used for all mixing-layer calculations. For the separated flow cases, the experimental separation location and extrapolated jet wake model were used.

The comparisons for attached boundary-layer flow on a circular-arc boattail nozzle with $\ell/D = 1.768$ and $D_b/D = 0.51$ are shown in figure 4 at several nozzle pressure ratios (NPR) and free-stream Mach numbers. Predicted and experimental pressure distributions agree very well in almost all cases. The only significant differences occur at $M_\infty = 0.96$ and NPR = 2.0 (fig. 4(c)) where shock—boundary-layer interactions are expected.

The comparisons for slightly separated flow on a circular-arc nozzle with $\ell/D = 1.0$ and for significantly separated flow on a nozzle with $\ell/D = 0.8$ are given in figures 5 and 6, respectively. Again the agreement between prediction and experiment is excellent except for the $\ell/D = 0.8$ nozzle at Mach numbers of 0.9 and

0.94 (fig. 6(c)). While converged solutions were obtained and reasonable levels for the separation plateau pressures were predicted, the results at Mach numbers of 0.9 and 0.94 are quite poor in the region of shocks and in the jet wake. Furthermore, calculations at these Mach numbers made with the Presz model gave poor predictions of the separation location, and attempts to improve the predictions by iterating on the separation location sometimes led to divergent solutions. Thus it appears that strong interaction modeling is needed to treat flows with shock-induced separation. Therefore, RAXJET is not recommended when separation Mach numbers are supersonic.

Calculations made with the Presz model to predict separation location are compared to those made with the experimentally determined location in figure 7 for the $\iota/D = 1.0$ and $\iota/D = 0.8$ nozzles. In both cases the integral wake model was used, and the predicted separation location was frozen after the first iteration. For the $\iota/D = 1.0$ nozzle, the separation was predicted at $\Delta x/D = 0.71$, well upstream of the experimental value of 0.84 which resulted in a significant underprediction of the pressures near the end of the afterbody. For the $\iota/D = 0.8$ nozzle the predicted separation was at $\Delta x/D = 0.54$, compared to an experimental value of 0.51, and much better agreement is seen. In principle, better predictions of separation location could be obtained by updating the predicted location for additional iterations since the inviscid pressure should be approaching a more correct solution. However, the Presz model was found to be so sensitive to the imposed pressure distribution that significant amounts of underrelaxation were required to achieve convergence, and the predicted separation locations were not found to be consistently improved over those obtained on the first iteration. This sensitivity of separation predictions is typical of separation criteria that are based on calculating a pressure rise to separation (see ref. 10).

Predicted results with the integral and extrapolated jet wake models are compared in figure 8. Both sets of calculations used the experimental separation location. Slight differences are noted between the results of the two methods, and the judgment as to which is the better method seems to depend on which aspect of the prediction is most important to a particular problem. From these and similar results at other flow conditions, the integral method seems to yield more accurate flow-field predictions, while the extrapolated method seems to yield more accurate drag predictions.

Predicted and experimental boattail pressure drag for the data of figures 4 and 6 are compared in figure 9. Predicted drag obtained with the Presz separation model and the integral wake model and with the experimental separation location and the extrapolated wake model are shown for the separated flow cases. The drag calculated with the experimental separation location and the integral wake model fell between these two curves. Predicted results from reference 6 which neglect entrainment effects downstream of reattachment are also included. Generally, the agreement between the present results and experiment is good with noticeable improvement over the results of reference 6. This improvement is primarily due to the inclusion of jet entrainment effects. Although there is an undesirable sensitivity of the present predictions to the separation and jet wake model used, the present method does correctly predict the qualitative behavior for a given model. Thus, for parametric drag studies it is recommended that a particular combination of separation and wake models be used consistently.

In figure 10, predicted pitot pressures across the jet and mixing layer are compared with the data of Mason and Putnam (ref. 24). Figure 10(a) gives the results for a nozzle with attached flow at a Mach number of 0.4 and a nearly fully expanded jet (NPR = 2.0). The agreement is reasonably good, except that the spread rate of

the mixing layer is underpredicted. Cline and Wilmoth (ref. 25), who used a Navier-Stokes solution method with essentially the same turbulence model, found a similar trend. The results of reference 14 suggest that at least some of the discrepancy may be due to deficiencies in the turbulence modeling. However, the overall afterbody flow-field predictions were found to be relatively insensitive to the turbulence model used in the mixing-layer calculation.

Figure 10(b) gives results for a nozzle with separated flow at a Mach number of 0.8 and a moderately underexpanded jet (NPR = 5.0). The prediction was made with the integral jet wake model. Note that the wake defect predicted by this model agrees with the experimental profile nearest the nozzle exit ($\Delta x/r_j = 0.1$). Also, the predicted structure of the inviscid plume flow field is in excellent agreement with the experimental structure. The location and strength of the barrel shock and Mach disk normal shock and the size of the Mach disk streamtube are all correctly predicted. Since this shock structure is known to be sensitive to the external pressure distribution imposed (see ref. 24), the present results suggest that the basic plume interaction model is reasonably correct.

DESCRIPTION OF COMPUTER PROGRAM

The organization of computer program RAXJET is presented in figure 11. The program is written in overlay form and consists of the main overlay (0,0) and six primary overlays (fig. 11(a)). The main overlay, RAXJET, controls the input and output of data and the viscous-inviscid iteration scheme. Primary overlay (1,0) contains the program RAXBOD which calculates the inviscid external flow. Primary overlay (2,0) contains the program SCIPAC which calculates the inviscid jet exhaust flow. Primary overlay (3,0) contains the program VISCOUS which calculates the boundary-layer growth and performs the separation analysis. Primary overlay (4,0) contains the program BOATAC which performs the overlaid mixing analysis. Primary overlay (5,0) contains the program INPT which reads the input data, and primary overlay (6,0) contains the program OUTPT which prints the computed results.

The program uses six disk files. Input data are obtained from file TAPE5 and the results are written to file TAPE6 which is equated to file OUTPUT. The remaining disk files are used internally by the program and are described later. RAXJET requires about 76 000 octal storage locations on the Control Data CYBER 175 computer and executes 20 viscous-inviscid iterations in approximately 12 minutes of CPU time for separated flow on an afterbody with a fully expanded jet. Attached flow computations generally require fewer iterations and therefore less computer time. Underexpanded or overexpanded jets generally require more computer time.

A brief description of each of the main routines is given in the following list:

1. Program RAXJET.- RAXJET initiates a run by calling program INPT to read the input data. Then an initial call is made to program RAXBOD to set up the inviscid external grid. This grid is used to define various grid indices used by other routines and to initialize various geometric arrays. RAXJET then starts the viscous-inviscid loop by calling RAXBOD, SCIPAC, VISCOUS, and BOATAC, successively. Then program OUTPT is called to print the results. Finally, RAXJET calculates the new effective body and repeats the viscous-inviscid iteration until the specified number of iterations is completed. RAXJET also calls subroutine AINTPL to interpolate the original body geometry onto the inviscid grid (which changes slightly during each iteration) and subroutine SMOOTH to smooth the effective body geometry for separated flows.

2. Program RAXBOD.- RAXBOD solves the exact nonlinear potential flow equation for the inviscid external flow and consists of the primary overlay (1,0) and four secondary overlays (see fig. 11(b)). RAXBOD first calls ONE1 (overlay (1,1)) to set up the tangential grid and ONE2 (overlay (1,2)) to set up the normal grid. Since the effective body shape may change with each iteration, these routines must be called before each inviscid calculation. For the first iteration only, subroutine ESTIM is called to initialize the perturbation potential to zero. For each succeeding iteration, potential values from the previous iteration are used as the initial estimate. Program ONE3 (overlay (1,3)) is then called to solve the exact potential equation by the South-Jameson relaxation scheme. The relaxation is continued until either the specified maximum number of relaxation iterations are performed or the specified convergence tolerance is reached. Finally, program ONE4 (overlay (1,4)) is called to calculate the flow quantities (velocity, pressure, etc.) from the perturbation potential and to transfer the results to disk file TAPE4.

3. Program SCIPAC.- SCIPAC solves the inviscid jet exhaust region by a shock-capturing—shock-fitting procedure and consists of the main program, 24 subroutines, and 6 function subroutines (see fig. 11(c)). SCIPAC initializes a jet calculation by calling SCIPPB which reads the external flow properties from TAPE4 and determines the pressure to be specified along the plume boundary. Then SCIPIN is called to generate the initial conditions at the nozzle exit from the input data and to discretize the initial flow conditions for the finite-difference marching procedure. Also, from nozzle exit conditions, SCIPIN estimates the length of the first inviscid cell which is used to terminate the marching procedure. Then SCIPCT is called to integrate the finite-difference flow equations and to perform the iterative Mach disk calculation. For the Mach disk calculation, disk files TAPE1 and TAPE2 store conditions upstream of the predicted Mach disk location while trial solutions downstream are attempted. Details of the Mach disk procedure are given in reference 17. Depending on certain input parameters and the predicted inviscid cell length, the marching procedure terminates either downstream of the Mach disk or at the end of the first or second inviscid cell. Properties downstream of this termination point are calculated by a simple isentropic expansion to local external pressure by calling subroutine SCIPDK. Jet exhaust properties at axial locations corresponding to the external inviscid grid are transferred to disk file TAPE3 by calling SCIPOT. Finally, SCIPPL is called to determine the coordinates of the inviscid plume boundary and to store them for later use.

4. Program VISCOUS.- Program VISCOUS calculates the boundary-layer growth, separation location, and discriminating streamline shape by calls to subroutines ONE, TWO, and THREE (see fig. 11(d)). Subroutine ONE calculates the boundary-layer displacement thickness, skin friction, and power-law exponent by a modified Reshotko-Tucker integral procedure with the inviscid pressure gradient imposed by the external flow solution. Subroutine TWO calculates the separation location by the Presz control volume method. Subroutine THREE calls B834 which calculates the discriminating streamline shape by the modified discrete control volume method of Presz et al. If the integral wake model is specified, B834 calls JET to calculate the discriminating streamline from the end of the body to the end of the recirculation region. If the integral wake model is not specified, B834 linearly extrapolates the discriminating streamline until it intersects the inviscid plume boundary.

5. Program BOATAC.- Program BOATAC calculates the turbulent mixing layer and the plume displacement thickness and consists of the primary overlay (4,0) and two secondary overlays (see fig. 11(e)). BOATAC first calls BOATSA (overlay (4,1)) which in turn calls (1) BOATIP to read the inviscid flow field from TAPE3 and TAPE4, (2) BOATIP and BOATKE to generate the initial velocity, temperature, and turbulence

profiles, and (3) BOATSB to map the profiles into equally spaced streamline coordinates. BOATAC then calls BOATM1 (overlay (4,2)) which in turns calls (1) BOATS3 to integrate the parabolized flow equations, (2) BOATDS to calculate the plume displacement thickness, (3) BOATEN to estimate the necessary computational boundary growth rate, (4) BOATM2 to reset the discretized profile to begin the next marching step, and (5) BOATOT to transfer the results to disk file TAPE2 at axial locations corresponding to the external grid. BOATAC starts at the nozzle exit for attached flows or at the reattachment location for separated flows and marches downstream the user-specified number of jet radii. Mixing-layer properties downstream of this axial location are not calculated.

6. Program INPT.- INPT reads the input data from TAPE5, checks for possible input errors, and prints the appropriate warning messages (fig. 11(f)). If certain RAXBOD grid parameters are not input, INPT calls subroutine OPTIM which attempts to optimize those parameters not given so that a maximum number of grid points are located on the afterbody consistent with an accurate solution of the total flow field. Finally, INPT calls subroutine IOUTPT to print the input data.

7. Program OUTPT.- OUTPT prints the surface quantities, drag coefficients, and convergence history (fig. 11(f)). If requested, OUTPT calls subroutine OFFOUT to generate and print a composite viscous-inviscid flow field.

Description of Input Data

The program input data are entered by a title card followed by eight namelists. A sample input data deck is given in the appendix. Some of the geometric input quantities are defined in figure 12, and certain input parameters for the off-body flow-field output are given in figure 13.

1. Title card.- The first card of each data deck consists of 80 alphanumeric characters that identify the case. The eight namelists must then appear in the following order.

2. Namelist CNTRLN.- CNTRLN contains the input parameters that control the main logic of the program:

IMAX Integer that specifies the number of grid points in the streamwise direction for the inviscid external flow solution (81 maximum). The default value is 81.

JMAX Integer that specifies the number of grid points in the body normal or radial direction for the inviscid external flow solution (41 maximum). The default value is 41.

MIT Integer that specifies the number of relaxation cycles used per viscous-inviscid iteration for the inviscid external flow solution. The default value is 20.

MVI Integer that specifies the number of viscous-inviscid iterations (30 maximum). The default value is 1.

ISEP Integer that specifies the separation model used:
If ISEP = 0, no separation model is used.
If ISEP = 1, the Presz control volume method is used.

If ISEP = 2, the separation location is specified by the user.
The default value is 0.

NSEP — Integer that specifies the number of viscous-inviscid iterations after which the separation location is held fixed (needed only if ISEP = 1). The default value is 1.

IWAKE — Integer that specifies the jet wake model (needed for ISEP = 1 or 2):
If IWAKE = 0, the integral wake model is used.
If IWAKE = 1, the extrapolated wake model is used.
The default value is 0.

XSEP — Axial coordinate of the separation location nondimensionalized by REFL (needed only if ISEP = 2). The default value is XM.

IUI — Integer that specifies the type of units used for input quantities:
If IUI = 0, lengths are input in feet, temperatures in Rankine, and pressures in pounds per square foot (psf).
If IUI = 1, lengths are input in meters, temperatures in kelvin, and pressures in atmospheres (1 atm = 101.325 kPa).
The default value is 0.

IUO — Same as IUI except it applies to output quantities.

3. Namelist FSC.- FSC contains the free-stream conditions and reference quantities:

GAM — Ratio of specific heats. The default value is 1.4.

AMINF — Free-stream Mach number. No default value is specified.

PT — Free-stream total pressure in pounds per square foot or atmospheres. The default value is 2116 psf or 1 atm, depending on IUI.

TT — Free-stream total temperature in °R or K. The default value is 530°R or 294 K, depending on IUI.

REFL — Reference length used to convert input coordinates to feet (IUI = 0) or meters (IUI = 1). All other inputs having dimensions of lengths are assumed to be nondimensionalized by REFL. The default value is 1.0.

SREF — Reference area in square feet or square meters used to calculate drag coefficients. The default value is $(\pi/4)(\text{REFL})^2$.

ALPHAE — Array containing the mole fractions of the six species in the following order: N_2, O_2, CO_2, H_2O, CO, and CH_4. The default values are the nominal values for air: ALPHAE(1) = 0.79, ALPHAE(2) = 0.21, ALPHAE(3) = ALPHAE(4) = ALPHAE(5) = ALPHAE(6) = 0.0

4. Namelist JETDAT.- JETDAT contains the nozzle exit conditions and control parameters for the inviscid jet exhaust solution:

XNPR — Nozzle pressure ratio, ratio of jet total pressure to free-stream static pressure. No default value is specified.

EMJET — Nozzle exit Mach number (EMJET > 1.05). The default value is 1.05.

TTJET — Nozzle exit total temperature in °R or K. The default value is 530°R or 294 K, depending on IUI.

RJET — Nozzle exit radius nondimensionalized by REFL. No default value is specified. (See fig. 12.)

THLIP — Nozzle exit lip angle in degrees. The default value is 0.0. (See fig. 12.)

NMAXJ — Integer that specifies the number of radial grid points used in the inviscid jet solution (81 maximum). The default value is 81.

IGAS — Integer that specifies the thermodynamic option for the inviscid jet solution:
If IGAS = 0, a perfect gas is assumed and GAMJ = 1.4.
If IGAS = 1, a perfect gas is assumed and GAMJ must be input.
If IGAS = 2, a calorically imperfect gas is assumed and GAMJ will be calculated.
If IGAS = 3, a perfect gas is assumed but GAMJ will be calculated based on nozzle exit conditions and held constant downstream.
The default value is 0.

GAMJ — Ratio of specific heats for inviscid jet exhaust. See IGAS for defaults.

IDK — Integer that controls the solution method downstream of a Mach disk:
If IDK = 0, an isentropic decay is imposed.
If IDK = 1, a finite-difference shock-capturing solution will be attempted.
The default value is 0.

ALPHAJ — Array containing the mole fractions of the six jet species. Same as ALPHAE (namelist FSC) except it applies to the inviscid jet.

5. Namelist MIXDAT.- MIXDAT contains the input quantities that control the overlaid mixing-layer calculation:

IVIS — Integer that specifies the turbulence model.
If IVIS = -2, the $k\varepsilon 2$ model is used.
If IVIS = 0, the Prandtl mixing-length model is used.
If IVIS = 2, a laminar model is used.
The default value is -2.

MPSI — Integer that specifies the number of radial grid points used in the mixing-layer calculation (50 maximum). The default value is 31.

FDL — Factor that multiplies the marching step size (FDL ≤ 1.0). The default value is 1.0.

FFF — Mixing-length scale used in the Prandtl mixing model in the near-field region. The default value is 0.065.

GGG — Mixing-length scale used in the Prandtl mixing model in the fully developed region. The default value is 0.080.

SIGMA — Turbulent Prandtl number. The default value is 1.0.

TCONT — Maximum allowable temperature change in one marching step in °R or K, depending on IUI. The default value is 400/(MPSI - 1) K.

XJENT — Axial distance in jet radii from the nozzle exit where the mixing calculation will be terminated. The default value is 15.

KMAXJ — Integer that specifies the number of mapped radial grid points in the inviscid jet solution that are used in the overlaid mixing calculation (25 maximum). The default value is 25.

KMAXE — Same as KMAXJ except it applies to the inviscid external flow solution.

TKEJ — Factor that multiplies the initial turbulent kinetic energy in the jet at the nozzle exit. The default value is 1.0.

TKEX — Same as TKEJ except it applies to the external flow side of the initial profile.

6. Namelist RELAX.- RELAX contains various relaxation parameters used in the inviscid external flow solution and viscous-inviscid interaction:

RF1 — Relaxation factor for subsonic points in the inviscid external flow solution ($0 < RF1 < 2$). The default value is 1.4.

QF3 — Supersonic damping factor for improving iterative stability in the inviscid external flow solution ($QF3 > 0$). The default value is 0.1.

COVERG — Convergence criterion for inviscid external flow solution. Inviscid relaxation cycles stop for a given iteration when the average residual is less than COVERG/(IMAX - 1)^2 or MIT cycles are completed, whichever occurs first. The default value is 1.0.

WB and WBF — Underrelaxation parameters for adding the displacement thickness and discriminating streamline to the body. WB is the value for the first iteration and WBF is the value for the final iteration. For intermediate iterations, the underrelaxation factor is varied linearly from WB to WBF. (WB and WBF must be in the range from 0 to 1.) The default values are 0.5. Larger values of WB or WBF give more underrelaxation.

7. Namelist GRID.- GRID contains the parameters that control the body-fitted grid used in the inviscid external flow solution:

XBT — Axial location of the start of the afterbody nondimensionalized by REFL. No default value is specified. (See fig. 12.)

XM — Axial location of the end of the body nondimensionalized by REFL. No default value is specified. (See fig. 12.)

DXIDXO — Derivative of the tangential coordinate stretching function at the nose, $(d\xi/dX)_{X=0}$. A reasonable value can be estimated from DXIDXO $\approx$ (IMAX - 1)$\Delta\xi_o$ where $\Delta\xi_o$ is the desired grid size at the

nose. If no input value is given, the program will attempt to calculate an optimum value.

DXIDXM — Derivative of the tangential stretching function at the end of the body, $(dF/dX)_{X=XM}$. A reasonable value can be estimated from DXIDXM = (IMAX - 1)ΔF_M where ΔF_M is the desired grid size at the end of the body. If no input value is given, the program will attempt to calculate an optimum value.

CXM — Fraction of streamwise grid points that lie on the body (0 < X < XM). (CXM must be in the range from 0 to 1.) The default value is 0.75. Note that if no input value of DXIDXM is given, CXM may be changed in an attempt to find an optimum value for DXIDXM.

DNDYO — Derivative of normal coordinate stretching function at the body surface, $(d\eta/dY)_{Y=0}$. A reasonable value may be estimated from DNDYO = $(1 - \Delta Y)^{\alpha} \Delta\eta_o/\Delta Y$ where $\Delta\eta_o$ is the desired grid size at the surface, α is the stretching exponent, and $\Delta Y = 1/(JMAX - 1)$. If no input value is given, the program will attempt to calculate an optimum value.

ALF — Exponent in the normal coordinate stretching function. (ALF > 0.) The default value is 1.3. Larger values of ALF move the last finite value of η farther away from the body and smaller values move it closer.

8. Namelist OUTPTC.- OUTPTC contains parameters which control the printing of results. Some of the parameters used to generate the composite flow-field output are defined graphically in figure 13. Figure 14 shows how the composite flow field is constructed.

IOUT — Integer that specifies the iteration number at which the printing of results will begin. All iterations from IOUT to MVI will be printed. The default value is 0.

IAFT — Integer that controls the amount of results printed:
If IAFT = 0, results will be printed starting at the nose.
If IAFT = 1, results will be printed starting at the first grid point ahead of the afterbody.
The default value is 0.

IOFF — Integer that controls the printing of the off-body flow-field results:
If IOFF = 0, no off-body results will be printed.
If IOFF = 1, off-body results will be printed.
The default value is 0.

XSTRT — Axial location (nondimensionalized by REFL) at which the printing of off-body results will begin. No default value is specified.

XEND — Axial location (nondimensionalized by REFL) at which the printing of off-body results will end. No default value is specified.

ROB — Radial outer boundary (nondimensionalized by REFL) for printing off-body results. No default value is specified.

IMAP — Integer that specifies the number of mapped output points between the body (or inviscid plume boundary) and r = ROB (see fig. 13). (IMAP ≤ 100 - JMAP.) The default value is 25.

JMAP — Integer that specifies the number of mapped output points across the jet exhaust (0 ≤ r ≤ Inviscid plume boundary). (JMAP ≤ 100 - IMAP.) The default value is 25.

ALFO — Exponent in radial stretching function used to distribute output points in off-body results. AFLO > 1 will pack points in the boundary layer and mixing layer. ALFO = 1 will give equally spaced points. The default value is 1.

9. Namelist GEOMN.- GEOMN contains the body geometry data. Note that a finite-length forebody geometry must be input even if only afterbody results are desired. The forebody nose may be blunt or pointed, and the input coordinates are assumed to be referenced to the nose (x = 0, r = 0 in fig. 12).

IXY — Integer that specifies the number of body input coordinates (140 maximum). No default value is specified.

IORDER — Integer that specifies the type of interpolation used to determine the geometry at the inviscid grid points:
If IORDER = 1, first order will be used.
If IORDER = 2, second order will be used.
The default value is 1.

XO — Array of IXY axial body coordinates (nondimensionalized by REFL) with origin at the nose of the body of revolution. No default values are specified.

YO — Array of IXY radial body coordinates (nondimensionalized by REFL) with origin at the nose of the body of revolution. No default values are specified. Note that the first point of the XO and YO arrays must correspond to the nose, XO(1) = 0, and the last point to the end of the body, XO(IXY) = XM.

Description of Output

An example of the printed output is given in the appendix for the sample input data also presented there. The first two pages are duplicate output with RAXJET bannerized followed by the case title, date, and time of run. Warning messages generated by the input data are printed on the third page and diagnostic messages from the grid optimization routine are printed on the fourth page. The fifth page contains the program title and abstract, case title, and free-stream and jet exhaust conditions. On the sixth page, the gas composition and remaining input parameters are printed. The next two pages list the input geometry. The tabular input geometry has been augmented with points that define a cylindrical sting starting at the end of the body as an initial guess for the plume shape.

The following pages list the results. For each iteration starting with IOUT the case title, iteration number, free-stream Mach number MO, jet pressure ratio, and reference length L are given. If boundary-layer separation is predicted, the separation and reattachment locations are also printed. A tabulation is given of

Axial grid point number I

Body axial coordinate X/L

Body radial coordinate R/L

Pressure coefficient CP

Local Mach number ML

Skin-friction coefficient CF

Body radius corrected for the discriminating streamline and inviscid plume shape RDS/L

Effective body radius REFF/L

Radial location of the outer edge of the viscous layer RVI/L

Displacement thickness DEL*/L

Boundary-layer momentum thickness THETA/L

Compressible shape factor H

Note that REFF/L is the effective body obtained by underrelaxation, while RDS/L + DEL*/L is the calculated displacement body for a given iteration. Note also that the definition of DEL*/L for the plume mixing layer used here differs from that presented in reference 14. Here, values of DEL*/L for X/L downstream of the nozzle exit include only the contribution due to jet entrainment and do not include the inviscid plume blockage. However, the effective body definition used here is the same as in reference 14. After the final iteration is printed, the following drag coefficients for each iteration are tabulated:

Afterbody pressure drag CDP,AFT

Afterbody friction drag CDT,AFT

Total (pressure and friction) afterbody drag CDT,AFT

External pressure drag for the complete body of revolution (forebody and afterbody) CDP,BOD

Body friction drag CDF,BOD

Total body drag CDT,BOD

Next, the maximum residual RPMAX and average residual RPAVG for the RAXBOD calculation are listed as an indication of the convergence history.

If off-body flow-field results are requested, the remaining pages tabulate

Axial location X/L

Radial location R/L

Nondimensionalized pressure P/PINF

Nondimensionalized temperature T/TINF

Nondimensionalized axial velocity U/UINF

Nondimensionalized radial velocity V/UINF

Mach number M

Ratio of specific heats GAMMA

Nondimensionalized pitot pressure PT/PTINF

Pressures, temperatures, and velocities are determined by linear interpolation directly from the appropriate flow solution as indicated in figure 14 except for points in the boundary layer (denoted by BL). For the BL points, edge conditions and pressures are determined by interpolation from the inviscid solution, streamwise velocities are calculated from a power-law profile, and temperatures are calculated by assuming a constant total temperature across the layer. Axial and radial velocity components are determined from the streamwise values by assuming a linear variation in streamline slope across the layer from the local body slope at the surface to the inviscid streamline slope at the outer BL edge. For all points, local Mach number and pitot pressure are computed from these interpolated and calculated quantities. Note that for supersonic points, the pitot pressure is obtained by normal shock relations for an adiabatic, perfect gas. Points in the inviscid jet region that are computed from isentropic theory are denoted by (*) and points in the mixing layer downstream of where the mixing solution terminates are denoted by (**). Note that the axial location of points in the inviscid jet and mixing layer may not correspond exactly to the grid location in the external flow. These points correspond to actual marching step locations that are nearest the external grid location. No attempt was made to interpolate these points in the axial direction since the discrepancy is usually quite small. Also note that flow-field results are not given within the separated region.

Instructions to the User

The following special instructions are provided to assist the user in applications of program RAXJET. These instructions do not cover all possible user problems but are intended to assist the user in anticipating cases where the physical and computational models may not give accurate results. Many of the problems associated with inappropriate input data are flagged by the program followed by explanatory warning messages, and these are not discussed here.

Grid generation.- The user has input control over the streamwise and normal grid used by RAXBOD, and the radial grid used by SCIPAC and BOATAC. The streamwise grid used by VISCOUS for the boundary-layer calculation is the same as that for RAXBOD. For most problems, the built-in procedures for optimizing the RAXBOD grid parameters give satisfactory results as long as the afterbody length comprises approximately 10 to 25 percent of the total body length. For shorter afterbodies, other unusual geometries, or much fewer than the maximum allowable number of grid points (IMAX,JMAX), the user should verify that the grid is adequate. For the SCIPAC calculation, accurate shock-capturing may require nearly the maximum allowable number of

points (NMAXJ = 81). If fewer points are used, SCIPAC gives less accurately defined shocks and may encounter problems when computing cases with small Mach disks or regular barrel shock reflections or when attempting to extend the computation beyond the first Mach disk or reflection (IDK = 1). If such problems are encountered, the user should try increasing NMAXJ. For the BOATAC calculation, the default value of MPSI = 31 may be adequate for the basic entrainment interaction; however, larger values of MPSI are recommended if accurate mixing-layer profiles are desired.

Convergence.- The convergence history of the RAXBOD calculation is given as part of the output. If convergence is not achieved by the final iteration, the number of global iterations MVI, the number of relaxation cycles MIT, or both should be increased. An indication of the global convergence of the viscous-inviscid calculation can be obtained by monitoring the afterbody pressure drag (CDP,AFT) or selected pressures and, for separated flows, the separation location (if ISEP = 1, NSEP > 1).

Attached flows (ISEP = 0).- Calculations in which attached flow is anticipated generally converge in 5 to 10 iterations with most input parameters set at their default values. Flows with incipient separation may also be run as attached flows but may require greater amounts of underrelaxation (increased WB and WBF) and more iterations to converge.

Separated flows (ISEP > 0).- Separated flows require considerably more user intervention in selecting appropriate control parameters than attached flows. The greatest source of error generally lies in prediction of the separation location. More accurate flow predictions can be made if the separation location is known and is input by the user (ISEP = 2). If the separation location is not known, it is recommended that a solution first be attempted as for attached flow (ISEP = 0). If the solution diverges or if the boundary-layer shape factor exceeds a value of 2, then assume that the flow is separated and attempt a solution with ISEP = 1. A value of NSEP = 1 (the default value) is recommended which bases the separation location prediction on the initial inviscid solution. This procedure yields reasonable results except where the flow is approaching shock-induced separation. RAXJET is not recommended for strong shock-induced separation. More accurate predictions of the separation location can sometimes be obtained by allowing the predicted location to be updated over several iterations (NSEP > 1), but larger amounts of underrelaxation are usually necessary (WB = 0.75, 0.5 < WBF < 0.75, typically). The choice of the wake model depends on the type of result that is of primary interest. If afterbody pressures and drag are the main interest, IWAKE = 1 is recommended. If mixing-layer profile results are important, IWAKE = 0 is recommended.

Real gas thermodynamics.- The real gas thermodynamics used in SCIPAC and BOATAC contain built-in data for the six species, N_2, O_2, CO_2, H_2O, CO, and CH_4. Alternate species may be used by replacing the appropriate polynomial coefficient data in subroutines SCIPCF and BOATSD with that for the alternate species. Detailed definition of these coefficients is given in reference 17.

CONCLUDING REMARKS

A viscous-inviscid interacton method has been developed to compute the subsonic and transonic flow over nozzle afterbodies with supersonic jet exhausts. The method accounts for the interaction between the inviscid external flow, an underexpanded jet exhaust, an attached or separated boundary layer, and the turbulent jet mixing layer. A computer algorithm called RAXJET has been written which iteratively combines

solutions for the various flow regions by a relaxation procedure. The results of the method are in good agreement with experiment for afterbodies with attached flow up to moderately high transonic speeds. For afterbodies with separated flow, the agreement is good except when shock-induced separation is encountered. The results indicate a need for improved modeling of separated flows where strong interactions occur. The method correctly predicts the effects of jet entrainment and plume blockage on nozzle drag. Good agreement is obtained with flow-field data for moderately underexpanded jet exhausts.

Langley Research Center
National Aeronautics and Space Administration
Hampton, VA 23665
January 4, 1982

APPENDIX

SAMPLE INPUT AND OUTPUT FOR PROGRAM RAXJET

Sample Input Data

```
L/D=0.8, DB/D=0.51 CIRCULAR ARC BOATTAIL - M = 0.8, NPR = 5.0
$CNTRLN IMAX=77,JMAX=39,NVI=20,MIT=40,ISEP=1,IUO=1 $
$FSC GAM=1.4, AMINF=0.8,PT=2116.,TT=560.,REFL=0.5 $
$JETDAT XNPR=5.0,TTJET=530.,RJET=0.25,NMAXJ=41,IGAS=2,IDK=0,
EMJET=1.05 $
$MIXDAT NPSI=41 $
$RELAX WB=0.75,WBF=0.5 $
$GRID CXM=.75, XBT=8.0,XM=8.8 $
$OUTPTC IOUT=20,IAFT=1,IOFF=1,XSTRT=8.0,XEND=9.4,ROH=0.75 $
$GEOMN IXY=89,
X0(1)=0.0,.1,.2,.3,.4,.5,.6,.7,.8,.9,1.0,1.1,1.2,1.3,1.4,1 .1,6,1.7,
1.8,1.9,2.0,2.1,2.2,2.3,2.4,2.5,2.6,2.7,2.8,2.9,3.0,3.1,3.2,3.3,3.4,
3.5,3.6,3.7,3.8,3.9,4.0,4.1,4.2,4.3,4.4,4.5,4.6,4.7,4.8,4.9,5.0,5.1,
5.2,5.3,5.4,5.5,5.6,5.7,5.8,5.9,6.0,6.1,6.2,6.3,6.4,6.5,6.6,6.7,6.8,
6.9,7.0,7.1,7.2,7.3,7.4,7.5,7.6,7.7,7.8,7.9,8.0,8.1,8.2,8.3,8.4,8.5,
8.6,8.7,8.8,
Y0(1)=0.0,.025013,.050026,.075038,.100051,.125064,.150077,.175090,
.200102,.225115,.250128,.275141,.300154,.325166,.350179,.375192,
.400205,.425218,.450230,.475630,.489760,.498360,59*.5,.496496,
.485932,.466146,.442860,.409646,.367897,.316754,.255 $
```

Sample Output

```
RRRRRRRR      AAAAAA     XXX     XXX          JJJ  EEEEEEEEEE  TTTTTTTTTTT
RRRRRRRRR    AAAAAAAA    XXX     XXX          JJJ  EEEEEEEEEE  TTTTTTTTTTT
RRR     RRR  AAA    AAA   XXX   XXX          JJJ  EEE             TTT
RRR     RRR  AAA    AAA   XXX   XXX          JJJ  EEE             TTT
RRR     RRR  AAA    AAA    XXXXXX            JJJ  EEE             TTT
RRRRRRRRRR   AAAAAAAAAA      XXXX             JJJ  EEEEEEEE        TTT
RRRRRRRRR    AAAAAAAAAA       XX              JJJ  EEEEEEEE        TTT
RRRRR        AAA    AAA      XXXX             JJJ  EEE             TTT
RRRRRR       AAA    AAA     XXXXXX            JJJ  EEE             TTT
RRR RRR      AAA    AAA    XXX  XXX           JJJ  EEE             TTT
RRR  RRR     AAA    AAA    XXX  XXX    JJJ    JJJ  EEE             TTT
RRR   RRR    AAA    AAA   XXX    XXX   JJJJJJJJ   EEEEEEEEEE      TTT
RRR    RRR   AAA    AAA   XXX    XXX    JJJJJJ    EEEEEEEEEE      TTT
```

CASE - L/D=0.8, DH/D=0.51 CIRCULAR ARC BOATTAIL - M = 0.8, NPR = 5.0

DATE - 81/07/16. TIME - 08.57.57.

Pages 1 and 2. (Note that page 2 is a duplicate of page 1.)

```
---WARNING MESSAGES---

 INPUT VALUE OF DXIDX0 NOT GIVEN OR < 0, WILL TRY TO CALCULATE AN OPTIMUM VALUE
 INPUT VALUE OF DXIDXM NOT GIVEN OR < 0, WILL TRY TO CALCULATE AN OPTIMUM VALUE
 INPUT VALUE OF DNDYU  NOT GIVEN OR < 0, WILL TRY TO CALCULATE AN OPTIMUM VALUE
 NOZZLE GEOMETRY GIVEN HAS A BASE THICKNESS OF       .005000, TOO LARGE A BASE MAY GIVE UNRELIABLE RESULTS
```

--TYPE 8 GRID OPTIMIZATION REQUESTED

CXM	CHANGED FROM	.75 TO	.82
DXIDX0	CHANGED FROM	0.0000 TO	5.5488
DXIDXM	CHANGED FROM	0.0000 TO	5.5488
DNDY0	CHANGED FROM	0.0000 TO	2.6799

RAXJET --- A VISCOUS/INVISCID PROGRAM FOR TRANSONIC, AXISYMMETRIC FLOW
OVER NOZZLE AFTERBODIES WITH SUPERSONIC JET EXHAUSTS

BY RICHARD G. WILMOTH, NASA, LANGLEY RESEARCH CENTER

PROGRAM ABSTRACT -

THE VISCOUS/INVISCID SOLUTION IS OBTAINED USING THE FULL POTENTIAL, RELAXATION METHOD OF SOUTH AND JAMESON FOR THE TRANSONIC, EXTERNAL FLOW COMBINED WITH: (1) THE SHOCK-CAPTURING/SHOCK-FITTING INVISCID PLUME MODEL OF DASH, PERGAMENT AND THORPE; (2) A MODIFIED RESHOTKO-TUCKER INTEGRAL BOUNDARY-LAYER SOLUTION; AND (3) THE OVERLAID, NEARFIELD MIXING MODEL OF DASH AND PERGAMENT. FOR SEPARATED FLOWS, PRESZ'S SEPARATION CRITERIA AND MODIFIED DISCRIMINATING STREAMLINE SOLUTION ARE USED. THE VISCOUS/INVISCID INTERACTION IS TAKEN INTO ACCOUNT BY AN ITERATIVE UNDERRELAXATION PROCEDURE.

CASE TITLE -

L/D=0.8, DB/D=0.51 CIRCULAR ARC BOATTAIL - M = 0.8, NPR = 5.0

FREE STREAM CONDITIONS -

MACH NUMBER	=	.800
GAMMA	=	1.400
TOTAL PRESSURE	=	1.000 ATM
TOTAL TEMPERATURE	=	311.111 KELVIN
REYNOLDS NUMBER	=	12.929 MILLION PER METER

JET EXHAUST CONDITIONS -

MACH NUMBER	=	1.050
PRESSURE RATIO	=	5.000
TOTAL TEMPERATURE	=	294.444 KELVIN
NOZZLE EXIT RADIUS	=	.038 METERS
NOZZLE LIP ANGLE	=	0.000 DEGREES

APPENDIX

COMPOSITION - SPECIES

SPECIES	JET	FREESTREAM
N2	.790E+00	.790E+00
O2	.210E+00	.210E+00
CO2	0.	0.
H2O	0.	0.
CO	0.	0.
CH4	0.	0.

CONTROL PARAMETERS -

IMAX =	77
JMAX =	39
MIT =	40
MVI =	20
ISEP =	1
NSEP =	1
IWAKE=	0

RELAXATION PARAMETERS -

RF1 =	1.40
QF3 =	.10
COVERG =	1.00
WB =	.75
WBF =	.50

GRID PARAMETERS -

CXM =	.82
DXIDXO =	5.548830
DXIDXM =	5.548830
DNDYO =	2.679878
ALF =	1.30

MIXING CONTROL PARAMETERS -

IVIS =	-2
MPSI =	41
KMAXJ=	25
KMAXE=	25

FDL =	1.00
FFF =	.065
GGG =	.080
SIGMA =	1.000

TCONT =	10.00
XJENT =	15.00
TKEJ =	1.00
TKEX =	1.00

JET CONTROL PARAMETERS - NMAXJ = 41, IGAS = 2, IDK = 0

OUTPUT CONTROL - IOUT =20, IAFT = 1, IOFF = 1, IUO = 1

INPUT GEOMETRY - 1ST-ORDER INTERPOLATION WILL BE USED TO FIT THE INVISCID GRID

THE AFTERBODY STARTS AT X/REFL = 8.000000 AND ENDS AT X/REFL = 8.800000
THE BODY SLOPE AT THE NOSE IS = .250130

I	X/REFL	R/REFL	I	X/REFL	R/REFL
1	0.000000	0.000000	36	3.500000	.500000
2	.100000	.025013	37	3.600000	.500000
3	.200000	.050026	38	3.700000	.500000
4	.300000	.075038	39	3.800000	.500000
5	.400000	.100051	40	3.900000	.500000
6	.500000	.125064	41	4.000000	.500000
7	.600000	.150077	42	4.100000	.500000
8	.700000	.175090	43	4.200000	.500000
9	.800000	.200102	44	4.300000	.500000
10	.900000	.225115	45	4.400000	.500000
11	1.000000	.250128	46	4.500000	.500000
12	1.100000	.275141	47	4.600000	.500000
13	1.200000	.300154	48	4.700000	.500000
14	1.300000	.325166	49	4.800000	.500000
15	1.400000	.350179	50	4.900000	.500000
16	1.500000	.375192	51	5.000000	.500000
17	1.600000	.400205	52	5.100000	.500000
18	1.700000	.425218	53	5.200000	.500000
19	1.800000	.450230	54	5.300000	.500000
20	1.900000	.473630	55	5.400000	.500000
21	2.000000	.489760	56	5.500000	.500000
22	2.100000	.498366	57	5.600000	.500000
23	2.200000	.500000	58	5.700000	.500000
24	2.300000	.500000	59	5.800000	.500000
25	2.400000	.500000	60	5.900000	.500000
26	2.500000	.500000	61	6.000000	.500000
27	2.600000	.500000	62	6.100000	.500000
28	2.700000	.500000	63	6.200000	.500000
29	2.800000	.500000	64	6.300000	.500000
30	2.900000	.500000	65	6.400000	.500000
31	3.000000	.500000	66	6.500000	.500000
32	3.100000	.500000	67	6.600000	.500000
33	3.200000	.500000	68	6.700000	.500000
34	3.300000	.500000	69	6.800000	.500000
35	3.400000	.500000	70	6.900000	.500000

I	X/REFL	R/REFL
71	7.000000	.500000
72	7.100000	.500000
73	7.200000	.500000
74	7.300000	.500000
75	7.400000	.500000
76	7.500000	.500000
77	7.600000	.500000
78	7.700000	.500000
79	7.800000	.500000
80	7.900000	.500000
81	8.000000	.500000
82	8.100000	.496496
83	8.200000	.485932
84	8.300000	.468146
85	8.400000	.442860
86	8.500000	.409646
87	8.600000	.367897
88	8.700000	.316754
89	8.800000	.255000
90	9.050000	.250000
91	9.300000	.250000
92	9.550000	.250000
93	9.800000	.250000
94	10.050000	.250000
95	10.300000	.250000
96	10.550000	.250000
97	10.800000	.250000
98	11.050000	.250000
99	11.300000	.250000

L/D=0.8, DB/D=0.51 CIRCULAR ARC BOATTAIL - M = 0.8, NPR = 5.0 ITERATION NO 20

MO = .800 JET PRESSURE RATIO = 5.000 L = .1524 METERS

BOUNDARY LAYER SEPARATION AT X/L = 8.5380 BOUNDARY LAYER REATTACHMENT AT X/L = 8.8678

I	X/L	R/L	CP	ML	CF	RDS/L	REFF/L	RVI/L	DELR/L	THETA/L	H
51	7.8975	.5000	-.1851	.8839	.0025	.5000	.5123	.5973	.0123	.0079	1.5565
52	8.0098	.4997	-.3003	.9368	.0026	.4997	.5106	.5965	.0110	.0070	1.5570
53	8.1121	.4952	-.4010	.9840	.0028	.4952	.5055	.5928	.0102	.0065	1.5686
54	8.2046	.4851	-.4009	.9840	.0027	.4851	.4959	.5852	.0108	.0068	1.5752
55	8.2882	.4702	-.3085	.9407	.0025	.4702	.4829	.5747	.0127	.0079	1.5757
56	8.3637	.4520	-.1836	.8852	.0023	.4520	.4678	.5629	.0158	.0096	1.5857
57	8.4322	.4322	-.0646	.8292	.0020	.4322	.4522	.5514	.0200	.0119	1.6139
58	8.4952	.4112	.0412	.7814	.0017	.4112	.4370	.5410	.0260	.0146	1.6645
59	8.5544	.3870	.1072	.7516	0.0000	.3895	.4233	.5315	.0323	.0174	1.7148
60	8.6118	.3619	.1225	.7447	0.0000	.3746	.4115	.5283	.0364	.0191	1.7258
61	8.6699	.3321	.1130	.7490	0.0000	.3597	.4001	.5274	.0398	.0205	1.7117
62	8.7316	.2973	.1023	.7538	0.0000	.3440	.3886	.5316	.0445	.0226	1.6987
63	8.8000	.2550	.1663	.7248	0.0000	.3235	.3745	.5500	.0539	.0295	1.7686
64	8.8786	.2534	.2570	.6834	0.0000	.2714	.3576	.5358	.0806		
65	8.9704	.2516	.2503	.6865	0.0000	.2895	.3451	.5112	.0529		
66	9.0788	.2500	.1904	.7139	0.0000	.3036	.3346	.5043	.0281		
67	9.2089	.2500	.1378	.7377	0.0000	.3119	.3253	.4996	.0125		
68	9.3679	.2500	.1112	.7498	0.0000	.3079	.3147	.4936	.0070		
69	9.5666	.2500	.1033	.7534	0.0000	.2967	.3027	.4843	.0033		
70	9.8222	.2500	.0839	.7621	0.0000	.2902	.2920	.4777	-.0014		
71	10.1629	.2500	.0568	.7744	0.0000	.2866	.2833	.4724	-.0071		
72	10.6399	.2500	.0326	.7853	0.0000	.2873	.2769	.4700	-.0126		
73	11.3554	.2500	.0170	.7923	0.0000	.2878	.2712	.4678	-.0183		
74	12.5479	.2500	.0080	.7964	0.0000	.2881	.2663	.4773	-.0250		
75	14.9329	.2500	.0024	.7989	0.0000	.2882	.2635	.4826	-.0268		
76	22.0880	.2500	.0003	.7999	0.0000	.2883	.2635	.4826	-.0268		

DRAG COEFFICIENTS (REFERENCE AREA = .018241 SQ METERS)

ITERATION	CDP,AFT	CDF,AFT	CDT,AFT	CDP,BOD	CDF,BOD	CDT,BOD
1	.0123	.0066	.0190	.0352	.0845	.1197
2	.0126	.0068	.0194	.0256	.0850	.1106
3	.0090	.0068	.0158	.0174	.0851	.1025
4	.0033	.0067	.0100	.0091	.0850	.0941
5	-.0020	.0066	.0045	.0021	.0849	.0870
6	-.0011	.0065	.0054	.0019	.0848	.0867
7	.0063	.0065	.0128	.0085	.0847	.0932
8	.0164	.0065	.0229	.0181	.0847	.1028
9	.0259	.0065	.0325	.0271	.0847	.1119
10	.0283	.0066	.0349	.0292	.0848	.1140
11	.0255	.0066	.0321	.0261	.0848	.1109
12	.0228	.0066	.0293	.0231	.0848	.1079
13	.0221	.0066	.0287	.0222	.0848	.1070
14	.0219	.0066	.0285	.0218	.0848	.1066
15	.0218	.0066	.0284	.0216	.0848	.1064
16	.0221	.0066	.0286	.0217	.0848	.1065
17	.0223	.0066	.0288	.0218	.0848	.1066
18	.0226	.0066	.0291	.0220	.0848	.1068
19	.0227	.0066	.0292	.0221	.0848	.1069
20	.0229	.0056	.0285	.0223	.0838	.1061

RAXBOD CONVERGENCE HISTORY FOR INVISCID RELAXATION SOLUTION

FOR CONVERGENCE, RPAVG MUST BE LESS THAN .17E-03 IN 40 RELAXATION CYCLES

ITERATION	RPMAX	RPAVG	CONVERGED?
1	.52E+00	.12E-01	* NO
2	.22E+00	.56E-02	* NO
3	.13E+00	.33E-02	* NO
4	.85E-01	.21E-02	* NO
5	.61E-01	.14E-02	* NO
6	.46E-01	.11E-02	* NO
7	.35E-01	.85E-03	* NO
8	.28E-01	.77E-03	* NO
9	.23E-01	.70E-03	* NO
10	.19E-01	.56E-03	* NO
11	.16E-01	.42E-03	* NO
12	.14E-01	.33E-03	* NO
13	.12E-01	.28E-03	* NO
14	.10E-01	.25E-03	* NO
15	.87E-02	.22E-03	* NO
16	.77E-02	.20E-03	* NO
17	.68E-02	.19E-03	* NO
18	.61E-02	.17E-03	* NO
19	.57E-02	.17E-03	YES
20	.59E-02	.17E-03	YES

FLOW FIELD RESULTS FROM X/L = 8.0000 TO X/L = 9.4000 AND TO R/L = .7500

NOTE: POINTS DENOTED BY (BL) ARE BOUNDARY-LAYER PROPERTIES CALCULATED FROM POWER-LAW PROFILE;
POINTS DENOTED BY (*) ARE INVISCID JET PROPERTIES CALCULATED FROM 1-D ISENTROPIC THEORY;
POINTS DENOTED BY (**) ARE MIXING LAYER PROPERTIES FROM LAST X/L-STATION & SHOULD NOT BE USED.

	I	X/L	R/L	P/PINF	T/TINF	U/UINF	V/UINF	M	GAMMA	PT/PTINF
BL	1	7.8975	.5000	.9171	1.1280	0.0000	0.0000	0.0000	1.4000	.6016
BL	2	7.8975	.5104	.9171	1.0387	.8354	-.0060	.6558	1.4000	.8030
BL	3	7.8975	.5208	.9179	1.0231	.9051	-.0078	.7159	1.4000	.8473
BL	4	7.8975	.5312	.9190	1.0128	.9486	-.0087	.7541	1.4000	.8790
BL	5	7.8975	.5417	.9201	1.0049	.9807	-.0095	.7827	1.4000	.9045
BL	6	7.8975	.5521	.9212	.9984	1.0063	-.0103	.8057	1.4000	.9264
BL	7	7.8975	.5625	.9222	.9928	1.0277	-.0110	.8252	1.4000	.9459
BL	8	7.8975	.5729	.9233	.9879	1.0462	-.0118	.8422	1.4000	.9636
BL	9	7.8975	.5833	.9244	.9835	1.0625	-.0125	.8572	1.4000	.9799
BL	10	7.8975	.5937	.9254	.9795	1.0771	-.0131	.8707	1.4000	.9950
	11	7.8975	.6042	.9264	.9784	1.0810	-.0135	.8744	1.4000	1.0000
	12	7.8975	.6146	.9274	.9787	1.0799	-.0139	.8734	1.4000	1.0000
	13	7.8975	.6250	.9284	.9790	1.0788	-.0143	.8724	1.4000	1.0000
	14	7.8975	.6354	.9294	.9793	1.0778	-.0146	.8714	1.4000	1.0000
	15	7.8975	.6458	.9304	.9796	1.0767	-.0150	.8703	1.4000	1.0000
	16	7.8975	.6562	.9314	.9799	1.0756	-.0154	.8693	1.4000	1.0000
	17	7.8975	.6667	.9323	.9802	1.0745	-.0157	.8684	1.4000	1.0000
	18	7.8975	.6771	.9332	.9805	1.0735	-.0159	.8674	1.4000	1.0000
	19	7.8975	.6875	.9342	.9807	1.0725	-.0161	.8665	1.4000	1.0000
	20	7.8975	.6979	.9351	.9810	1.0715	-.0163	.8656	1.4000	1.0000
	21	7.8975	.7083	.9360	.9813	1.0705	-.0166	.8646	1.4000	1.0000
	22	7.8975	.7187	.9369	.9815	1.0695	-.0168	.8637	1.4000	1.0000
	23	7.8975	.7292	.9378	.9818	1.0685	-.0170	.8628	1.4000	1.0000
	24	7.8975	.7396	.9387	.9821	1.0675	-.0172	.8619	1.4000	1.0000
	25	7.8975	.7500	.9396	.9824	1.0665	-.0174	.8610	1.4000	1.0000
BL	1	8.0098	.4997	.8655	1.1280	0.0000	0.0000	0.0000	1.4000	.5678
BL	2	8.0098	.5101	.8655	1.0248	.8975	-.0255	.7096	1.4000	.7944
BL	3	8.0098	.5205	.8685	1.0096	.9614	-.0276	.7657	1.4000	.8399
BL	4	8.0098	.5309	.8717	.9997	1.0008	-.0288	.8011	1.4000	.8726
BL	5	8.0098	.5414	.8749	.9922	1.0297	-.0297	.8274	1.4000	.8993
BL	6	8.0098	.5518	.8780	.9860	1.0528	-.0304	.8485	1.4000	.9224
BL	7	8.0098	.5622	.8812	.9808	1.0720	-.0310	.8663	1.4000	.9431
BL	8	8.0098	.5727	.8844	.9762	1.0885	-.0315	.8817	1.4000	.9621
BL	9	8.0098	.5831	.8876	.9722	1.1030	-.0320	.8953	1.4000	.9798
BL	10	8.0098	.5935	.8901	.9685	1.1159	-.0324	.9075	1.4000	.9957
	11	8.0098	.6040	.8925	.9680	1.1174	-.0325	.9090	1.4000	1.0000

	I	X/L	R/L	P/PINF	T/TINF	U/UINF	V/UINF	M	GAMMA	PT/PTINF
	12	8.0098	.6144	.8950	.9688	1.1148	-.0325	.9065	1.4000	1.0000
	13	8.0098	.6248	.8974	.9695	1.1121	-.0324	.9040	1.4000	1.0000
	14	8.0098	.6353	.8999	.9703	1.1095	-.0324	.9015	1.4000	1.0000
	15	8.0098	.6457	.9023	.9711	1.1068	-.0324	.8989	1.4000	1.0000
	16	8.0098	.6561	.9048	.9718	1.1042	-.0323	.8964	1.4000	1.0000
	17	8.0098	.6666	.9070	.9725	1.1018	-.0323	.8942	1.4000	1.0000
	18	8.0098	.6770	.9089	.9731	1.0997	-.0322	.8922	1.4000	1.0000
	19	8.0098	.6874	.9108	.9737	1.0976	-.0321	.8903	1.4000	1.0000
	20	8.0098	.6978	.9127	.9742	1.0955	-.0320	.8883	1.4000	1.0000
	21	8.0098	.7083	.9146	.9748	1.0935	-.0320	.8864	1.4000	1.0000
	22	8.0098	.7187	.9165	.9754	1.0914	-.0319	.8844	1.4000	1.0000
	23	8.0098	.7291	.9185	.9760	1.0895	-.0318	.8825	1.4000	1.0000
	24	8.0098	.7396	.9204	.9766	1.0872	-.0317	.8805	1.4000	1.0000
	25	8.0098	.7500	.9221	.9771	1.0853	-.0316	.8787	1.4000	1.0000
BL	1	8.1121	.4952	.8204	1.1280	0.0000	0.0000	0.0000	1.4000	.5382
BL	2	8.1121	.5058	.8206	1.0135	.9431	-.0718	.7516	1.4000	.7830
BL	3	8.1121	.5165	.8259	.9986	1.0028	-.0748	.8051	1.4000	.8300
BL	4	8.1121	.5271	.8312	.9889	1.0395	-.0759	.8385	1.4000	.8641
BL	5	8.1121	.5377	.8365	.9817	1.0664	-.0762	.8632	1.4000	.8923
BL	6	8.1121	.5483	.8416	.9758	1.0877	-.0760	.8831	1.4000	.9171
BL	7	8.1121	.5589	.8471	.9708	1.1055	-.0755	.8997	1.4000	.9396
BL	8	8.1121	.5695	.8524	.9665	1.1208	-.0747	.9141	1.4000	.9604
BL	9	8.1121	.5801	.8575	.9626	1.1342	-.0738	.9268	1.4000	.9797
BL	10	8.1121	.5908	.8614	.9592	1.1462	-.0733	.9382	1.4000	.9968
	11	8.1121	.6014	.8654	.9595	1.1450	-.0720	.9370	1.4000	1.0000
	12	8.1121	.6120	.8693	.9608	1.1408	-.0705	.9329	1.4000	1.0000
	13	8.1121	.6226	.8733	.9620	1.1366	-.0690	.9288	1.4000	1.0000
	14	8.1121	.6332	.8772	.9632	1.1324	-.0675	.9247	1.4000	1.0000
	15	8.1121	.6438	.8812	.9645	1.1282	-.0660	.9206	1.4000	1.0000
	16	8.1121	.6545	.8851	.9657	1.1241	-.0644	.9166	1.4000	1.0000
	17	8.1121	.6651	.8883	.9667	1.1207	-.0633	.9133	1.4000	1.0000
	18	8.1121	.6757	.8912	.9676	1.1176	-.0622	.9104	1.4000	1.0000
	19	8.1121	.6863	.8941	.9685	1.1145	-.0611	.9074	1.4000	1.0000
	20	8.1121	.6969	.8970	.9694	1.1114	-.0600	.9044	1.4000	1.0000
	21	8.1121	.7075	.8999	.9703	1.1083	-.0589	.9014	1.4000	1.0000
	22	8.1121	.7182	.9029	.9712	1.1052	-.0578	.8984	1.4000	1.0000
	23	8.1121	.7288	.9058	.9721	1.1021	-.0567	.8954	1.4000	1.0000
	24	8.1121	.7394	.9087	.9730	1.0990	-.0556	.8924	1.4000	1.0000
	25	8.1121	.7500	.9109	.9737	1.0966	-.0548	.8901	1.4000	1.0000
BL	1	8.2046	.4851	.8204	1.1280	0.0000	0.0000	0.0000	1.4000	.5382
BL	2	8.2046	.4961	.8205	1.0147	.9331	-.1216	.7473	1.4000	.7797

	I	X/L	R/L	P/PINF	T/TINF	U/UINF	V/UINF	M	GAMMA	PT/PTINF
BL	3	8.2046	.5072	.8262	.9996	.9938	-.1262	.8016	1.4000	.8275
BL	4	8.2046	.5182	.8319	.9898	1.0313	-.1276	.8356	1.4000	.8623
BL	5	8.2046	.5293	.8376	.9824	1.0586	-.1274	.8608	1.4000	.8913
BL	6	8.2046	.5403	.8433	.9764	1.0808	-.1265	.8810	1.4000	.9167
BL	7	8.2046	.5513	.8490	.9713	1.0992	-.1249	.8980	1.4000	.9399
BL	8	8.2046	.5624	.8547	.9669	1.1151	-.1228	.9127	1.4000	.9614
BL	9	8.2046	.5734	.8597	.9630	1.1290	-.1209	.9256	1.4000	.9811
BL	10	8.2046	.5844	.8640	.9594	1.1413	-.1194	.9373	1.4000	.9987
	11	8.2046	.5955	.8682	.9604	1.1382	-.1162	.9341	1.4000	1.0000
	12	8.2046	.6065	.8724	.9617	1.1340	-.1129	.9297	1.4000	1.0000
	13	8.2046	.6176	.8767	.9631	1.1297	-.1095	.9253	1.4000	1.0000
	14	8.2046	.6286	.8809	.9644	1.1255	-.1062	.9210	1.4000	1.0000
	15	8.2046	.6396	.8851	.9657	1.1212	-.1029	.9166	1.4000	1.0000
	16	8.2046	.6507	.8890	.9669	1.1173	-.0999	.9126	1.4000	1.0000
	17	8.2046	.6617	.8921	.9679	1.1141	-.0975	.9094	1.4000	1.0000
	18	8.2046	.6727	.8952	.9688	1.1109	-.0951	.9062	1.4000	1.0000
	19	8.2046	.6838	.8983	.9698	1.1077	-.0927	.9031	1.4000	1.0000
	20	8.2046	.6948	.9014	.9708	1.1046	-.0903	.8999	1.4000	1.0000
	21	8.2046	.7059	.9045	.9717	1.1014	-.0879	.8967	1.4000	1.0000
	22	8.2046	.7169	.9076	.9727	1.0982	-.0854	.8935	1.4000	1.0000
	23	8.2046	.7279	.9107	.9736	1.0950	-.0830	.8904	1.4000	1.0000
	24	8.2046	.7390	.9132	.9744	1.0924	-.0811	.8878	1.4000	1.0000
	25	8.2046	.7500	.9155	.9751	1.0901	-.0793	.8855	1.4000	1.0000
BL	1	8.2882	.4702	.8618	1.1280	0.0000	0.0000	0.0000	1.4000	.5653
BL	2	8.2882	.4819	.8618	1.0271	.8734	-.1597	.7009	1.4000	.7848
BL	3	8.2882	.4936	.8657	1.0114	.9400	-.1650	.7592	1.4000	.8321
BL	4	8.2882	.5052	.8701	1.0011	.9815	-.1669	.7961	1.4000	.8667
BL	5	8.2882	.5169	.8745	.9933	1.0123	-.1666	.8235	1.4000	.8954
BL	6	8.2882	.5285	.8788	.9869	1.0371	-.1649	.8457	1.4000	.9205
BL	7	8.2882	.5402	.8832	.9814	1.0579	-.1623	.8643	1.4000	.9432
BL	8	8.2882	.5518	.8875	.9766	1.0759	-.1590	.8804	1.4000	.9643
BL	9	8.2882	.5635	.8912	.9723	1.0917	-.1564	.8947	1.4000	.9832
	10	8.2882	.5751	.8944	.9686	1.1052	-.1538	.9071	1.4000	1.0000
	11	8.2882	.5868	.8976	.9696	1.1023	-.1489	.9038	1.4000	1.0000
	12	8.2882	.5985	.9008	.9706	1.0994	-.1441	.9005	1.4000	1.0000
	13	8.2882	.6101	.9041	.9716	1.0965	-.1392	.8972	1.4000	1.0000
	14	8.2882	.6218	.9073	.9726	1.0936	-.1343	.8939	1.4000	1.0000
	15	8.2882	.6334	.9105	.9736	1.0908	-.1294	.8906	1.4000	1.0000
	16	8.2882	.6451	.9130	.9743	1.0885	-.1258	.8881	1.4000	1.0000
	17	8.2882	.6567	.9154	.9750	1.0862	-.1223	.8856	1.4000	1.0000
	18	8.2882	.6684	.9178	.9758	1.0840	-.1187	.8832	1.4000	1.0000
	19	8.2882	.6801	.9202	.9765	1.0817	-.1152	.8807	1.4000	1.0000

	I	X/L	H/L	P/PINF	T/TINF	U/UINF	V/UINF	M	GAMMA	PT/PTINF
	20	8.2882	.6917	.9226	.9772	1.0794	-.1117	.8783	1.4000	1.0000
	21	8.2882	.7034	.9250	.9780	1.0772	-.1081	.8758	1.4000	1.0000
	22	8.2882	.7150	.9274	.9787	1.0749	-.1046	.8734	1.4000	1.0000
	23	8.2882	.7267	.9294	.9793	1.0730	-.1018	.8714	1.4000	1.0000
	24	8.2882	.7383	.9312	.9798	1.0713	-.0992	.8695	1.4000	1.0000
	25	8.2882	.7500	.9330	.9804	1.0695	-.0967	.8677	1.4000	1.0000
BL	1	8.3637	.4520	.9177	1.1280	0.0000	0.0000	0.0000	1.4000	.6021
BL	2	8.3637	.4644	.9177	1.0435	.7922	-.1800	.6362	1.4000	.7906
BL	3	8.3637	.4769	.9194	1.0272	.8680	-.1835	.7003	1.4000	.8368
BL	4	8.3637	.4893	.9216	1.0163	.9153	-.1866	.7413	1.4000	.8708
BL	5	8.3637	.5017	.9238	1.0078	.9508	-.1866	.7721	1.4000	.8989
BL	6	8.3637	.5141	.9260	1.0008	.9795	-.1848	.7971	1.4000	.9233
BL	7	8.3637	.5265	.9282	.9948	1.0038	-.1818	.8183	1.4000	.9453
BL	8	8.3637	.5389	.9304	.9895	1.0250	-.1779	.8367	1.4000	.9656
BL	9	8.3637	.5514	.9322	.9847	1.0436	-.1751	.8531	1.4000	.9839
	10	8.3637	.5638	.9338	.9806	1.0590	-.1720	.8668	1.4000	1.0000
	11	8.3637	.5762	.9355	.9811	1.0581	-.1661	.8651	1.4000	1.0000
	12	8.3637	.5886	.9372	.9816	1.0571	-.1602	.8634	1.4000	1.0000
	13	8.3637	.6010	.9388	.9821	1.0562	-.1543	.8618	1.4000	1.0000
	14	8.3637	.6134	.9405	.9826	1.0553	-.1485	.8601	1.4000	1.0000
	15	8.3637	.6258	.9420	.9831	1.0543	-.1435	.8586	1.4000	1.0000
	16	8.3637	.6383	.9433	.9835	1.0534	-.1392	.8572	1.4000	1.0000
	17	8.3637	.6507	.9446	.9839	1.0525	-.1349	.8559	1.4000	1.0000
	18	8.3637	.6631	.9460	.9843	1.0515	-.1307	.8545	1.4000	1.0000
	19	8.3637	.6755	.9473	.9846	1.0506	-.1264	.8532	1.4000	1.0000
	20	8.3637	.6879	.9486	.9850	1.0497	-.1222	.8518	1.4000	1.0000
	21	8.3637	.7003	.9500	.9854	1.0487	-.1179	.8505	1.4000	1.0000
	22	8.3637	.7128	.9511	.9858	1.0478	-.1145	.8494	1.4000	1.0000
	23	8.3637	.7252	.9522	.9861	1.0470	-.1114	.8483	1.4000	1.0000
	24	8.3637	.7376	.9532	.9864	1.0461	-.1083	.8472	1.4000	1.0000
	25	8.3637	.7500	.9543	.9867	1.0452	-.1052	.8461	1.4000	1.0000
BL	1	8.4322	.4322	.9711	1.1280	0.0000	0.0000	0.0000	1.4000	.6370
BL	2	8.4322	.4454	.9711	1.0595	.7075	-.1854	.5684	1.4000	.7931
BL	3	8.4322	.4586	.9710	1.0429	.7941	-.1848	.6387	1.4000	.8383
BL	4	8.4322	.4719	.9710	1.0314	.8479	-.1896	.6844	1.4000	.8715
BL	5	8.4322	.4851	.9709	1.0222	.8888	-.1906	.7192	1.4000	.8989
BL	6	8.4322	.4984	.9708	1.0146	.9221	-.1894	.7476	1.4000	.9229
BL	7	8.4322	.5116	.9707	1.0079	.9505	-.1866	.7719	1.4000	.9444
BL	8	8.4322	.5249	.9707	1.0020	.9754	-.1827	.7931	1.4000	.9641
BL	9	8.4322	.5381	.9707	.9966	.9972	-.1803	.8121	1.4000	.9825
BL	10	8.4322	.5513	.9708	.9916	1.0169	-.1774	.8293	1.4000	.9998

	I	X/L	R/L	P/PINF	T/TINF	U/UINF	V/UINF	M	GAMMA	PT/PTINF
	11	8.4322	.5646	.9709	.9916	1.0179	-.1711	.8293	1.4000	1.0000
	12	8.4322	.5778	.9710	.9916	1.0188	-.1648	.8293	1.4000	1.0000
	13	8.4322	.5911	.9710	.9916	1.0198	-.1585	.8292	1.4000	1.0000
	14	8.4322	.6043	.9711	.9917	1.0208	-.1523	.8291	1.4000	1.0000
	15	8.4322	.6176	.9713	.9917	1.0212	-.1476	.8289	1.4000	1.0000
	16	8.4322	.6308	.9715	.9918	1.0215	-.1430	.8287	1.4000	1.0000
	17	8.4322	.6441	.9717	.9918	1.0219	-.1384	.8285	1.4000	1.0000
	18	8.4322	.6573	.9720	.9919	1.0223	-.1338	.8283	1.4000	1.0000
	19	8.4322	.6705	.9722	.9920	1.0227	-.1292	.8281	1.4000	1.0000
	20	8.4322	.6838	.9724	.9920	1.0231	-.1246	.8278	1.4000	1.0000
	21	8.4322	.6970	.9727	.9921	1.0232	-.1208	.8276	1.4000	1.0000
	22	8.4322	.7103	.9730	.9922	1.0233	-.1174	.8273	1.4000	1.0000
	23	8.4322	.7235	.9733	.9923	1.0233	-.1140	.8270	1.4000	1.0000
	24	8.4322	.7368	.9736	.9924	1.0233	-.1106	.8266	1.4000	1.0000
	25	8.4322	.7500	.9739	.9925	1.0234	-.1072	.8263	1.4000	1.0000
BL	1	8.4952	.4112	1.0185	1.1280	0.0000	0.0000	0.0000	1.4000	.6581
BL	2	8.4952	.4254	1.0185	1.0742	.6211	-.1860	.5005	1.4000	.7928
BL	3	8.4952	.4395	1.0180	1.0575	.7215	-.1728	.5771	1.4000	.8369
BL	4	8.4952	.4536	1.0154	1.0455	.7824	-.1796	.6280	1.4000	.8689
BL	5	8.4952	.4677	1.0128	1.0358	.8291	-.1821	.6673	1.4000	.8956
BL	6	8.4952	.4818	1.0102	1.0274	.8676	-.1821	.6997	1.4000	.9190
BL	7	8.4952	.4959	1.0076	1.0200	.9006	-.1803	.7275	1.4000	.9401
BL	8	8.4952	.5100	1.0050	1.0134	.9297	-.1772	.7521	1.4000	.9594
BL	9	8.4952	.5242	1.0036	1.0072	.9553	-.1755	.7742	1.4000	.9785
BL	10	8.4952	.5383	1.0021	1.0016	.9786	-.1731	.7944	1.4000	.9965
	11	8.4952	.5524	1.0006	1.0002	.9850	-.1676	.7994	1.4000	1.0000
	12	8.4952	.5665	.9991	.9998	.9877	-.1614	.8009	1.4000	1.0000
	13	8.4952	.5806	.9977	.9993	.9905	-.1552	.8024	1.4000	1.0000
	14	8.4952	.5947	.9965	.9990	.9927	-.1498	.8035	1.4000	1.0000
	15	8.4952	.6088	.9957	.9988	.9942	-.1451	.8044	1.4000	1.0000
	16	8.4952	.6230	.9949	.9985	.9958	-.1405	.8052	1.4000	1.0000
	17	8.4952	.6371	.9941	.9983	.9973	-.1359	.8060	1.4000	1.0000
	18	8.4952	.6512	.9933	.9981	.9989	-.1312	.8068	1.4000	1.0000
	19	8.4952	.6653	.9924	.9978	1.0004	-.1266	.8076	1.4000	1.0000
	20	8.4952	.6794	.9918	.9977	1.0016	-.1225	.8082	1.4000	1.0000
	21	8.4952	.6935	.9914	.9975	1.0025	-.1190	.8086	1.4000	1.0000
	22	8.4952	.7077	.9910	.9974	1.0033	-.1155	.8090	1.4000	1.0000
	23	8.4952	.7218	.9906	.9973	1.0041	-.1120	.8094	1.4000	1.0000
	24	8.4952	.7359	.9902	.9972	1.0050	-.1085	.8098	1.4000	1.0000
	25	8.4952	.7500	.9898	.9971	1.0058	-.1050	.8102	1.4000	1.0000
	1	8.5544	.3870	*** SEPARATED FLOW ***						

I	X/L	R/L	P/PINF	T/TINF	U/UINF	V/UINF	M	GAMMA	PT/PTINF
2	8.5544	.4021	*** SEPARATED FLOW ***						
3	8.5544	.4172	*** SEPARATED FLOW ***						
4	8.5544	.4323	*** SEPARATED FLOW ***						
5	8.5544	.4475	*** SEPARATED FLOW ***						
6	8.5544	.4626	*** SEPARATED FLOW ***						
7	8.5544	.4777	*** SEPARATED FLOW ***						
8	8.5544	.4928	*** SEPARATED FLOW ***						
9	8.5544	.5080	*** SEPARATED FLOW ***						
10	8.5544	.5231	*** SEPARATED FLOW ***						
11	8.5544	.5382	1.0222	1.0063	.9621	-.1582	.7776	1.4000	1.0000
12	8.5544	.5533	1.0198	1.0056	.9657	-.1529	.7801	1.4000	1.0000
13	8.5544	.5685	1.0173	1.0049	.9694	-.1476	.7826	1.4000	1.0000
14	8.5544	.5836	1.0154	1.0044	.9722	-.1429	.7845	1.4000	1.0000
15	8.5544	.5987	1.0139	1.0040	.9746	-.1385	.7860	1.4000	1.0000
16	8.5544	.6139	1.0124	1.0035	.9769	-.1342	.7875	1.4000	1.0000
17	8.5544	.6290	1.0109	1.0031	.9792	-.1299	.7891	1.4000	1.0000
18	8.5544	.6441	1.0093	1.0027	.9815	-.1256	.7906	1.4000	1.0000
19	8.5544	.6592	1.0078	1.0022	.9838	-.1213	.7921	1.4000	1.0000
20	8.5544	.6744	1.0069	1.0020	.9852	-.1179	.7931	1.4000	1.0000
21	8.5544	.6895	1.0059	1.0017	.9867	-.1144	.7940	1.4000	1.0000
22	8.5544	.7046	1.0050	1.0014	.9881	-.1110	.7950	1.4000	1.0000
23	8.5544	.7197	1.0040	1.0012	.9896	-.1076	.7959	1.4000	1.0000
24	8.5544	.7349	1.0031	1.0009	.9910	-.1042	.7969	1.4000	1.0000
25	8.5544	.7500	1.0022	1.0006	.9925	-.1008	.7978	1.4000	1.0000
1	8.6118	.3619	*** SEPARATED FLOW ***						
2	8.6118	.3780	*** SEPARATED FLOW ***						
3	8.6118	.3942	*** SEPARATED FLOW ***						
4	8.6118	.4104	*** SEPARATED FLOW ***						
5	8.6118	.4266	*** SEPARATED FLOW ***						
6	8.6118	.4427	*** SEPARATED FLOW ***						
7	8.6118	.4589	*** SEPARATED FLOW ***						
8	8.6118	.4751	*** SEPARATED FLOW ***						
9	8.6118	.4912	*** SEPARATED FLOW ***						
10	8.6118	.5074	*** SEPARATED FLOW ***						
11	8.6118	.5236	*** SEPARATED FLOW ***						
12	8.6118	.5398	1.0326	1.0092	.9525	-.1438	.7672	1.4000	1.0000
13	8.6118	.5559	1.0302	1.0085	.9560	-.1391	.7696	1.4000	1.0000
14	8.6118	.5721	1.0281	1.0079	.9590	-.1348	.7717	1.4000	1.0000
15	8.6118	.5883	1.0263	1.0074	.9615	-.1309	.7735	1.4000	1.0000
16	8.6118	.6045	1.0245	1.0069	.9641	-.1269	.7753	1.4000	1.0000
17	8.6118	.6206	1.0227	1.0064	.9666	-.1229	.7771	1.4000	1.0000
18	8.6118	.6368	1.0210	1.0059	.9692	-.1189	.7789	1.4000	1.0000

I	X/L	H/L	P/PINF	T/TINF	U/UINF	V/UINF	M	GAMMA	PT/PTINF
19	8.6118	.6530	1.0194	1.0055	.9715	-.1152	.7805	1.4000	1.0000
20	8.6118	.6691	1.0181	1.0051	.9733	-.1119	.7818	1.4000	1.0000
21	8.6118	.6853	1.0168	1.0048	.9751	-.1086	.7831	1.4000	1.0000
22	8.6118	.7015	1.0155	1.0044	.9769	-.1053	.7843	1.4000	1.0000
23	8.6118	.7177	1.0143	1.0041	.9787	-.1020	.7856	1.4000	1.0000
24	8.6118	.7338	1.0130	1.0037	.9805	-.0988	.7869	1.4000	1.0000
25	8.6118	.7500	1.0120	1.0034	.9818	-.0960	.7879	1.4000	1.0000
1	8.6699	.3521	*** SEPARATED FLOW ***						
2	8.6699	.3496	*** SEPARATED FLOW ***						
3	8.6699	.3670	*** SEPARATED FLOW ***						
4	8.6699	.3844	*** SEPARATED FLOW ***						
5	8.6699	.4018	*** SEPARATED FLOW ***						
6	8.6699	.4192	*** SEPARATED FLOW ***						
7	8.6699	.4366	*** SEPARATED FLOW ***						
8	8.6699	.4540	*** SEPARATED FLOW ***						
9	8.6699	.4714	*** SEPARATED FLOW ***						
10	8.6699	.4888	*** SEPARATED FLOW ***						
11	8.6699	.5062	*** SEPARATED FLOW ***						
12	8.6699	.5237	*** SEPARATED FLOW ***						
13	8.6699	.5411	1.0381	1.0107	.9478	-.1329	.7616	1.4000	1.0000
14	8.6699	.5585	1.0363	1.0102	.9505	-.1285	.7634	1.4000	1.0000
15	8.6699	.5759	1.0346	1.0098	.9529	-.1246	.7651	1.4000	1.0000
16	8.6699	.5933	1.0329	1.0093	.9554	-.1207	.7668	1.4000	1.0000
17	8.6699	.6107	1.0312	1.0088	.9578	-.1168	.7686	1.4000	1.0000
18	8.6699	.6281	1.0295	1.0083	.9603	-.1128	.7703	1.4000	1.0000
19	8.6699	.6455	1.0279	1.0079	.9624	-.1093	.7719	1.4000	1.0000
20	8.6699	.6629	1.0265	1.0075	.9644	-.1061	.7733	1.4000	1.0000
21	8.6699	.6804	1.0251	1.0071	.9664	-.1029	.7747	1.4000	1.0000
22	8.6699	.6978	1.0236	1.0067	.9683	-.0996	.7762	1.4000	1.0000
23	8.6699	.7152	1.0222	1.0063	.9703	-.0964	.7776	1.4000	1.0000
24	8.6699	.7326	1.0209	1.0059	.9721	-.0934	.7790	1.4000	1.0000
25	8.6699	.7500	1.0198	1.0056	.9736	-.0908	.7801	1.4000	1.0000
1	8.7316	.2973	*** SEPARATED FLOW ***						
2	8.7316	.3161	*** SEPARATED FLOW ***						
3	8.7316	.3350	*** SEPARATED FLOW ***						
4	8.7316	.3539	*** SEPARATED FLOW ***						
5	8.7316	.3727	*** SEPARATED FLOW ***						
6	8.7316	.3916	*** SEPARATED FLOW ***						
7	8.7316	.4104	*** SEPARATED FLOW ***						
8	8.7316	.4293	*** SEPARATED FLOW ***						
9	8.7316	.4482	*** SEPARATED FLOW ***						

I	X/L	R/L	P/PINF	T/TINF	U/UINF	V/UINF	M	GAMMA	PT/PTINF
10	8.7316	.4670	*** SEPARATED FLOW ***						
11	8.7316	.4859	*** SEPARATED FLOW ***						
12	8.7316	.5048	*** SEPARATED FLOW ***						
13	8.7316	.5236	*** SEPARATED FLOW ***						
14	8.7316	.5425	1.0433	1.0122	.9431	-.1244	.7564	1.4000	1.0000
15	8.7316	.5614	1.0417	1.0117	.9454	-.1201	.7580	1.4000	1.0000
16	8.7316	.5802	1.0400	1.0113	.9478	-.1159	.7597	1.4000	1.0000
17	8.7316	.5991	1.0384	1.0108	.9502	-.1116	.7613	1.4000	1.0000
18	8.7316	.6180	1.0368	1.0104	.9526	-.1073	.7630	1.4000	1.0000
19	8.7316	.6368	1.0352	1.0099	.9548	-.1037	.7646	1.4000	1.0000
20	8.7316	.6557	1.0336	1.0095	.9569	-.1004	.7661	1.4000	1.0000
21	8.7316	.6745	1.0320	1.0091	.9590	-.0971	.7677	1.4000	1.0000
22	8.7316	.6934	1.0305	1.0086	.9612	-.0938	.7693	1.4000	1.0000
23	8.7316	.7123	1.0289	1.0082	.9633	-.0904	.7709	1.4000	1.0000
24	8.7316	.7311	1.0276	1.0078	.9651	-.0877	.7723	1.4000	1.0000
25	8.7316	.7500	1.0262	1.0074	.9668	-.0851	.7736	1.4000	1.0000
1	8.8000	0.0000	2.4859	.4860	.9145	0.0000	1.0500	1.3986	3.2735
2	8.8000	.0104	2.4859	.4860	.9145	0.0000	1.0500	1.3986	3.2735
3	8.8000	.0208	2.4859	.4860	.9145	0.0000	1.0500	1.3986	3.2735
4	8.8000	.0313	2.4859	.4860	.9145	0.0000	1.0500	1.3986	3.2735
5	8.8000	.0417	2.4859	.4860	.9145	0.0000	1.0500	1.3986	3.2735
6	8.8000	.0521	2.4859	.4860	.9145	0.0000	1.0500	1.3986	3.2735
7	8.8000	.0625	2.4859	.4860	.9145	0.0000	1.0500	1.3986	3.2735
8	8.8000	.0729	2.4859	.4860	.9145	0.0000	1.0500	1.3986	3.2735
9	8.8000	.0833	2.4859	.4860	.9145	0.0000	1.0500	1.3986	3.2735
10	8.8000	.0938	2.4859	.4860	.9145	0.0000	1.0500	1.3986	3.2735
11	8.8000	.1042	2.4859	.4860	.9145	0.0000	1.0500	1.3986	3.2735
12	8.8000	.1146	2.4859	.4860	.9145	0.0000	1.0500	1.3986	3.2735
13	8.8000	.1250	2.4859	.4860	.9145	0.0000	1.0500	1.3986	3.2735
14	8.8000	.1354	2.4859	.4860	.9145	0.0000	1.0500	1.3986	3.2735
15	8.8000	.1458	2.4859	.4860	.9145	0.0000	1.0500	1.3986	3.2735
16	8.8000	.1563	2.4859	.4860	.9145	0.0000	1.0500	1.3986	3.2735
17	8.8000	.1667	2.4859	.4860	.9145	0.0000	1.0500	1.3986	3.2735
18	8.8000	.1771	2.4859	.4860	.9145	0.0000	1.0500	1.3986	3.2735
19	8.8000	.1875	2.4859	.4860	.9145	0.0000	1.0500	1.3986	3.2735
20	8.8000	.1979	2.4859	.4860	.9145	0.0000	1.0500	1.3986	3.2735
21	8.8000	.2083	2.4859	.4860	.9145	0.0000	1.0500	1.3986	3.2735
22	8.8000	.2188	2.4859	.4860	.9145	0.0000	1.0500	1.3986	3.2735
23	8.8000	.2292	*** SEPARATED FLOW ***						
24	8.8000	.2396	*** SEPARATED FLOW ***						
25	8.8000	.2500	*** SEPARATED FLOW ***						
26	8.8000	.2708	*** SEPARATED FLOW ***						

I	X/L	H/L	P/PINF	T/TINF	U/UINF	V/UINF	M	GAMMA	PT/PTINF
27	8.8000	.2917	*** SEPARATED FLOW ***						
28	8.8000	.3125	*** SEPARATED FLOW ***						
29	8.8000	.3333	*** SEPARATED FLOW ***						
30	8.8000	.3542	*** SEPARATED FLOW ***						
31	8.8000	.3750	*** SEPARATED FLOW ***						
32	8.8000	.3958	*** SEPARATED FLOW ***						
33	8.8000	.4167	*** SEPARATED FLOW ***						
34	8.8000	.4375	*** SEPARATED FLOW ***						
35	8.8000	.4583	*** SEPARATED FLOW ***						
36	8.8000	.4792	*** SEPARATED FLOW ***						
37	8.8000	.5000	*** SEPARATED FLOW ***						
38	8.8000	.5208	*** SEPARATED FLOW ***						
39	8.8000	.5417	*** SEPARATED FLOW ***						
40	8.8000	.5625	1.0506	1.0142	.9361	-.1122	.7490	1.4000	1.0000
41	8.8000	.5833	1.0482	1.0135	.9395	-.1072	.7514	1.4000	1.0000
42	8.8000	.6042	1.0458	1.0129	.9428	-.1021	.7539	1.4000	1.0000
43	8.8000	.6250	1.0437	1.0123	.9457	-.0981	.7560	1.4000	1.0000
44	8.8000	.6458	1.0416	1.0117	.9484	-.0945	.7581	1.4000	1.0000
45	8.8000	.6667	1.0396	1.0111	.9511	-.0909	.7601	1.4000	1.0000
46	8.8000	.6875	1.0375	1.0106	.9538	-.0874	.7622	1.4000	1.0000
47	8.8000	.7083	1.0356	1.0100	.9562	-.0841	.7641	1.4000	1.0000
48	8.8000	.7292	1.0339	1.0096	.9584	-.0814	.7658	1.4000	1.0000
49	8.8000	.7500	1.0323	1.0091	.9605	-.0787	.7675	1.4000	1.0000
1	8.8802	0.0000	2.4859	.4860	.9145	0.0000	1.0500	1.3986	3.2735
2	8.8802	.0113	2.4451	.4837	.9247	.0034	1.0643	1.3986	3.2726
3	8.8802	.0226	2.3874	.4804	.9380	.0062	1.0833	1.3986	3.2720
4	8.8802	.0339	2.3510	.4781	.9467	.0102	1.0959	1.3986	3.2718
5	8.8802	.0452	2.3248	.4769	.9530	.0121	1.1047	1.3986	3.2699
6	8.8802	.0565	2.2816	.4741	.9635	.0166	1.1200	1.3986	3.2689
7	8.8802	.0678	2.2378	.4716	.9737	.0214	1.1352	1.3986	3.2659
8	8.8802	.0792	2.1781	.4680	.9880	.0288	1.1565	1.3986	3.2619
9	8.8802	.0905	2.1112	.4638	1.0040	.0381	1.1809	1.3986	3.2564
10	8.8802	.1018	2.0343	.4590	1.0225	.0496	1.2093	1.3986	3.2474
11	8.8802	.1131	1.9476	.4533	1.0430	.0640	1.2423	1.3986	3.2348
12	8.8802	.1244	1.8545	.4470	1.0651	.0816	1.2789	1.3986	3.2178
13	8.8802	.1357	1.7544	.4400	1.0888	.1021	1.3195	1.3986	3.1942
14	8.8802	.1470	1.6489	.4323	1.1137	.1262	1.3645	1.3986	3.1641
15	8.8802	.1583	1.5400	.4240	1.1391	.1540	1.4130	1.3986	3.1251
16	8.8802	.1696	1.4307	.4156	1.1630	.1856	1.4623	1.3986	3.0699
17	8.8802	.1809	1.3183	.4084	1.1814	.2189	1.5050	1.3986	2.9666
18	8.8802	.1922	1.2096	.4004	1.2001	.2560	1.5524	1.3986	2.8669
19	8.8802	.2035	1.1038	.3914	1.2195	.2967	1.6057	1.3986	2.7703

I	X/L	H/L	P/PINF	T/TINF	U/UINF	V/UINF	M	GAMMA	PT/PTINF
20	8.8802	.2149	1.0024	.3817	1.2405	.3352	1.6650	1.3986	2.6774
21	8.8802	.2262	.9355	.3742	1.2557	.3626	1.7102	1.3986	2.6175
22	8.8786	.2375	.9645	.4114	1.1340	0.0000	1.4115	1.4006	1.9553
23	8.8786	.2488	.9906	.5316	.5072	-.0003	.5629	1.4002	.8058
24	8.8786	.2601	1.0154	.6581	.1156	-.0028	.1130	1.3998	.6721
25	8.8786	.2714	1.0554	.8437	.1462	-.0069	.1257	1.3992	.7001
26	8.8786	.2913	1.1151	1.1197	.2038	-.0154	.1538	1.3983	.7437
27	8.8786	.3113	1.1151	1.1150	.2819	-.0309	.2133	1.3983	.7551
28	8.8786	.3312	1.1151	1.1082	.3644	-.0529	.2765	1.3983	.7714
29	8.8786	.3512	1.1151	1.0994	.4486	-.0810	.3418	1.3984	.7931
30	8.8786	.3711	1.1151	1.0890	.5330	-.1150	.4079	1.3985	.8203
31	8.8786	.3910	1.1151	1.0772	.6140	-.1281	.4725	1.3985	.8523
32	8.8786	.4110	1.1151	1.0646	.6900	-.1332	.5341	1.3986	.8882
33	8.8786	.4309	1.1135	1.0521	.7582	-.1345	.5903	1.3986	.9246
34	8.8786	.4509	1.1097	1.0406	.8157	-.1329	.6386	1.3986	.9576
35	8.8786	.4708	1.1056	1.0309	.8608	-.1328	.6770	1.3987	.9856
36	8.8786	.4908	1.1012	1.0243	.8907	-.1296	.7028	1.3987	1.0043
37	8.8786	.5107	1.0966	1.0214	.9033	-.1236	.7138	1.3987	1.0100
38	8.8786	.5306	1.0657	1.0184	.9196	-.1039	.7337	1.4000	1.0000
39	8.8786	.5506	1.0624	1.0174	.9239	-.0999	.7371	1.4000	1.0000
40	8.8786	.5705	1.0591	1.0165	.9282	-.0960	.7404	1.4000	1.0000
41	8.8786	.5905	1.0558	1.0156	.9324	-.0920	.7438	1.4000	1.0000
42	8.8786	.6104	1.0532	1.0149	.9357	-.0889	.7464	1.4000	1.0000
43	8.8786	.6303	1.0508	1.0142	.9387	-.0860	.7489	1.4000	1.0000
44	8.8786	.6503	1.0483	1.0136	.9418	-.0830	.7513	1.4000	1.0000
45	8.8786	.6702	1.0459	1.0129	.9449	-.0801	.7538	1.4000	1.0000
46	8.8786	.6902	1.0436	1.0123	.9477	-.0774	.7561	1.4000	1.0000
47	8.8786	.7101	1.0417	1.0117	.9500	-.0751	.7580	1.4000	1.0000
48	8.8786	.7301	1.0399	1.0112	.9523	-.0728	.7598	1.4000	1.0000
49	8.8786	.7500	1.0380	1.0107	.9546	-.0706	.7617	1.4000	1.0000
1	8.9716	0.0000	1.3728	.4099	1.1952	0.0000	1.4943	1.3986	3.0528
2	8.9716	.0121	1.3728	.4100	1.1951	.0189	1.4942	1.3986	3.0524
3	8.9716	.0241	1.3648	.4094	1.1968	.0373	1.4979	1.3986	3.0473
4	8.9716	.0362	1.3459	.4078	1.2015	.0544	1.5076	1.3986	3.0373
5	8.9716	.0482	1.3276	.4062	1.2056	.0749	1.5170	1.3986	3.0271
6	8.9716	.0603	1.3010	.4038	1.2117	.0948	1.5309	1.3986	3.0122
7	8.9716	.0724	1.2681	.4009	1.2194	.1154	1.5484	1.3986	2.9925
8	8.9716	.0844	1.2311	.3975	1.2279	.1372	1.5687	1.3986	2.9696
9	8.9716	.0965	1.1890	.3936	1.2376	.1601	1.5923	1.3986	2.9419
10	8.9716	.1085	1.1429	.3891	1.2482	.1842	1.6190	1.3986	2.9090
11	8.9716	.1206	1.0936	.3843	1.2592	.2103	1.6485	1.3986	2.8715
12	8.9716	.1327	1.0431	.3791	1.2703	.2381	1.6801	1.3986	2.8302

I	X/L	R/L	P/PINF	T/TINF	U/UINF	V/UINF	M	GAMMA	PT/PTINF
13	8.9716	.1447	.9885	.3733	1.2823	.2669	1.7157	1.3986	2.7815
14	8.9716	.1568	.9326	.3672	1.2941	.2976	1.7543	1.3986	2.7284
15	8.9716	.1689	.8754	.3606	1.3064	.3289	1.7958	1.3986	2.6686
16	8.9716	.1809	.8204	.3538	1.3186	.3600	1.8395	1.3986	2.6102
17	8.9716	.1930	.7779	.3493	1.3248	.3834	1.8678	1.3986	2.5432
18	8.9716	.2050	.7743	.3506	1.3215	.3825	1.8596	1.3986	2.5116
19	8.9716	.2171	.8304	.3596	1.3060	.3435	1.8025	1.3986	2.5483
20	8.9716	.2292	.8936	.3685	1.2888	.3043	1.7460	1.3986	2.5928
21	8.9716	.2412	.9426	.3791	1.2752	.2765	1.7054	1.3986	2.6247
22	8.9746	.2533	1.0068	.3763	1.2509	.1866	1.6453	1.4007	2.6370
23	8.9746	.2653	1.0416	.5011	.8490	.2026	.9873	1.4003	1.2746
24	8.9746	.2774	1.0830	.7764	.4228	.0695	.4061	1.3994	.7959
25	8.9746	.2895	1.1111	.9735	.3114	.0065	.2529	1.3988	.7620
26	8.9746	.3016	1.1111	1.0763	.3466	-.0239	.2673	1.3985	.7660
27	8.9746	.3278	1.1111	1.0959	.4118	-.0382	.3155	1.3984	.7809
28	8.9746	.3470	1.1111	1.0940	.4844	-.0473	.3717	1.3984	.8018
29	8.9746	.3662	1.1111	1.0853	.5590	-.0540	.4305	1.3985	.8278
30	8.9746	.3854	1.1111	1.0744	.6317	-.0588	.4889	1.3985	.8582
31	8.9746	.4046	1.1111	1.0628	.7002	-.0625	.5446	1.3986	.8916
32	8.9746	.4238	1.1095	1.0513	.7619	-.0648	.5956	1.3986	.9250
33	8.9746	.4430	1.1062	1.0407	.8151	-.0660	.6402	1.3986	.9559
34	8.9746	.4622	1.1027	1.0316	.8578	-.0660	.6765	1.3987	.9827
35	8.9746	.4814	1.0990	1.0248	.8882	-.0652	.7026	1.3987	1.0021
36	8.9746	.5005	1.0951	1.0218	.9014	-.0634	.7139	1.3987	1.0088
37	8.9704	.5197	1.0693	1.0193	.9177	-.0813	.7301	1.4000	1.0000
38	8.9704	.5389	1.0662	1.0185	.9216	-.0793	.7333	1.4000	1.0000
39	8.9704	.5581	1.0630	1.0176	.9254	-.0774	.7364	1.4000	1.0000
40	8.9704	.5773	1.0599	1.0168	.9292	-.0754	.7396	1.4000	1.0000
41	8.9704	.5965	1.0574	1.0161	.9322	-.0735	.7422	1.4000	1.0000
42	8.9704	.6157	1.0550	1.0154	.9351	-.0717	.7446	1.4000	1.0000
43	8.9704	.6349	1.0526	1.0148	.9380	-.0699	.7470	1.4000	1.0000
44	8.9704	.6541	1.0502	1.0141	.9408	-.0681	.7494	1.4000	1.0000
45	8.9704	.6732	1.0479	1.0135	.9436	-.0663	.7517	1.4000	1.0000
46	8.9704	.6924	1.0461	1.0130	.9458	-.0647	.7535	1.4000	1.0000
47	8.9704	.7116	1.0443	1.0125	.9480	-.0631	.7554	1.4000	1.0000
48	8.9704	.7308	1.0425	1.0120	.9502	-.0616	.7572	1.4000	1.0000
49	8.9704	.7500	1.0406	1.0114	.9523	-.0600	.7591	1.4000	1.0000
1	9.0846	0.0000	.6879	.3365	1.4149	0.0000	1.9526	1.3986	2.4355
2	9.0846	.0127	.6868	.3365	1.4151	.0273	1.9531	1.3986	2.4329
3	9.0846	.0253	.6830	.3359	1.4158	.0543	1.9569	1.3986	2.4277
4	9.0846	.0380	.6771	.3350	1.4168	.0817	1.9625	1.3986	2.4192
5	9.0846	.0506	.6685	.3338	1.4182	.1095	1.9707	1.3986	2.4067

I	X/L	R/L	P/PINF	T/TINF	U/UINF	V/UINF	M	GAMMA	PT/PTINF
6	9.0846	.0633	.6578	.3323	1.4200	.1376	1.9811	1.3986	2.3908
7	9.0846	.0759	.6449	.3304	1.4221	.1660	1.9938	1.3986	2.3714
8	9.0846	.0886	.6300	.3282	1.4245	.1947	2.0089	1.3986	2.3485
9	9.0846	.1012	.6136	.3257	1.4270	.2240	2.0259	1.3986	2.3227
10	9.0846	.1139	.5955	.3230	1.4296	.2539	2.0452	1.3986	2.2933
11	9.0846	.1265	.5757	.3198	1.4325	.2838	2.0669	1.3986	2.2603
12	9.0846	.1392	.5557	.3166	1.4350	.3136	2.0896	1.3986	2.2257
13	9.0846	.1518	.5375	.3136	1.4368	.3419	2.1110	1.3986	2.1932
14	9.0846	.1645	.5286	.3121	1.4361	.3610	2.1217	1.3986	2.1770
15	9.0846	.1771	.5540	.3164	1.4277	.3489	2.0917	1.3986	2.2231
16	9.0846	.1898	.6517	.3315	1.4005	.2805	1.9858	1.3986	2.3791
17	9.0846	.2024	.7689	.3474	1.3685	.2145	1.8812	1.3986	2.5461
18	9.0846	.2151	.8452	.3577	1.3439	.1809	1.8149	1.3986	2.6253
19	9.0846	.2277	.8902	.3650	1.3239	.1679	1.7682	1.3986	2.6409
20	9.0846	.2404	.9283	.3715	1.3058	.1590	1.7276	1.3986	2.6440
21	9.0846	.2530	.9670	.3773	1.2892	.1495	1.6910	1.3986	2.6532
22	9.0838	.2657	.9999	.3699	1.2712	.0839	1.6716	1.4007	2.6917
23	9.0838	.2783	1.0242	.4895	.9661	.1528	1.1162	1.4003	1.4615
24	9.0838	.2910	1.0366	.7047	.6620	.0978	.6406	1.3997	.8962
25	9.0838	.3036	1.0844	.9348	.5032	.0374	.4174	1.3989	.8019
26	9.0838	.3222	1.0844	1.0526	.4982	-.0033	.3879	1.3986	.7891
27	9.0838	.3408	1.0844	1.0757	.5068	-.0219	.4214	1.3985	.8037
28	9.0838	.3594	1.0844	1.0754	.6078	-.0337	.4688	1.3985	.8268
29	9.0838	.3780	1.0844	1.0674	.6711	-.0423	.5198	1.3986	.8551
30	9.0838	.3966	1.0844	1.0569	.7322	-.0486	.5701	1.3986	.8866
31	9.0838	.4152	1.0835	1.0462	.7880	-.0532	.6167	1.3986	.9185
32	9.0838	.4338	1.0817	1.0362	.8364	-.0563	.6577	1.3987	.9485
33	9.0838	.4524	1.0797	1.0275	.8762	-.0584	.6918	1.3987	.9751
34	9.0838	.4710	1.0775	1.0208	.9059	-.0594	.7176	1.3987	.9959
35	9.0838	.4896	1.0753	1.0170	.9222	-.0596	.7317	1.3987	1.0069
36	9.0788	.5082	1.0631	1.0176	.9264	-.0629	.7364	1.4000	1.0000
37	9.0788	.5268	1.0610	1.0171	.9289	-.0618	.7385	1.4000	1.0000
38	9.0788	.5454	1.0589	1.0165	.9314	-.0607	.7407	1.4000	1.0000
39	9.0788	.5640	1.0567	1.0159	.9340	-.0596	.7428	1.4000	1.0000
40	9.0788	.5826	1.0548	1.0154	.9362	-.0585	.7447	1.4000	1.0000
41	9.0788	.6012	1.0531	1.0149	.9383	-.0574	.7465	1.4000	1.0000
42	9.0788	.6198	1.0513	1.0144	.9404	-.0563	.7483	1.4000	1.0000
43	9.0788	.6384	1.0495	1.0139	.9425	-.0553	.7501	1.4000	1.0000
44	9.0788	.6570	1.0477	1.0134	.9447	-.0542	.7519	1.4000	1.0000
45	9.0788	.6756	1.0462	1.0130	.9465	-.0532	.7535	1.4000	1.0000
46	9.0788	.6942	1.0447	1.0126	.9482	-.0522	.7550	1.4000	1.0000
47	9.0788	.7128	1.0432	1.0122	.9499	-.0512	.7565	1.4000	1.0000
48	9.0788	.7314	1.0417	1.0117	.9517	-.0502	.7580	1.4000	1.0000

I	X/L	R/L	P/PINF	T/TINF	U/UINF	V/UINF	M	GAMMA	PT/PTINF
49	9.0788	.7500	1.0402	1.0113	.9534	-.0492	.7595	1.4000	1.0000
1	9.2144	0.0000	.3440	.2760	1.5729	0.0000	2.3967	1.3986	1.7760
2	9.2144	.0130	.3440	.2762	1.5727	.0299	2.3958	1.3986	1.7748
3	9.2144	.0260	.3425	.2757	1.5727	.0593	2.3992	1.3986	1.7717
4	9.2144	.0390	.3402	.2752	1.5727	.0888	2.4035	1.3986	1.7658
5	9.2144	.0520	.3371	.2745	1.5724	.1184	2.4093	1.3986	1.7579
6	9.2144	.0650	.3332	.2735	1.5722	.1481	2.4168	1.3986	1.7477
7	9.2144	.0780	.3285	.2724	1.5719	.1779	2.4257	1.3986	1.7352
8	9.2144	.0910	.3233	.2712	1.5713	.2075	2.4362	1.3986	1.7213
9	9.2144	.1040	.3179	.2699	1.5704	.2364	2.4469	1.3986	1.7067
10	9.2144	.1170	.3134	.2688	1.5689	.2633	2.4562	1.3986	1.6944
11	9.2144	.1300	.3165	.2696	1.5644	.2787	2.4497	1.3986	1.7029
12	9.2144	.1430	.3806	.2846	1.5355	.2184	2.3299	1.3986	1.8642
13	9.2144	.1560	.5792	.3214	1.4552	.0518	2.0562	1.3986	2.2526
14	9.2144	.1690	.6400	.3299	1.4331	.0352	1.9979	1.3986	2.3622
15	9.2144	.1820	.6742	.3347	1.4198	.0388	1.9652	1.3986	2.4150
16	9.2144	.1950	.7227	.3415	1.4013	.0327	1.9200	1.3986	2.4822
17	9.2144	.2079	.7644	.3467	1.3866	.0314	1.8854	1.3986	2.5414
18	9.2144	.2209	.8053	.3523	1.3708	.0302	1.8492	1.3986	2.5863
19	9.2144	.2339	.8457	.3591	1.3512	.0290	1.8052	1.3986	2.6023
20	9.2144	.2469	.8850	.3660	1.3311	.0279	1.7615	1.3986	2.6077
21	9.2144	.2599	.9230	.3722	1.3130	.0268	1.7230	1.3986	2.6166
22	9.2126	.2729	.9593	.3918	1.2255	-.0083	1.5645	1.4006	2.3058
23	9.2126	.2859	.9855	.5032	1.0232	.0854	1.1558	1.4003	1.4756
24	9.2126	.2989	1.0020	.6644	.8282	.0713	.8151	1.3998	1.0171
25	9.2126	.3119	1.0615	.8532	.6778	.0350	.5877	1.3992	.8797
26	9.2126	.3302	1.0615	1.0036	.6235	-.0012	.4971	1.3987	.8243
27	9.2126	.3484	1.0615	1.0468	.6471	-.0172	.5052	1.3986	.8288
28	9.2126	.3667	1.0615	1.0561	.6911	-.0257	.5375	1.3986	.8475
29	9.2126	.3849	1.0615	1.0530	.7412	-.0303	.5773	1.3986	.8727
30	9.2126	.4032	1.0613	1.0450	.7914	-.0329	.6188	1.3986	.9012
31	9.2126	.4214	1.0604	1.0358	.8378	-.0345	.6580	1.3987	.9301
32	9.2126	.4397	1.0595	1.0271	.8782	-.0353	.6926	1.3987	.9575
33	9.2126	.4579	1.0584	1.0197	.9107	-.0355	.7207	1.3987	.9810
34	9.2126	.4762	1.0573	1.0145	.9331	-.0354	.7403	1.3987	.9979
35	9.2126	.4945	1.0561	1.0128	.9399	-.0351	.7463	1.3987	1.0024
36	9.2089	.5127	1.0512	1.0144	.9410	-.0492	.7484	1.4000	1.0000
37	9.2089	.5310	1.0500	1.0140	.9423	-.0483	.7496	1.4000	1.0000
38	9.2089	.5492	1.0489	1.0137	.9437	-.0474	.7508	1.4000	1.0000
39	9.2089	.5675	1.0477	1.0134	.9450	-.0466	.7519	1.4000	1.0000
40	9.2089	.5857	1.0466	1.0131	.9464	-.0458	.7531	1.4000	1.0000
41	9.2089	.6040	1.0455	1.0128	.9477	-.0450	.7542	1.4000	1.0000

I	X/L	H/L	P/PINF	T/TINF	U/UINF	V/UINF	M	GAMMA	PT/PTINF
42	9.2089	.6222	1.0444	1.0125	.9490	-.0443	.7553	1.4000	1.0000
43	9.2089	.6405	1.0432	1.0122	.9503	-.0435	.7564	1.4000	1.0000
44	9.2089	.6587	1.0422	1.0119	.9516	-.0428	.7575	1.4000	1.0000
45	9.2089	.6770	1.0411	1.0116	.9527	-.0421	.7586	1.4000	1.0000
46	9.2089	.6952	1.0401	1.0113	.9539	-.0415	.7596	1.4000	1.0000
47	9.2089	.7135	1.0391	1.0110	.9551	-.0406	.7606	1.4000	1.0000
48	9.2089	.7317	1.0381	1.0107	.9563	-.0401	.7617	1.4000	1.0000
49	9.2089	.7500	1.0370	1.0104	.9575	-.0394	.7627	1.4000	1.0000
1	9.3692	0.0000	.1727	.2266	1.6909	0.0000	2.8429	1.3986	1.2321
2	9.3692	.0128	.1725	.2266	1.6910	.0275	2.8438	1.3986	1.2313
3	9.3692	.0257	.1722	.2265	1.6905	.0549	2.8445	1.3986	1.2298
4	9.3692	.0385	.1715	.2262	1.6900	.0822	2.8476	1.3986	1.2273
5	9.3692	.0513	.1708	.2259	1.6891	.1090	2.8504	1.3986	1.2244
6	9.3692	.0641	.1709	.2261	1.6872	.1337	2.8488	1.3986	1.2242
7	9.3692	.0770	.1937	.2349	1.6685	.1072	2.7616	1.3986	1.3075
8	9.3692	.0898	.4089	.3082	1.4743	-.2091	2.1520	1.3986	1.9821
9	9.3692	.1026	.5022	.3109	1.4713	-.1952	2.1308	1.3986	2.0847
10	9.3692	.1154	.5377	.3155	1.4606	-.1837	2.0977	1.3986	2.1690
11	9.3692	.1283	.5820	.3219	1.4441	-.1789	2.0530	1.3986	2.2569
12	9.3692	.1411	.6195	.3271	1.4307	-.1703	2.0164	1.3986	2.3248
13	9.3692	.1539	.6595	.3328	1.4161	-.1643	1.9779	1.3986	2.3900
14	9.3692	.1668	.6983	.3381	1.4019	-.1582	1.9420	1.3986	2.4483
15	9.3692	.1796	.7361	.3432	1.3885	-.1521	1.9087	1.3986	2.5018
16	9.3692	.1924	.7730	.3481	1.3753	-.1460	1.8765	1.3986	2.5483
17	9.3692	.2052	.8094	.3524	1.3630	-.1403	1.8485	1.3986	2.5977
18	9.3692	.2181	.8450	.3575	1.3494	-.1347	1.8155	1.3986	2.6263
19	9.3692	.2309	.8790	.3637	1.3323	-.1279	1.7764	1.3986	2.6288
20	9.3692	.2437	.9111	.3695	1.3155	-.1214	1.7396	1.3986	2.6265
21	9.3692	.2565	.9418	.3746	1.3010	-.1152	1.7083	1.3986	2.6302
22	9.3722	.2694	.9694	.4186	1.1794	-.0365	1.4555	1.4005	2.0661
23	9.3722	.2822	.9884	.5266	1.0109	-.0262	1.1129	1.4002	1.4048
24	9.3722	.2950	1.0012	.6693	.8526	-.0199	.8322	1.3998	1.0342
25	9.3722	.3079	1.0098	.8283	.7325	-.0201	.6428	1.3993	.9092
26	9.3722	.3263	1.0098	.9816	.6703	-.0253	.5407	1.3988	.8401
27	9.3722	.3447	1.0098	1.0533	.6862	-.0300	.5596	1.3987	.8394
28	9.3722	.3631	1.0098	1.0468	.7240	-.0334	.5657	1.3986	.8555
29	9.3722	.3815	1.0098	1.0462	.7689	-.0357	.6010	1.3986	.8789
30	9.3722	.4000	1.0095	1.0398	.8146	-.0371	.6387	1.3986	.9058
31	9.3722	.4184	1.0089	1.0315	.8576	-.0379	.6750	1.3987	.9335
32	9.3722	.4368	1.0082	1.0232	.8953	-.0382	.7074	1.3987	.9600
33	9.3722	.4552	1.0075	1.0162	.9255	-.0381	.7338	1.3987	.9827
34	9.3722	.4737	1.0067	1.0115	.9454	-.0377	.7515	1.3987	.9982

	I	X/L	R/L	P/PINF	T/TINF	U/UINF	V/UINF	M	GAMMA	PT/PTINF
	35	9.3722	.4921	1.0460	1.0110	.9476	-.0368	.7532	1.3987	.9993
	36	9.3679	.5105	1.0425	1.0120	.9512	-.0414	.7572	1.4000	1.0000
	37	9.3679	.5289	1.0417	1.0118	.9521	-.0403	.7580	1.4000	1.0000
	38	9.3679	.5474	1.0410	1.0115	.9531	-.0392	.7587	1.4000	1.0000
	39	9.3679	.5658	1.0402	1.0113	.9539	-.0383	.7595	1.4000	1.0000
	40	9.3679	.5842	1.0395	1.0111	.9548	-.0375	.7602	1.4000	1.0000
	41	9.3679	.6026	1.0387	1.0109	.9557	-.0367	.7610	1.4000	1.0000
	42	9.3679	.6210	1.0380	1.0107	.9566	-.0359	.7618	1.4000	1.0000
	43	9.3679	.6395	1.0372	1.0105	.9575	-.0351	.7625	1.4000	1.0000
	44	9.3679	.6579	1.0365	1.0103	.9583	-.0345	.7633	1.4000	1.0000
	45	9.3679	.6763	1.0358	1.0101	.9592	-.0339	.7640	1.4000	1.0000
	46	9.3679	.6947	1.0350	1.0099	.9600	-.0333	.7647	1.4000	1.0000
	47	9.3679	.7132	1.0343	1.0097	.9609	-.0327	.7654	1.4000	1.0000
	48	9.3679	.7316	1.0336	1.0095	.9617	-.0321	.7662	1.4000	1.0000
	49	9.3679	.7500	1.0329	1.0093	.9625	-.0315	.7669	1.4000	1.0000
*	1	9.5666	0.0000	1.2988	.4383	1.0994	0.0000	1.3292	1.3986	2.3918
*	2	9.5666	.0124	1.2988	.4383	1.0993	0.0000	1.3292	1.3986	2.3917
*	3	9.5666	.0247	1.2988	.4383	1.0993	0.0000	1.3291	1.3986	2.3915
*	4	9.5666	.0371	1.0176	.4124	1.1756	-.1585	1.4805	1.3986	2.2285
*	5	9.5666	.0494	.6510	.3472	1.3490	-.3126	1.8822	1.3986	2.1575
*	6	9.5666	.0618	.6259	.3355	1.3955	-.2524	1.9593	1.3986	2.2298
*	7	9.5666	.0742	.6711	.3400	1.3832	-.2492	1.9295	1.3986	2.3257
*	8	9.5666	.0865	.6914	.3401	1.3860	-.2328	1.9290	1.3986	2.3948
*	9	9.5666	.0989	.7185	.3427	1.3802	-.2232	1.9118	1.3986	2.4489
*	10	9.5666	.1113	.7442	.3453	1.3742	-.2142	1.8945	1.3986	2.4956
*	11	9.5666	.1236	.7691	.3480	1.3677	-.2057	1.8766	1.3986	2.5355
*	12	9.5666	.1360	.7938	.3509	1.3606	-.1980	1.8580	1.3986	2.5709
*	13	9.5666	.1483	.8182	.3538	1.3534	-.1907	1.8394	1.3986	2.6029
*	14	9.5666	.1607	.8418	.3566	1.3463	-.1834	1.8212	1.3986	2.6311
*	15	9.5666	.1731	.8644	.3593	1.3395	-.1763	1.8042	1.3986	2.6572
*	16	9.5666	.1854	.8863	.3618	1.3330	-.1693	1.7882	1.3986	2.6818
*	17	9.5666	.1978	.9073	.3642	1.3268	-.1623	1.7730	1.3986	2.7047
*	18	9.5666	.2102	.9275	.3681	1.3162	-.1549	1.7484	1.3986	2.6975
*	19	9.5666	.2225	.9465	.3724	1.3042	-.1474	1.7216	1.3986	2.6796
*	20	9.5666	.2349	.9651	.3763	1.2933	-.1404	1.6973	1.3986	2.6652
	21	9.5692	.2472	.9834	.3832	1.2532	-.0633	1.6183	1.4006	2.5037
	22	9.5692	.2596	.9980	.4589	1.1248	-.0706	1.3278	1.4004	1.8360
	23	9.5692	.2720	1.0085	.5587	.9936	-.0579	1.0657	1.4001	1.3507
	24	9.5692	.2843	1.0162	.6792	.8720	-.0490	.8464	1.3997	1.0652
	25	9.5692	.2967	1.0462	.8073	.7764	-.0444	.6917	1.3993	.9449
	26	9.5692	.3150	1.0462	.9552	.7083	-.0442	.5799	1.3989	.8618
	27	9.5692	.3345	1.0462	1.0172	.7129	-.0463	.5657	1.3987	.8526

I	X/L	H/L	P/PINF	T/TINF	U/UINF	V/UINF	M	GAMMA	PT/PTINF
28	9.5692	.3534	1.0462	1.0376	.7431	-.0480	.5858	1.3987	.8644
29	9.5692	.3722	1.0462	1.0410	.7825	-.0491	.6135	1.3986	.8847
30	9.5692	.3911	1.0459	1.0369	.8239	-.0496	.6473	1.3987	.9091
31	9.5692	.4100	1.0452	1.0297	.8641	-.0496	.6811	1.3987	.9351
32	9.5692	.4289	1.0444	1.0220	.9001	-.0492	.7121	1.3987	.9605
33	9.5692	.4478	1.0436	1.0153	.9294	-.0484	.7376	1.3987	.9826
34	9.5692	.4667	1.0428	1.0107	.9488	-.0473	.7546	1.3987	.9976
35	9.5666	.4856	1.0377	1.0106	.9570	-.0335	.7621	1.4000	1.0000
36	9.5666	.5045	1.0369	1.0104	.9579	-.0325	.7628	1.4000	1.0000
37	9.5666	.5233	1.0362	1.0102	.9588	-.0315	.7636	1.4000	1.0000
38	9.5666	.5422	1.0355	1.0100	.9596	-.0306	.7643	1.4000	1.0000
39	9.5666	.5611	1.0348	1.0098	.9604	-.0299	.7649	1.4000	1.0000
40	9.5666	.5800	1.0341	1.0096	.9612	-.0292	.7656	1.4000	1.0000
41	9.5666	.5989	1.0335	1.0095	.9619	-.0285	.7663	1.4000	1.0000
42	9.5666	.6178	1.0328	1.0093	.9627	-.0278	.7669	1.4000	1.0000
43	9.5666	.6367	1.0322	1.0091	.9634	-.0272	.7676	1.4000	1.0000
44	9.5666	.6556	1.0316	1.0089	.9641	-.0266	.7682	1.4000	1.0000
45	9.5666	.6744	1.0310	1.0088	.9648	-.0261	.7688	1.4000	1.0000
46	9.5666	.6933	1.0304	1.0086	.9655	-.0256	.7694	1.4000	1.0000
47	9.5666	.7122	1.0298	1.0084	.9662	-.0251	.7699	1.4000	1.0000
48	9.5666	.7311	1.0293	1.0083	.9668	-.0246	.7705	1.4000	1.0000
49	9.5666	.7500	1.0287	1.0081	.9674	-.0242	.7711	1.4000	1.0000

REFERENCES

1. Bergman, Dave: Effects of Engine Exhaust Flow on Boattail Drag. AIAA Paper 70-132, Jan. 1970.

2. Swanson, R. Charles, Jr.: Numerical Solutions of the Navier-Stokes Equations for Transonic Afterbody Flows. NASA TP-1784, 1980.

3. Diewert, G. S.: Numerical Simulation of Three-Dimensional Boattail Afterbody Flow Fields. AIAA-80-1347, July 1980.

4. Reubush, David E.; and Putnam, Lawrence E.: An Experimental and Analytical Investigation of the Effect on Isolated Boattail Drag of Varying Reynolds Number up to 130×10^6. NASA TN D-8210, 1976.

5. Wilmoth, Richard G.: Computation of Transonic Boattail Flow With Separation. NASA TP-1070, 1977.

6. Putnam, Lawrence E.: DONBOL: A Computer Program for Predicting Axisymmetric Nozzle Afterbody Pressure Distributions and Drag at Subsonic Speeds. NASA TM-78779, 1979.

7. Reshotko, Eli; and Tucker, Maurice: Approximate Calculation of the Compressible Turbulent Boundary Layer With Heat Transfer and Arbitrary Pressure Gradient. NACA TN 4154, 1957.

8. Presz, Walter Michael, Jr.: Turbulent Boundary Layer Separation of Axisymmetric Afterbodies. Ph. D. Thesis, Univ. of Connecticut, 1974.

9. South, Jerry C., Jr.; and Jameson, Antony: Relaxation Solutions for Inviscid Axisymmetric Transonic Flow Over Blunt or Pointed Bodies. AIAA Computational Fluid Dynamics Conference, July 1973, pp. 8-17.

10. Abeyounis, William Kelly: Boundary-Layer Separation on Isolated Boattail Nozzles. NASA TP-1226, 1978.

11. Presz, Walter M., Jr.; King, Ronald W.; and Buteau, John D.: An Improved Analytical Model of the Separation Region on Boattail Nozzles at Subsonic Speeds. NASA CR-3028, 1978.

12. Wilmoth, R. G.; and Dash, S. M.: A Viscous-Inviscid Interaction Model of Jet Entrainment. Computation of Viscous-Inviscid Interactions, AGARD-CP-291, Feb. 1981, pp. 13-1 - 13-15.

13. Dash, Sanford M.; and Pergament, Harold S.: A Computational Model for the Prediction of Jet Entrainment in the Vicinity of Nozzle Boattails (The BOAT Code). NASA CR-3075, 1978.

14. Wilmoth, Richard G.: Viscous-Inviscid Calculations of Jet Entrainment Effects on the Subsonic Flow Over Nozzle Afterbodies. NASA TP-1626, 1980.

15. Dash, S. M.; and Thorpe, R. D.: A New Shock-Capturing/Shock-Fitting Computational Model for Analyzing Supersonic Inviscid Flows (The SCIPPY Code). Rep. No. 366, Aeronaut. Res. Assoc. Princeton, Inc., Nov. 1978.

16. Keller, James D.; and South, Jerry C., Jr.: RAXBOD: A Fortran Program for Inviscid Transonic Flow Over Axisymmetric Bodies. NASA TM X-72831, 1976.

17. Dash, Sanford M.; Pergament, Harold S.; and Thorpe, Roger D.: Computational Models for the Viscous/Inviscid Analysis of Jet Aircraft Exhaust Plumes. NASA CR-3289, 1980.

18. Abbett, Michael: Mach Disk in Underexpanded Exhaust Plumes. AIAA J., vol. 9, no. 3, March 1971, pp. 512-514.

19. User's Manual for the External Drag and Internal Nozzle Performance Deck (Deck XI) - Supersonic Flow Analysis (Applicable to Deck VI). PWA-3465, Suppl. F, Pt. I (Contract No. AF33(615)-3128), Pratt and Whitney Aircraft, Sept. 1, 1968.

20. Peters, C. E.; and Phares, W. J.: An Integral Turbulent Kinetic Energy Analysis of Free Shear Flows. Free Turbulent Shear Flows. Volume I - Conference Proceedings, NASA SP-321, 1973, pp. 577-624.

21. Reubush, David E.: Experimental Study of the Effectiveness of Cylindrical Plume Simulators for Predicting Jet-On Boattail Drag at Mach Numbers up to 1.30. NASA TN D-7795, 1974.

22. Abeyounis, William K.; and Putnam, Lawrence E.: Experimental and Theoretical Study of Flow Fields Surrounding Boattail Nozzles at Subsonic Speeds. NASA TP-1633, 1980.

23. Reubush, David E.; and Runckel, Jack F.: Effect of Fineness Ratio on the Boattail Drag of Circular-Arc Afterbodies Having Closure Ratios of 0.50 With Jet Exhaust at Mach Numbers up to 1.30. NASA TN D-7192, 1973.

24. Mason, Mary L.; and Putnam, Lawrence E.: Pitot Pressure Measurements in Flow Fields Behind Circular-Arc Nozzles With Exhaust Jets at Subsonic Free-Stream Mach Numbers. NASA TM-80169, 1979.

25. Cline, Michael C.; and Wilmoth, Richard G.: Computation of High Reynolds Number Internal/External Flows. AIAA-81-1194, June 1981.

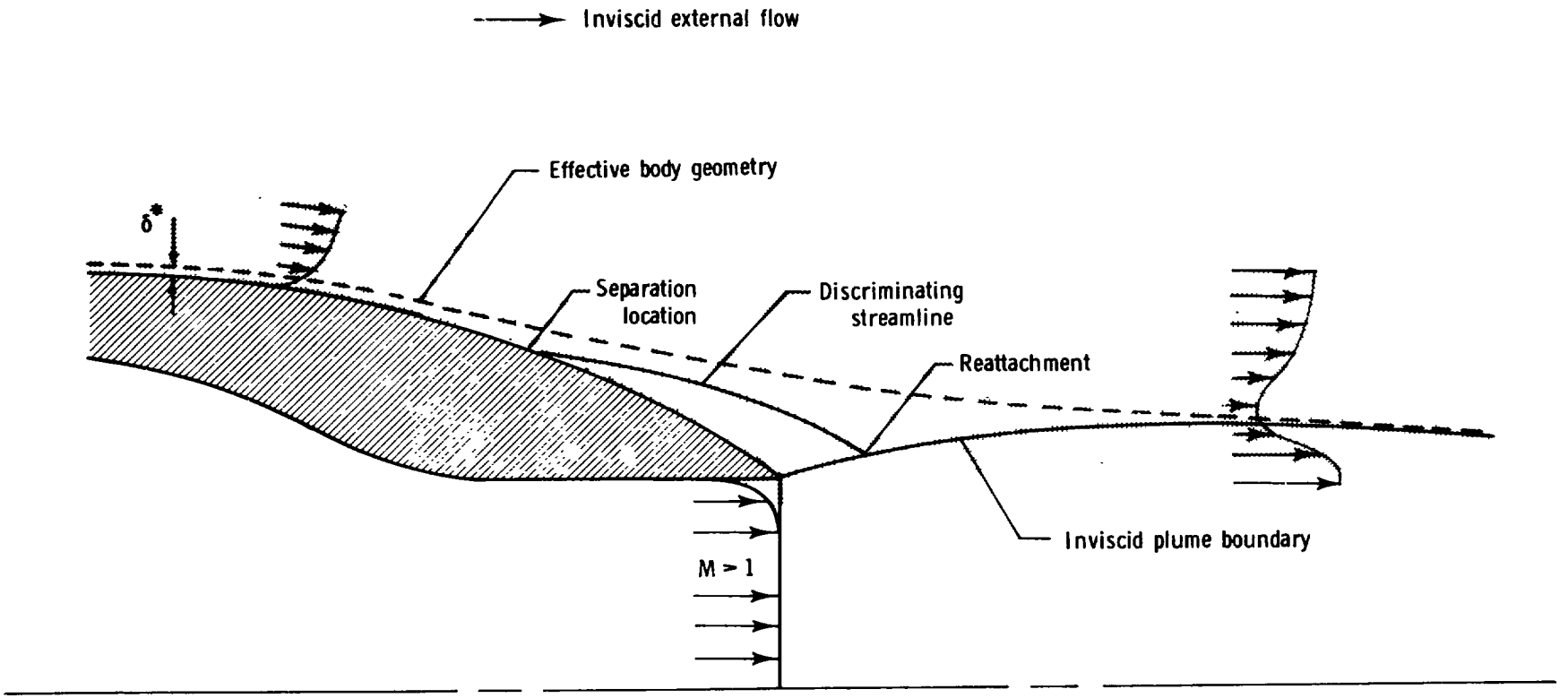

Figure 1.- Schematic of nozzle afterbody flow field.

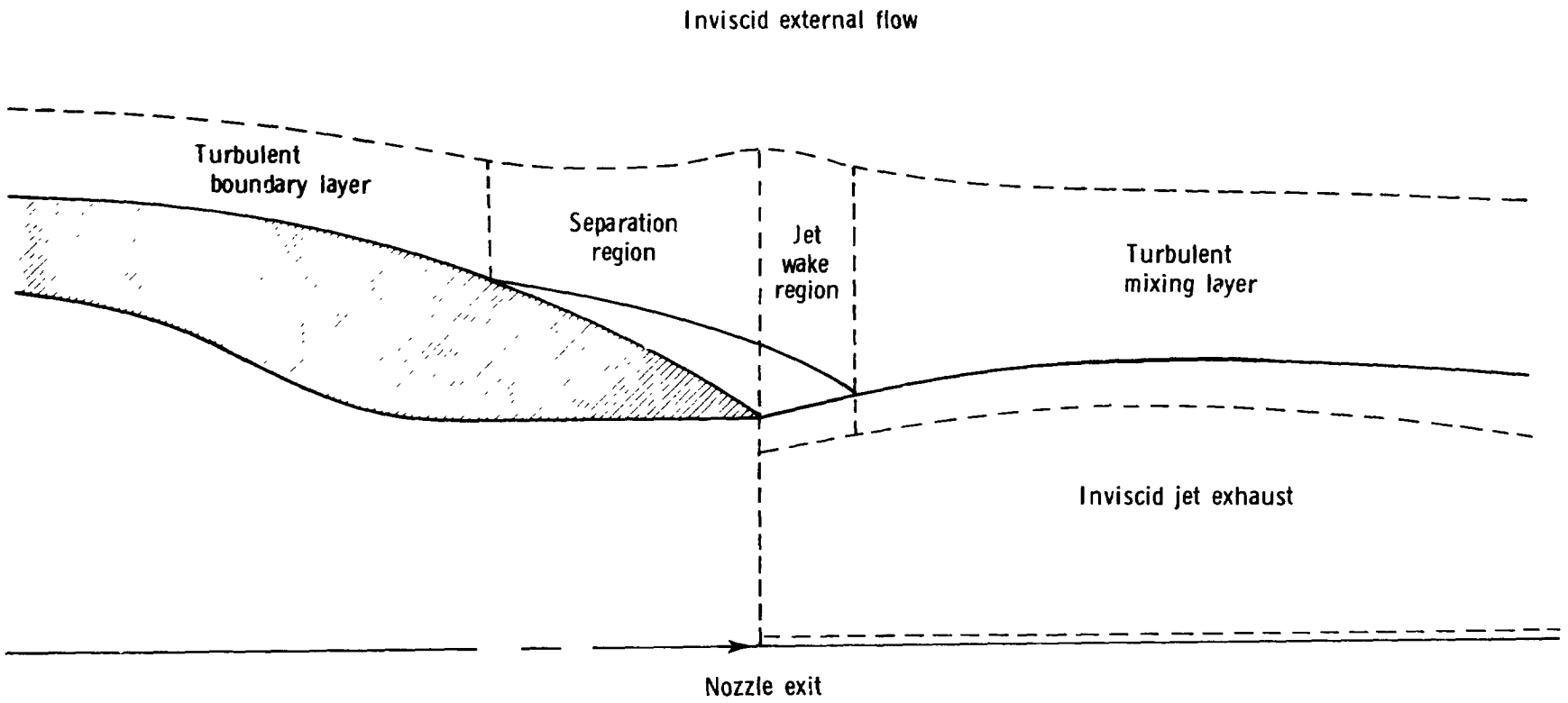

Figure 2.- Patched viscous-inviscid interaction model.

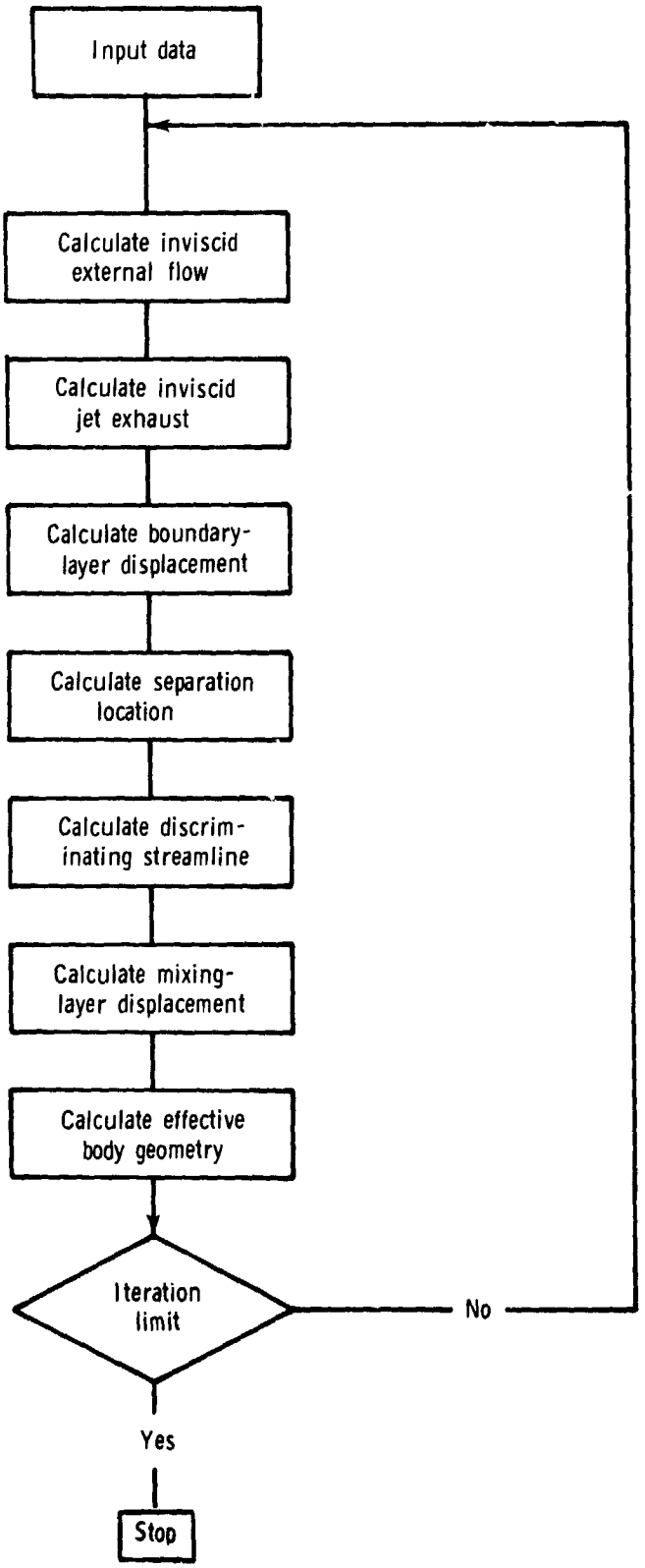

Figure 3.- Viscous-inviscid iteration scheme.

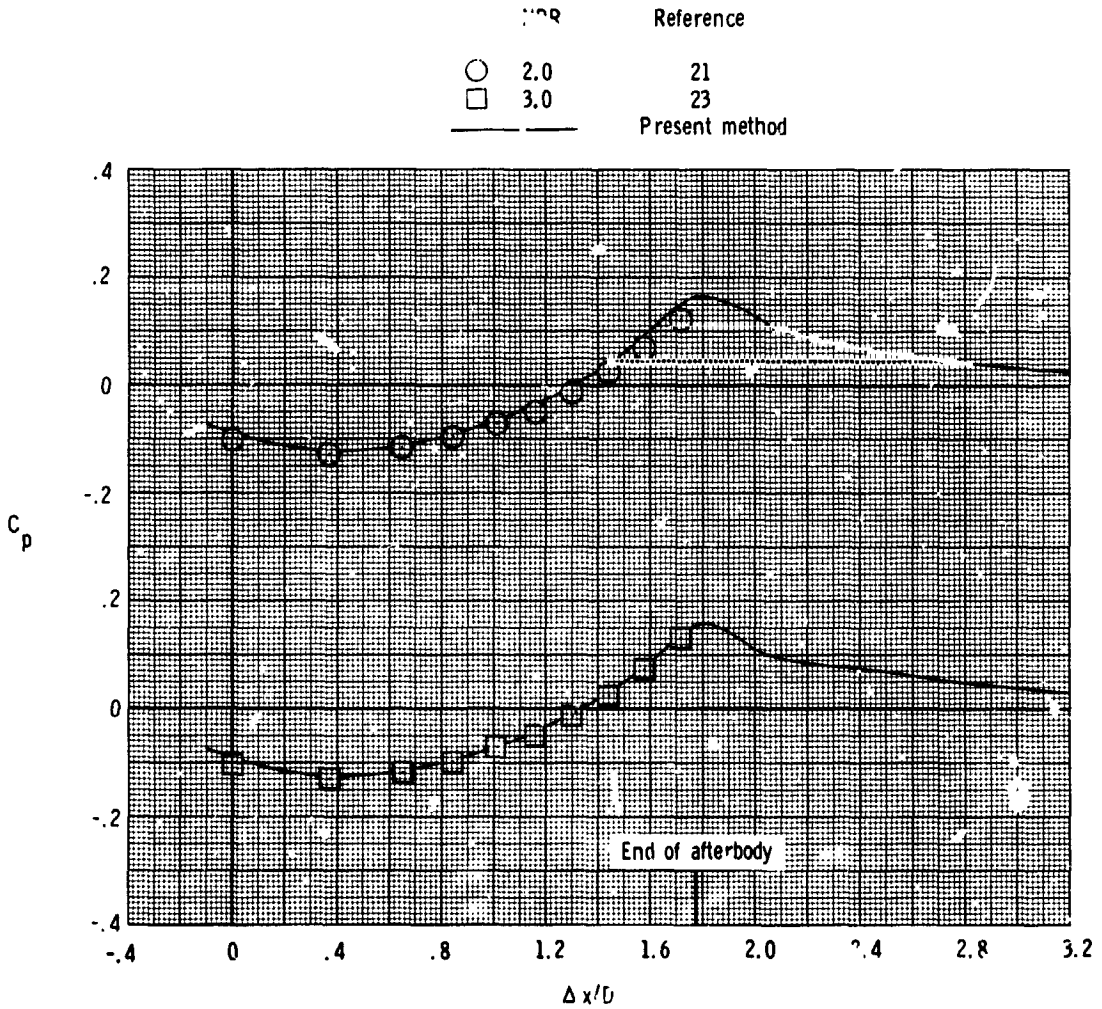

(a) Effect of NPR. $M_\infty = 0.4$.

Figure 4.- Predicted and experimental afterbody pressures for attached flow on a circular-arc boattail nozzle with $\ell/D = 1.768$ and $D_b/D = 0.51$. $\Delta x = x - x_A$.

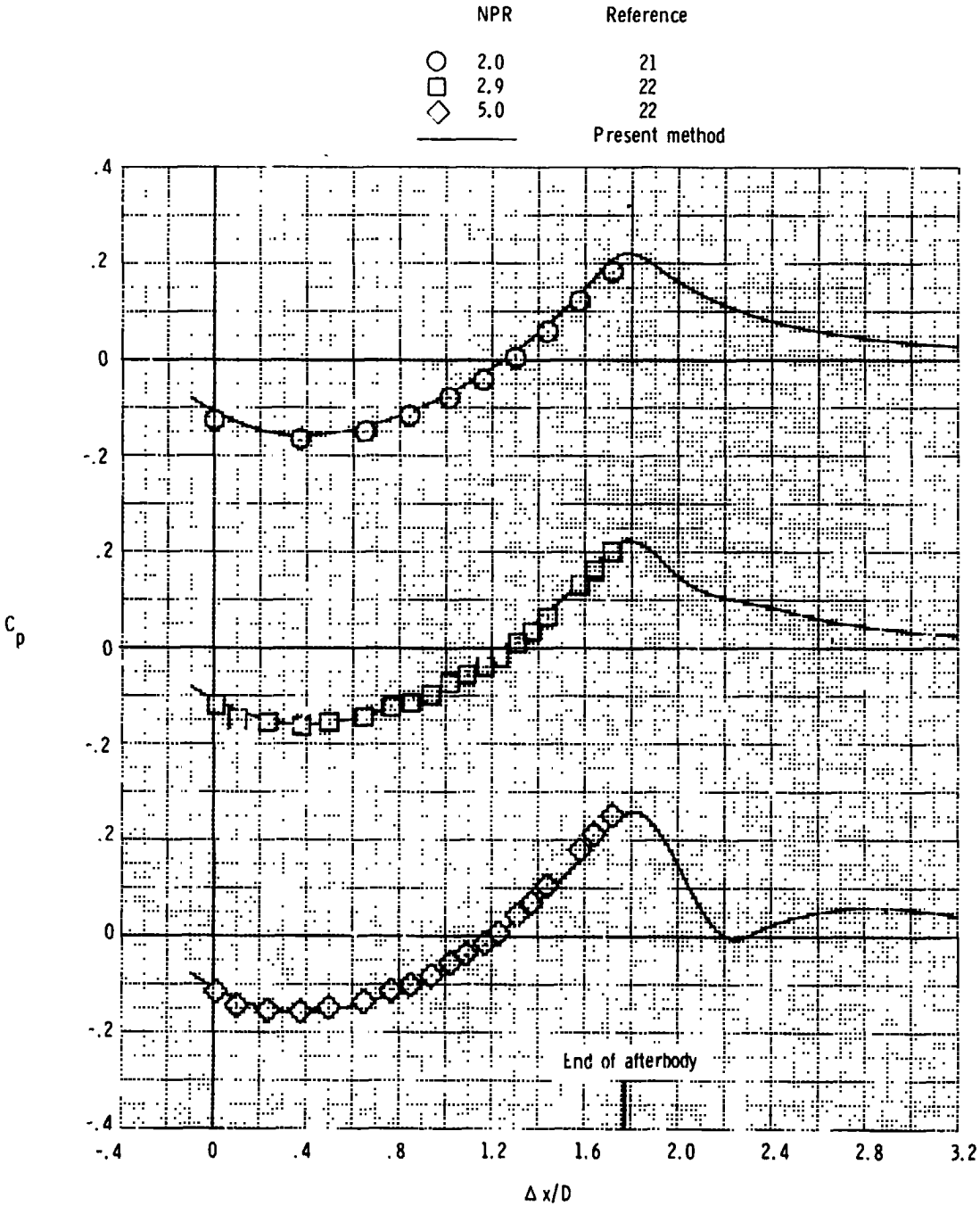

(b) Effect of NPR. $M_\infty = 0.8$.

Figure 4.- Continued.

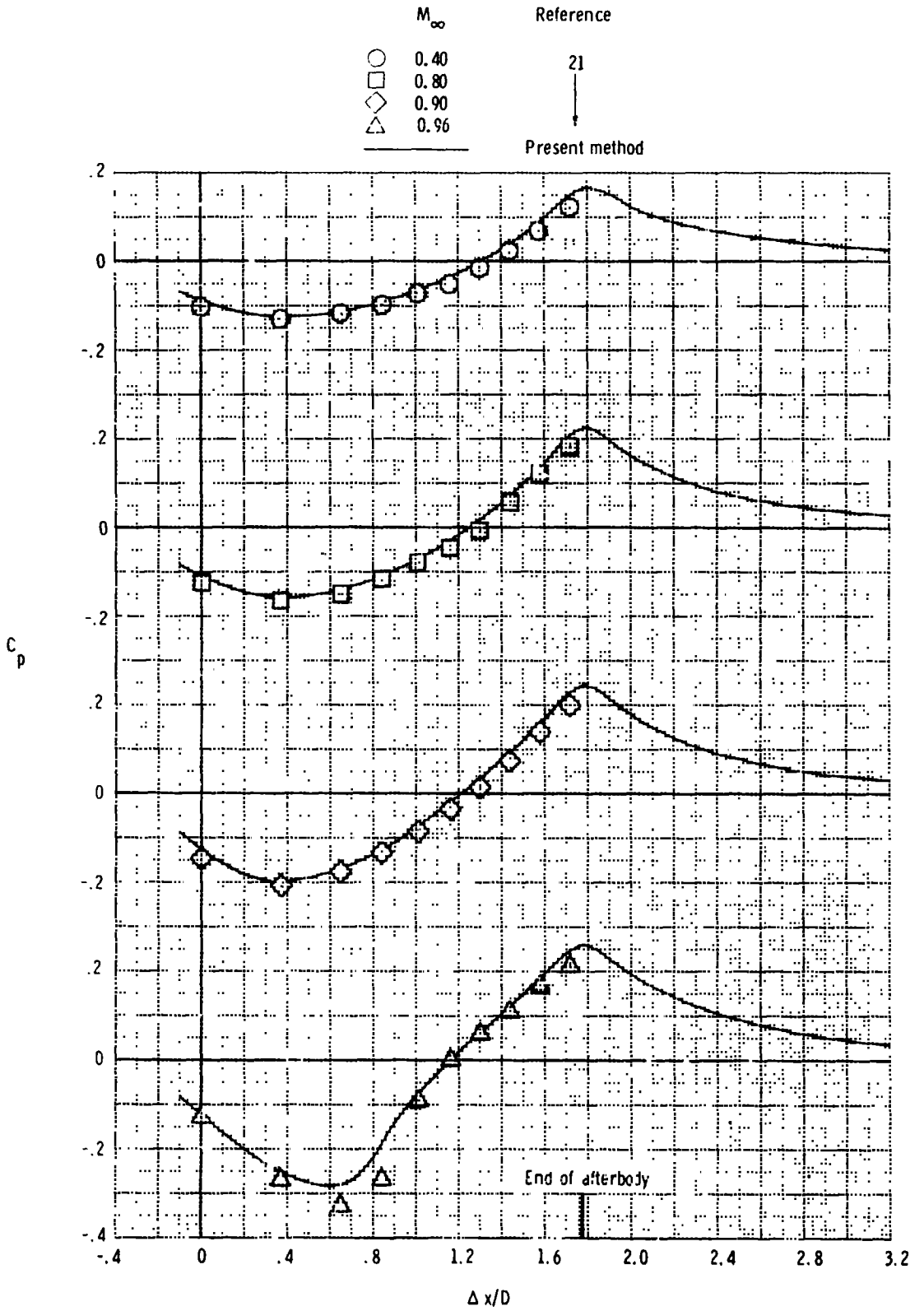

(c) Effect of M_∞. NPR = 2.0.

Figure 4.- Concluded.

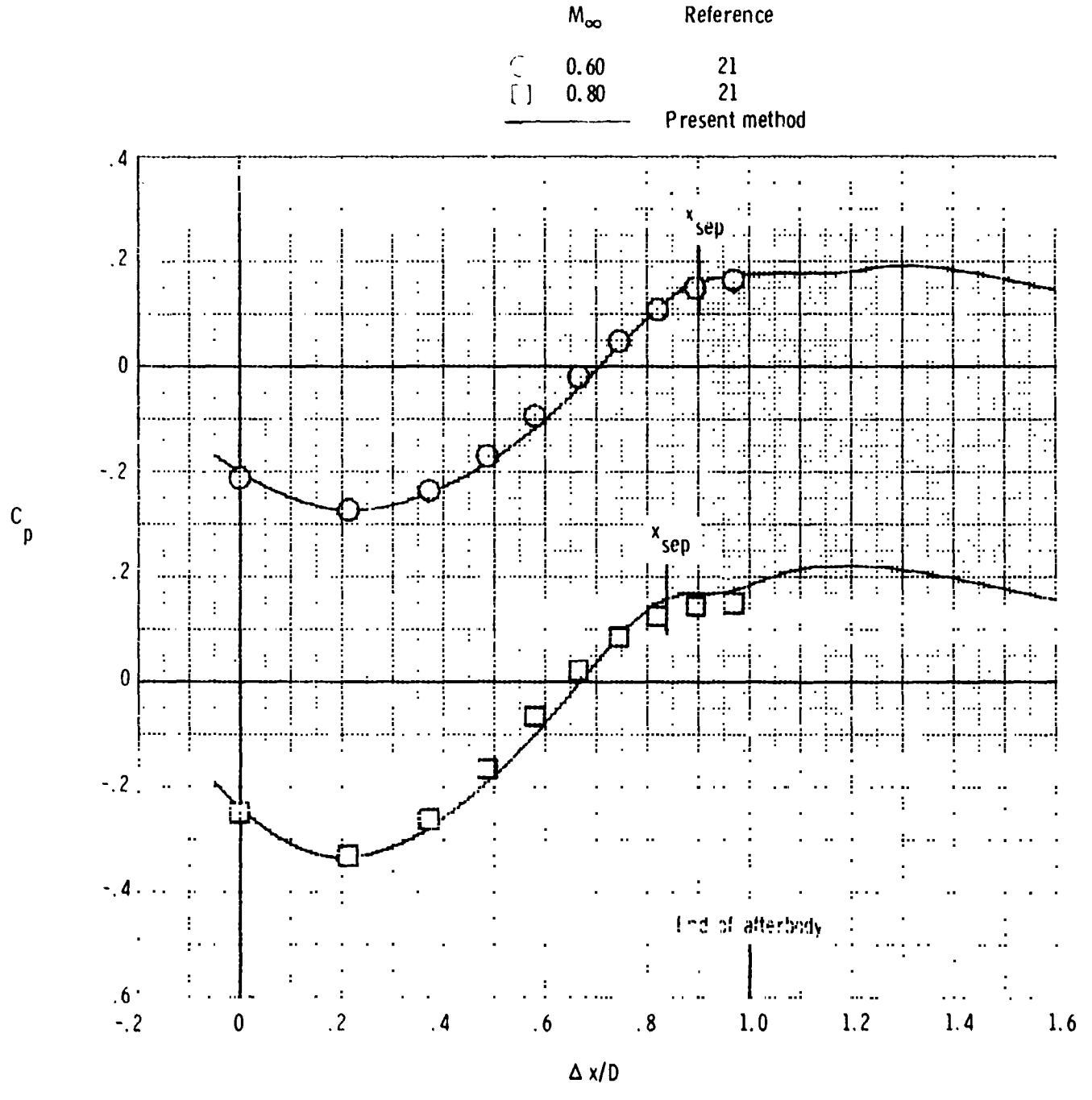

Figure 5.- Predicted and experimental afterbody pressures for separated flow on a circular-arc boattail nozzle with $\ell/D = 1.0$ and $D_b/D = 0.51$. NPR = 2.0. Experimental separation and extrapolated wake model used. $\Delta x = x - x_A$.

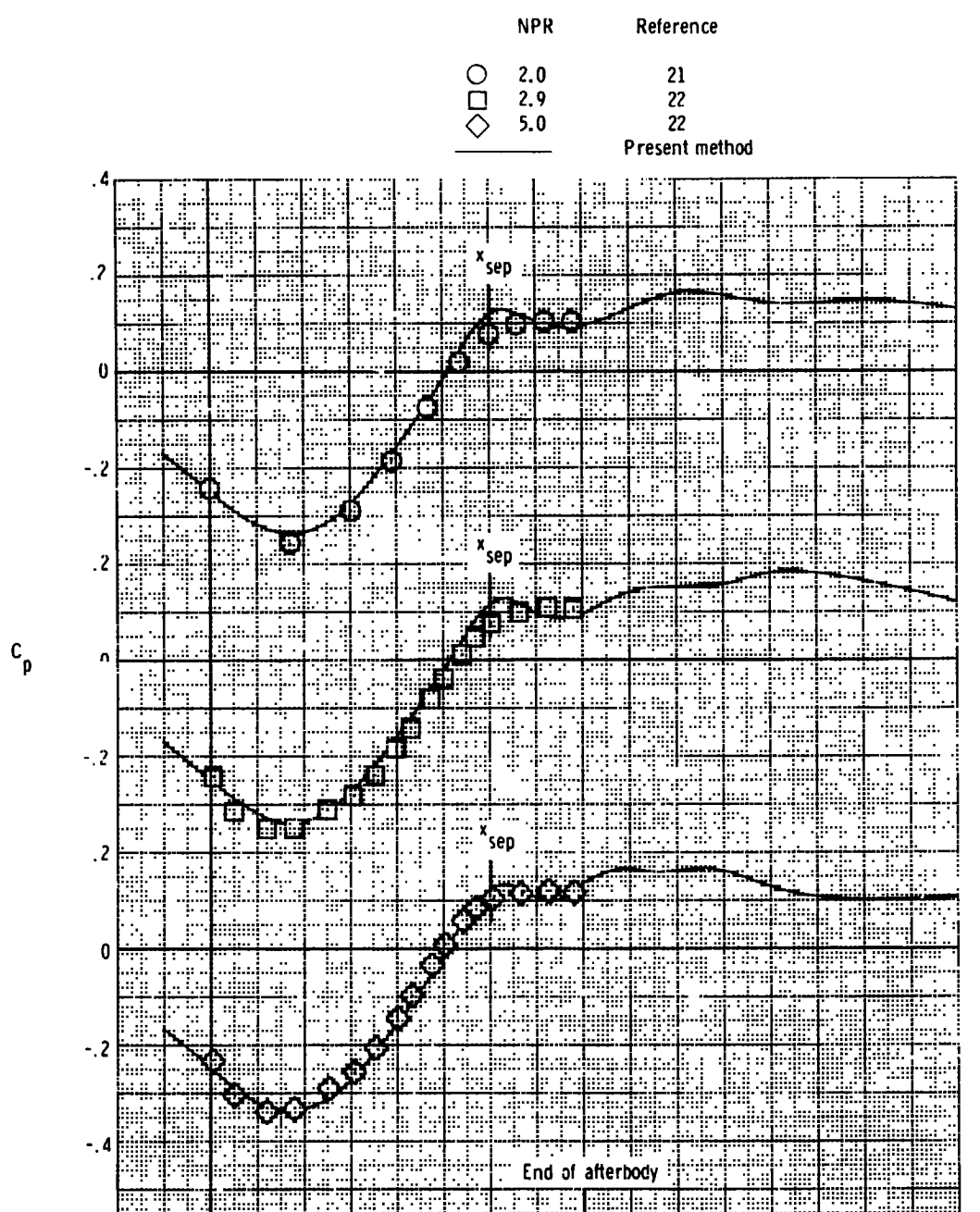

(a) $M_\infty = 0.6$.

Figure 6.- Predicted and experimental afterbody pressures for separated flow on a circular-arc boattail nozzle with $\ell/D = 0.8$ and $D_b/D = 0.51$. Experimental separation location and extrapolated wake model used. $\Delta x = x - x_A$.

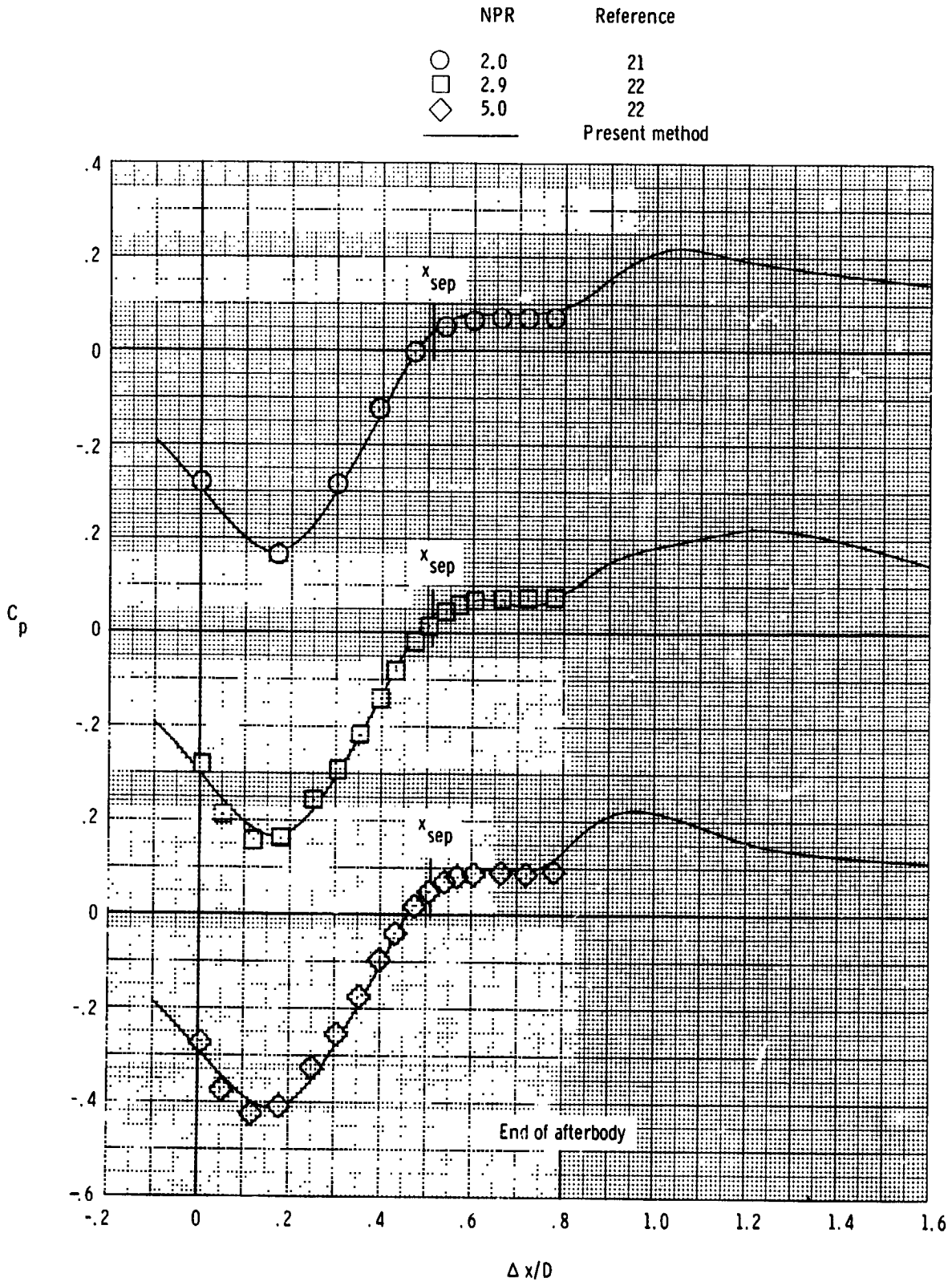

(b) $M_\infty = 0.8$.

Figure 6.- Continued.

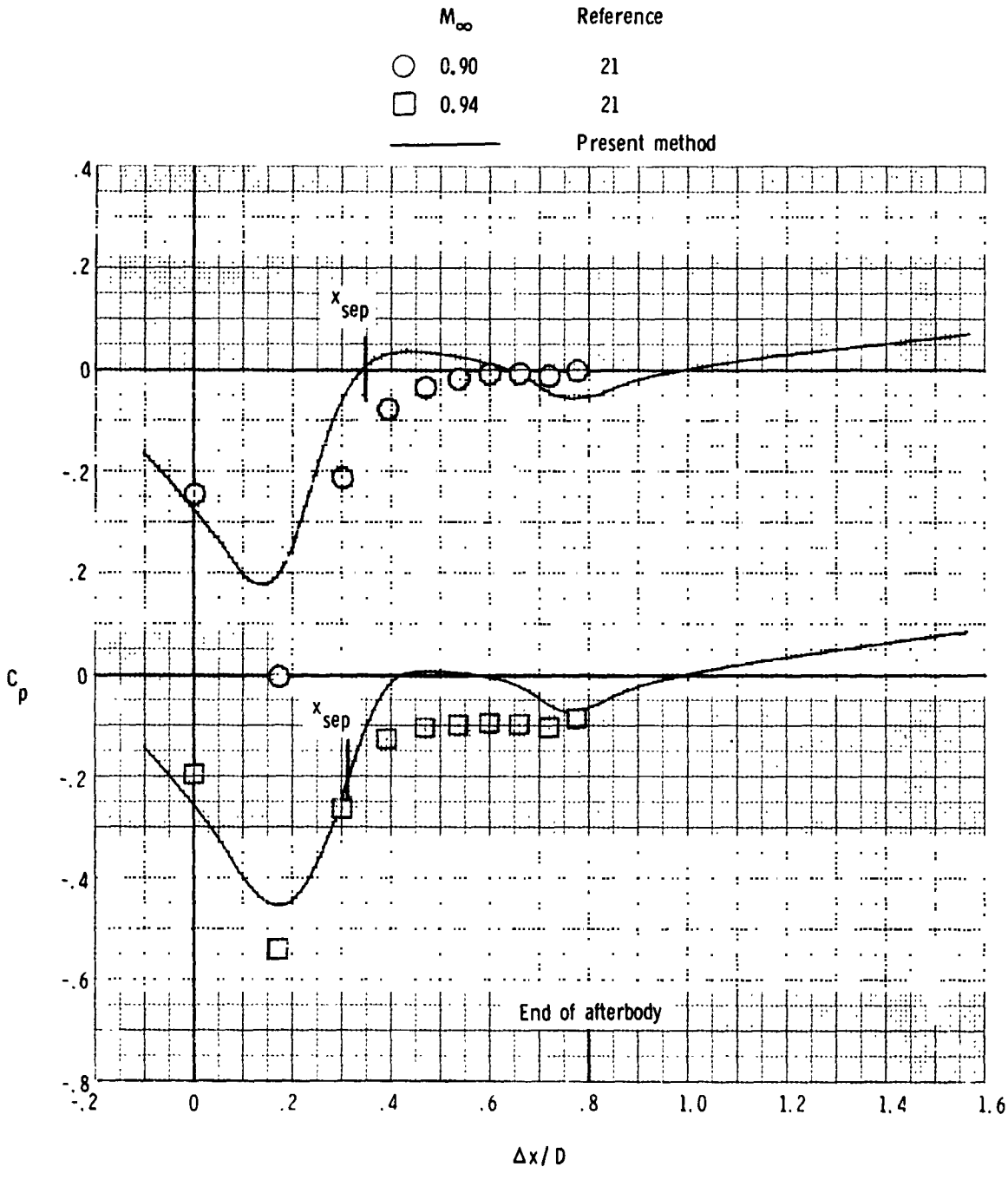

(c) M_∞ = 0.9 and 0.94; NPR = 2.0.

Figure 6.- Concluded.

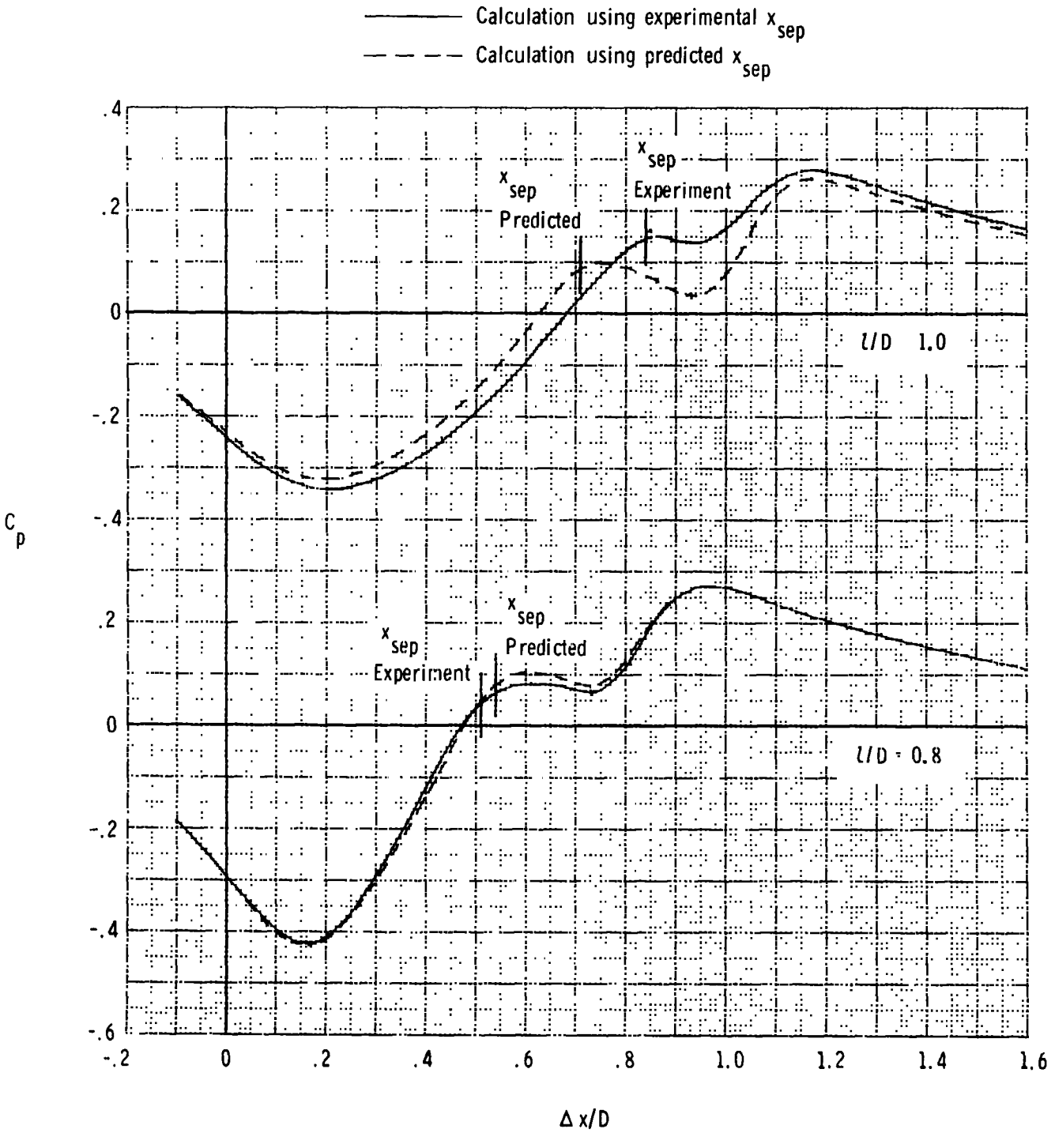

Figure 7.- Effect of separation location prediction on predicted afterbody pressures. Integral wake model used for both calculations. M_∞ = 0.8; NPR = 2.0; $\Delta x = x - x_A$.

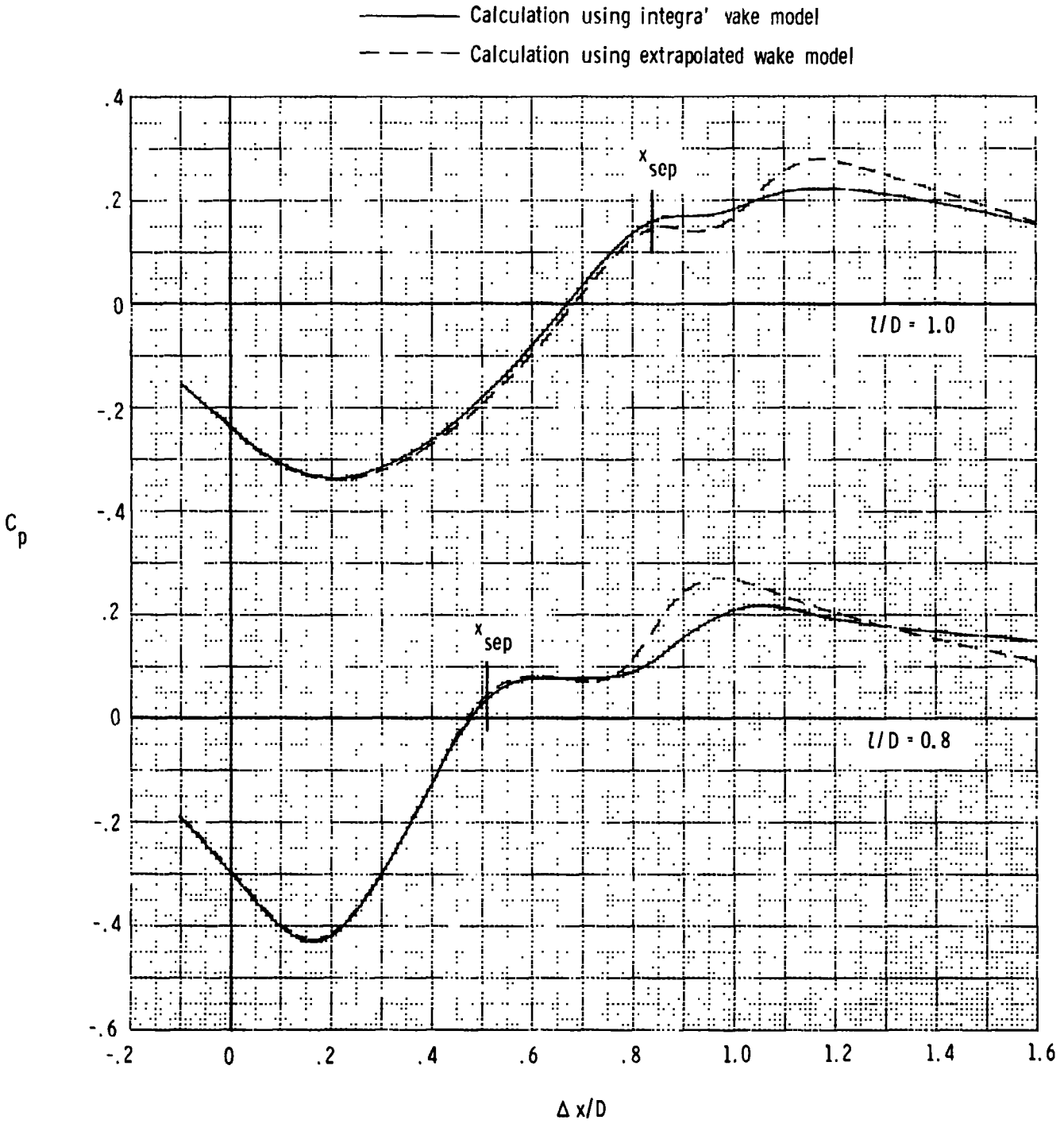

Figure 8.- Effect of jet wake model on predicted afterbody pressures. Experimental x_{sep} used for both calculations. M_∞ = 0.8; NPR = 2.0; $\Delta x = x - x_A$.

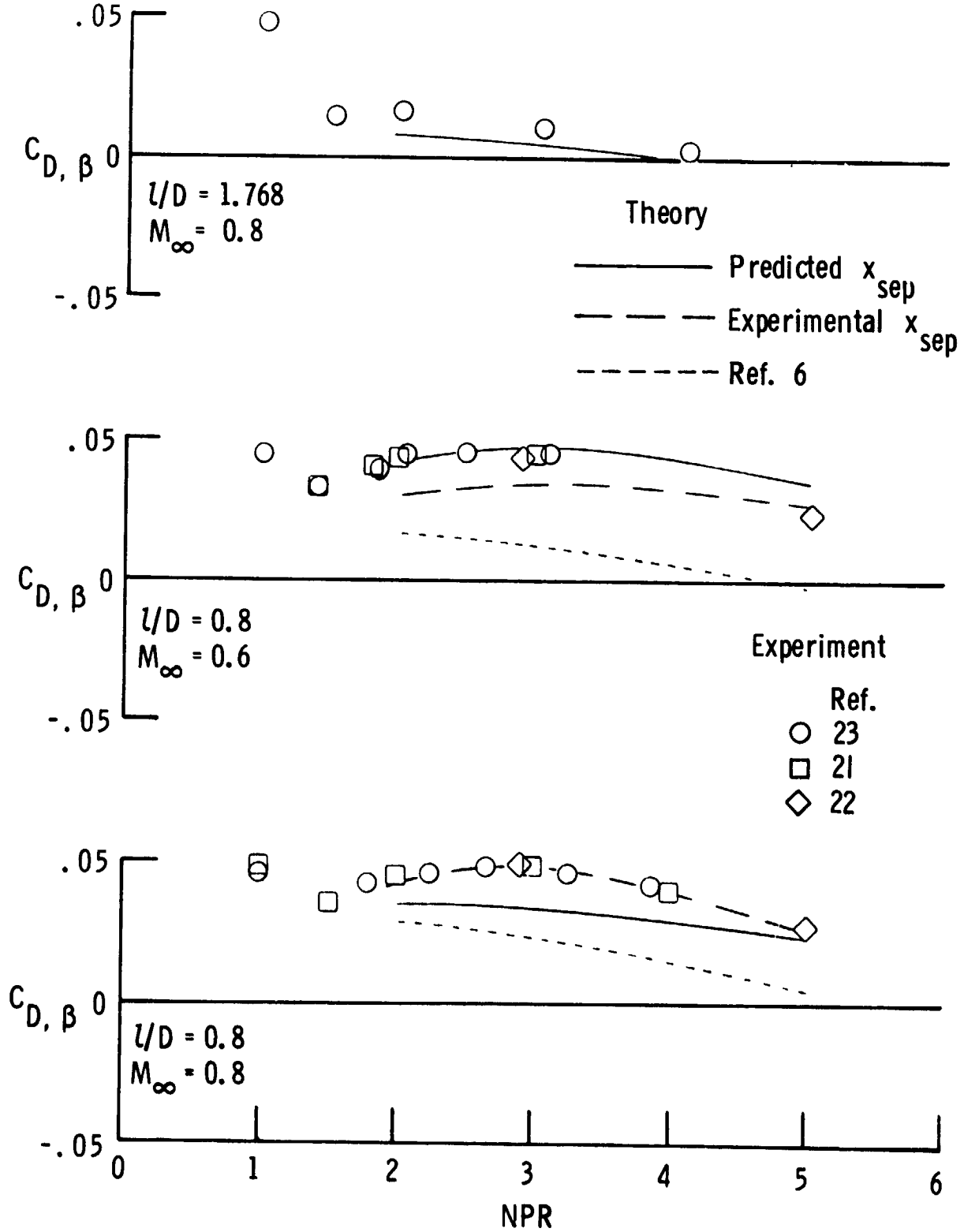

Figure 9.- Predicted and experimental afterbody pressure drag. Integral wake model used with predicted x_{sep} and extrapolated wake model used with experimental x_{sep}.

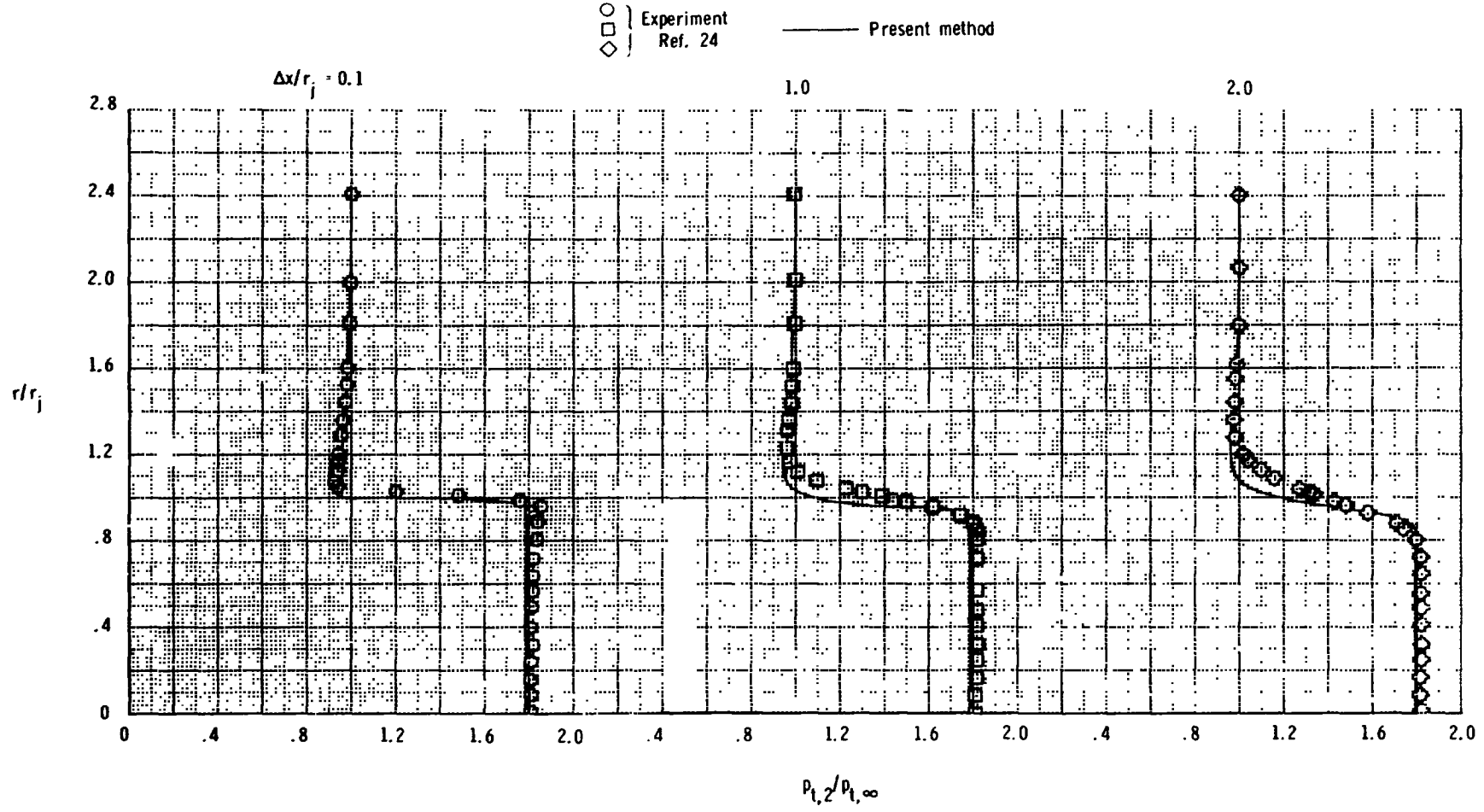

(a) $\iota/D = 1.768$; $M_\infty = 0.4$; NPR = 2.0.

Figure 10.- Predicted and experimental pitot pressure profiles across jet and mixing layer. $\Delta x = x - x_M$.

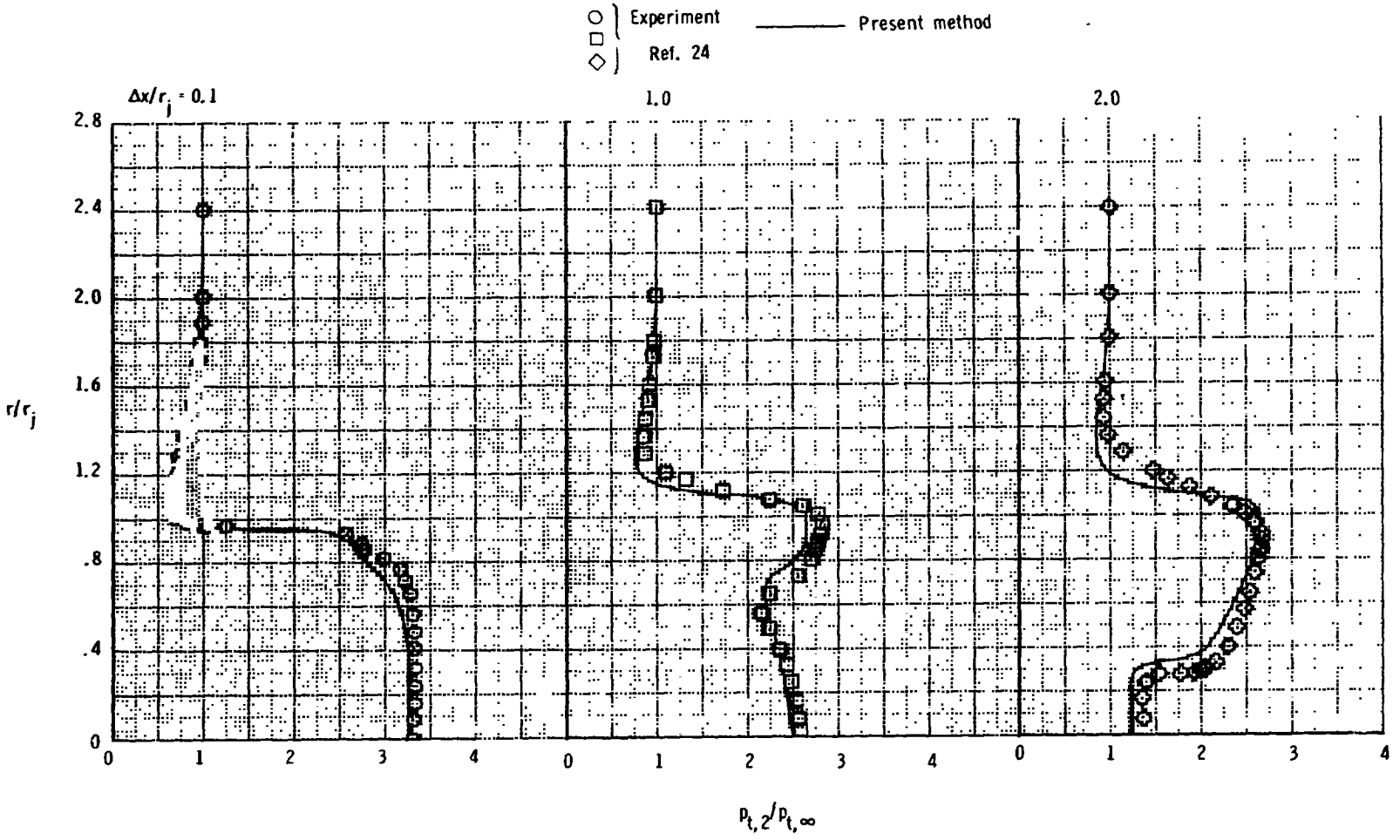

(b) $\iota/D = 0.8$; $M_\infty = 0.8$; NPR = 5.0.

Figure 10.- Concluded.

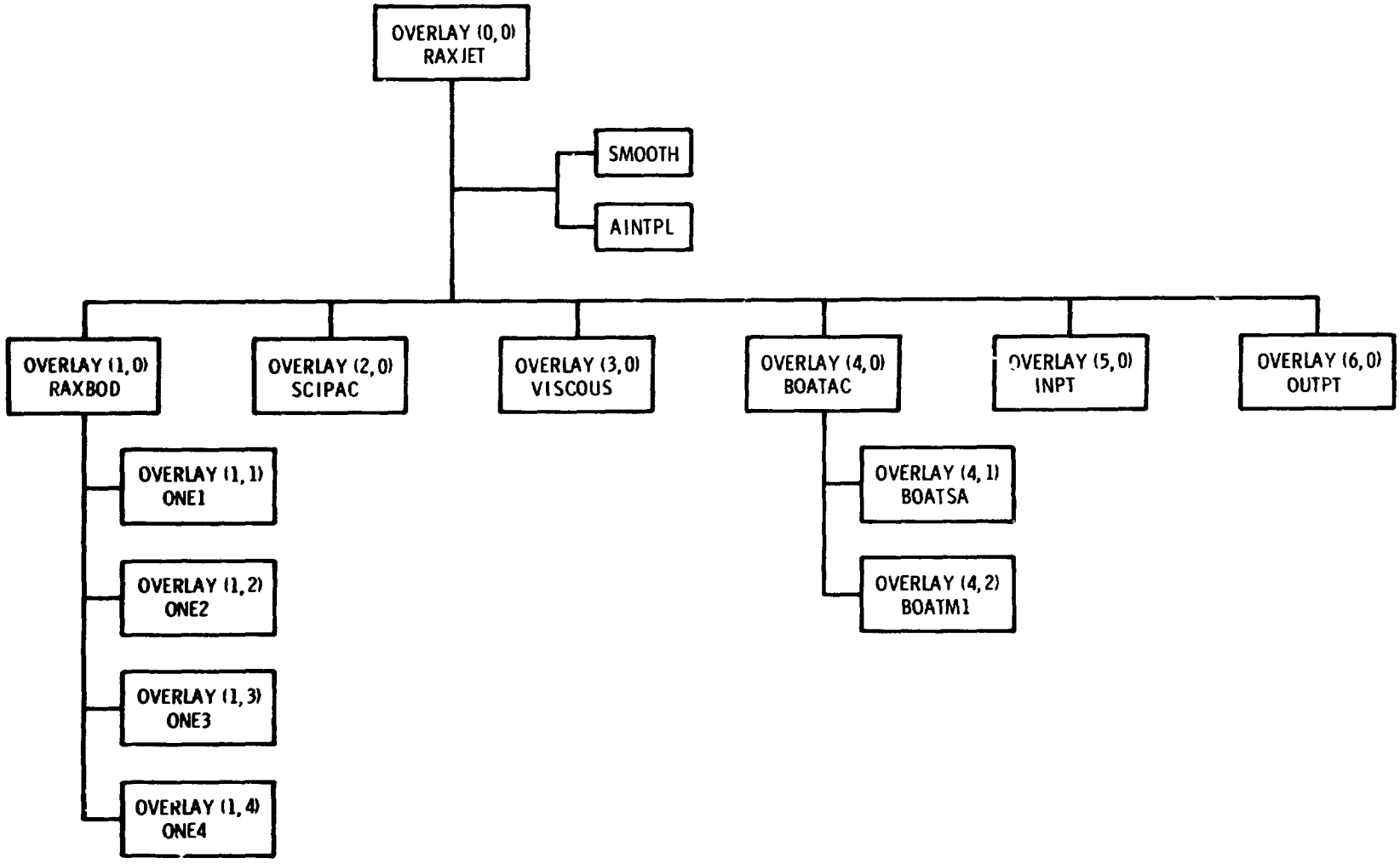

(a) Primary overlay chart.

Figure 11.- Organizational chart for program RAXJET.

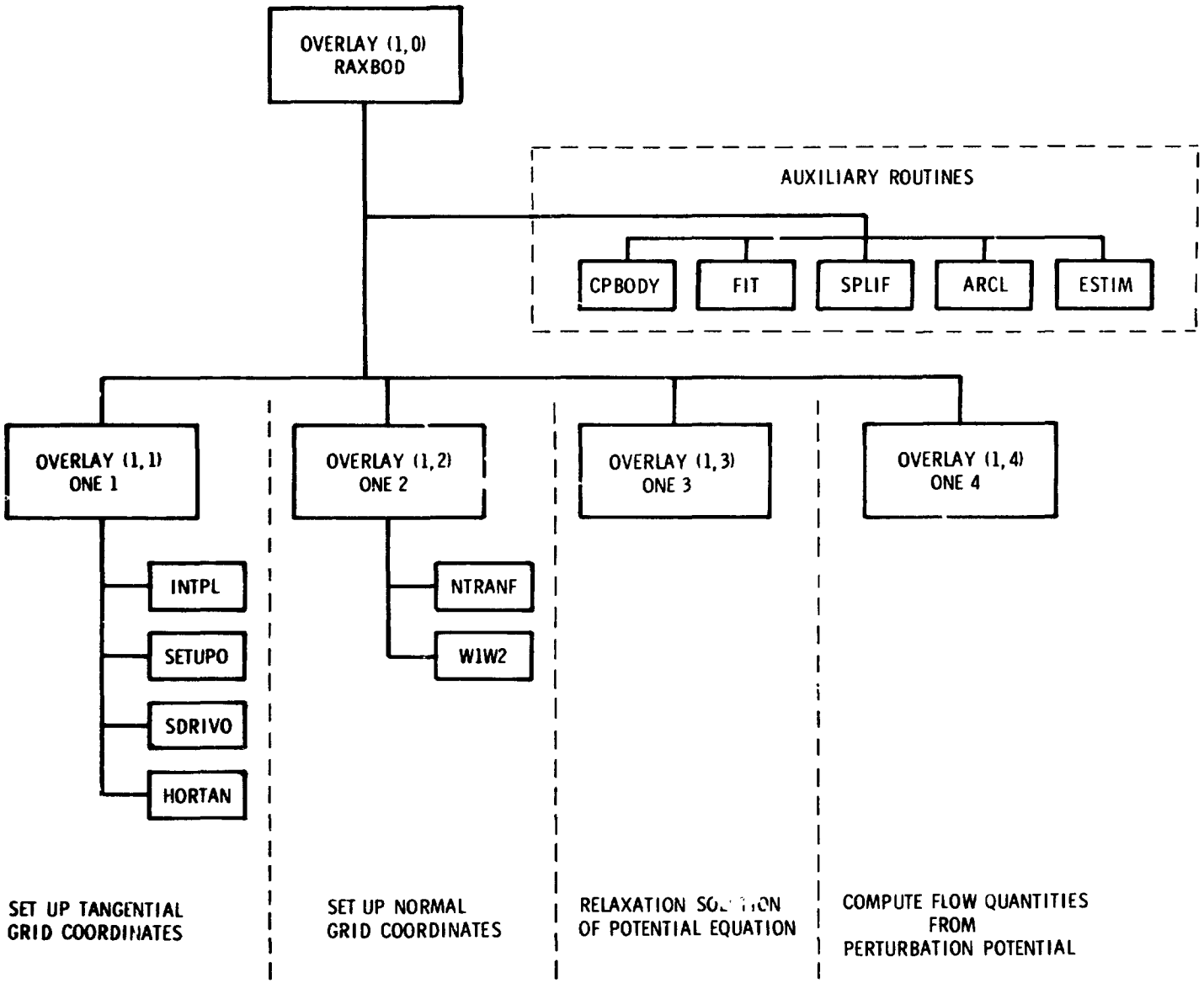

(b) Program RAXBOD.

Figure 11.- Continued.

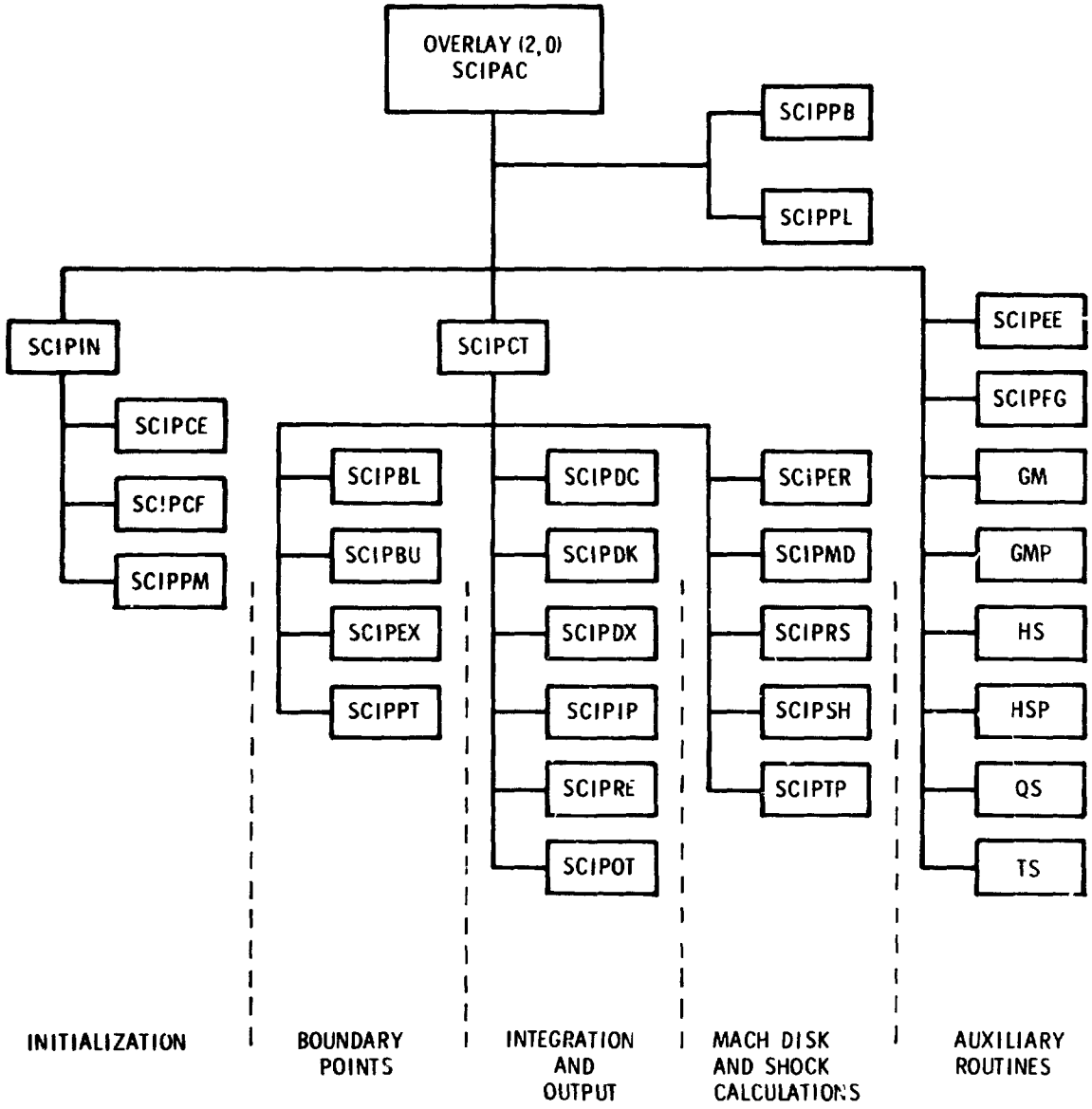

(c) Program SCIPAC.

Figure 11.- Continued.

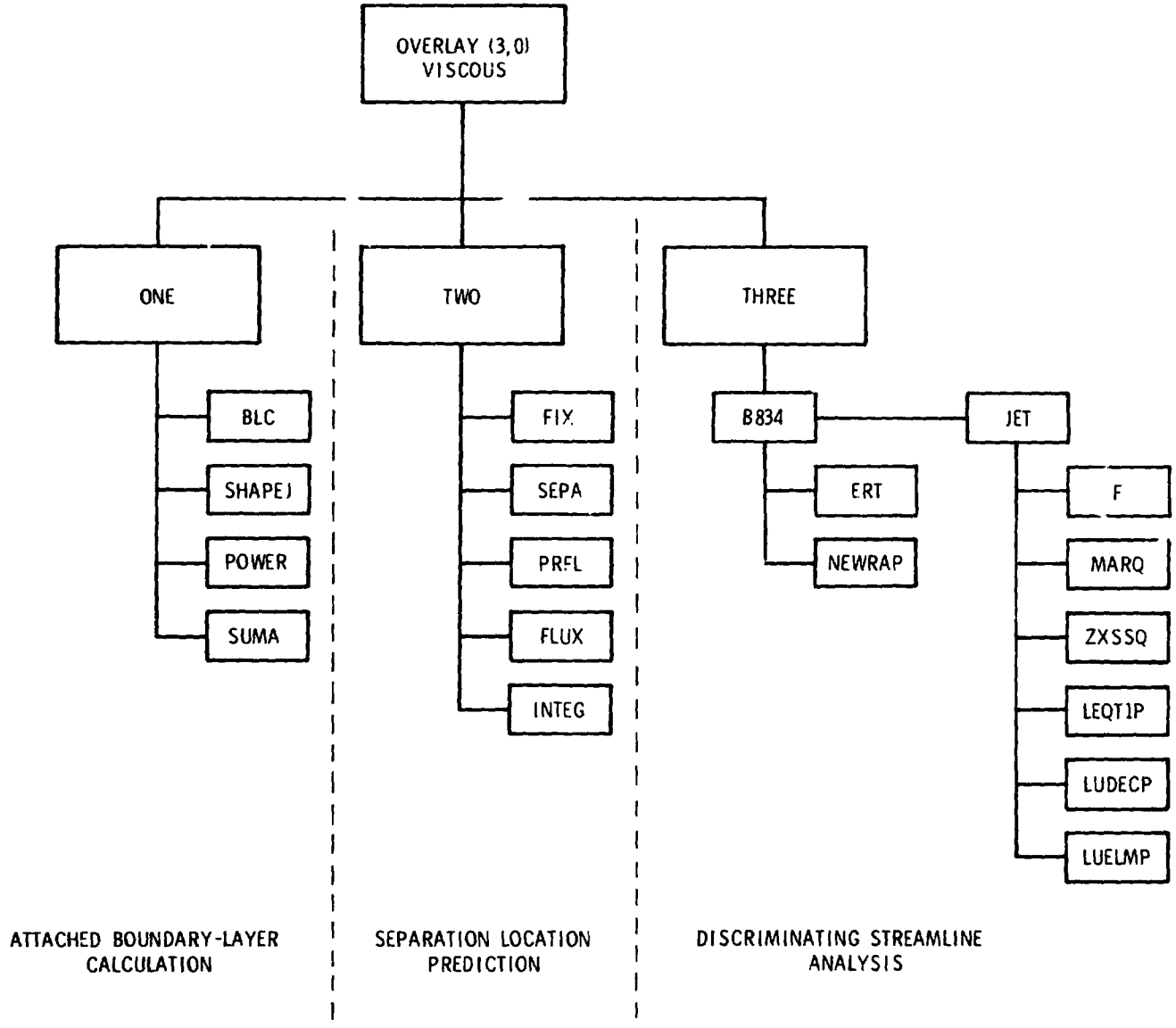

(d) Program VISCOUS.

Figure 11.- Continued.

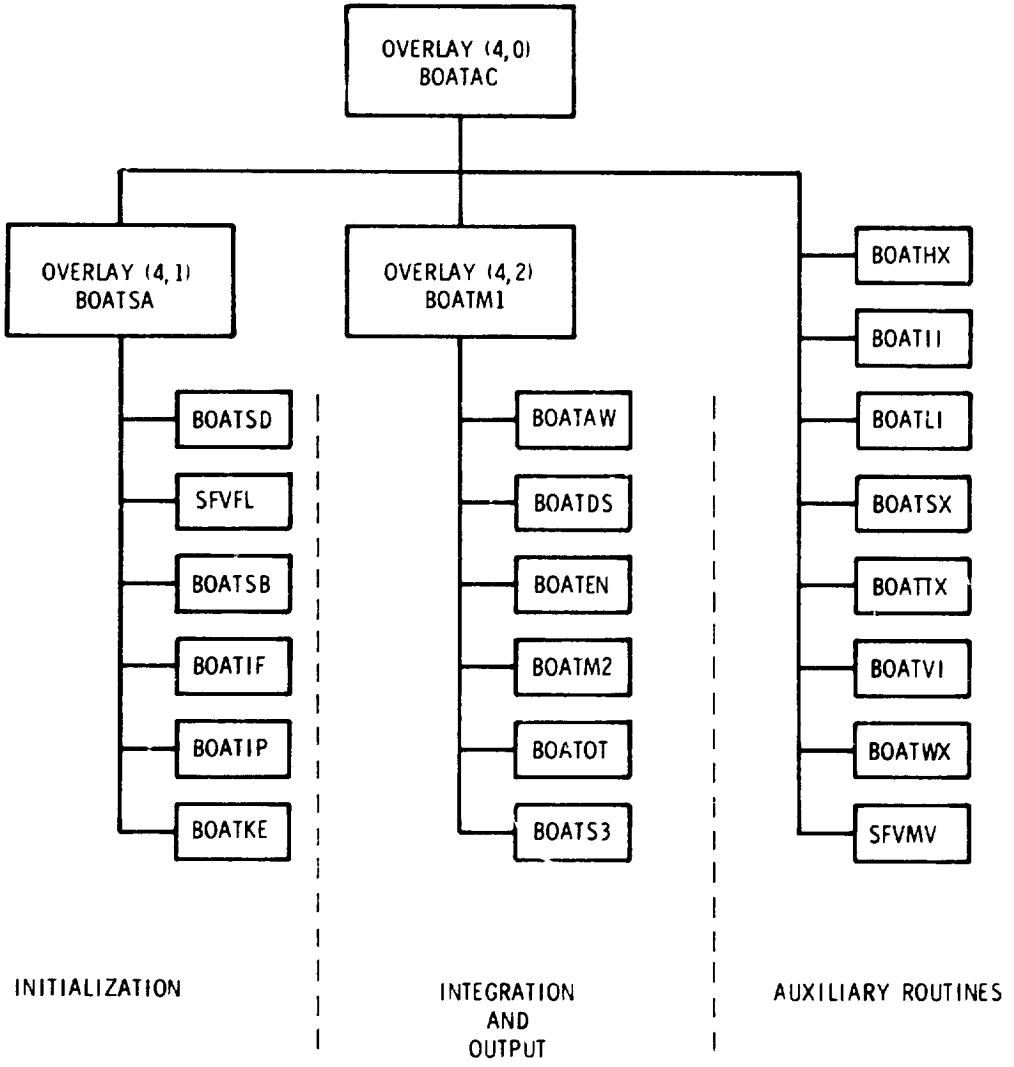

(e) Program BOATAC.

Figure 11.- Continued.

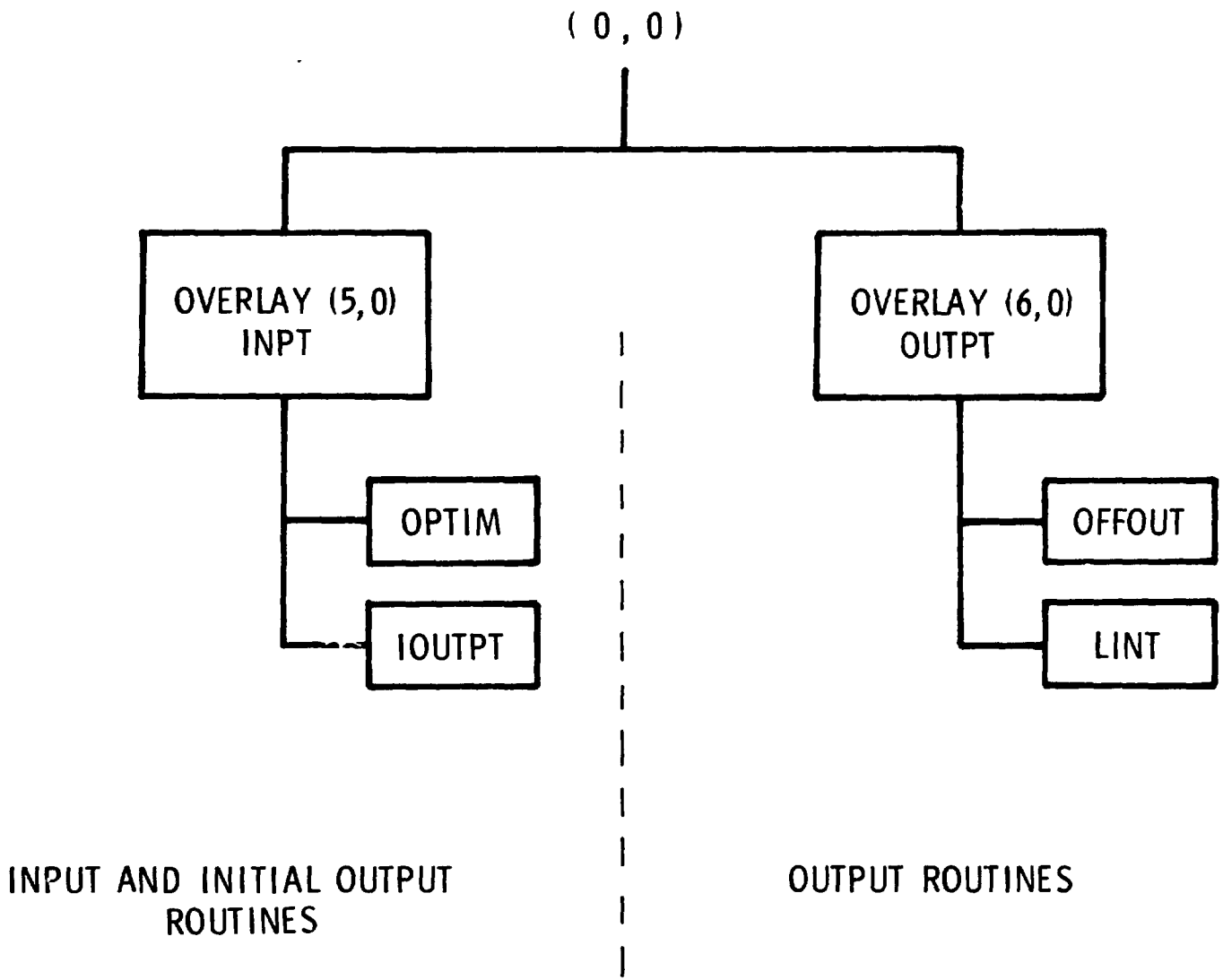

(f) Programs INPT and OUTPT.

Figure 11.- Concluded.

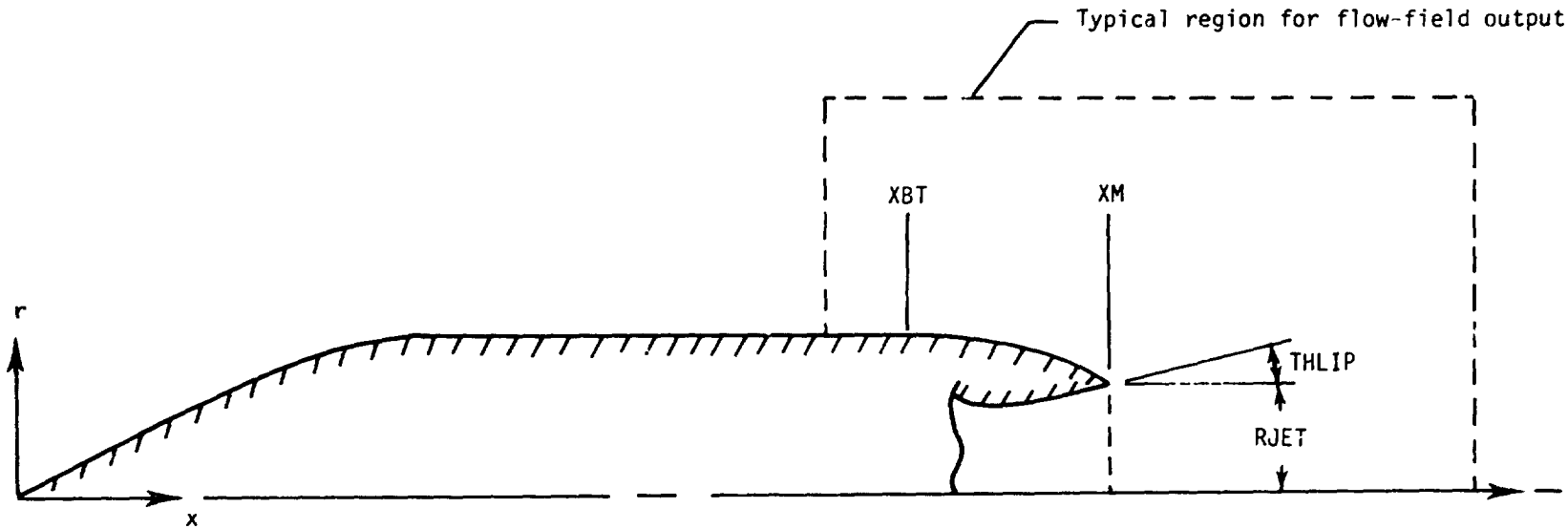

Figure 1 Definiton of geometric input parameters.

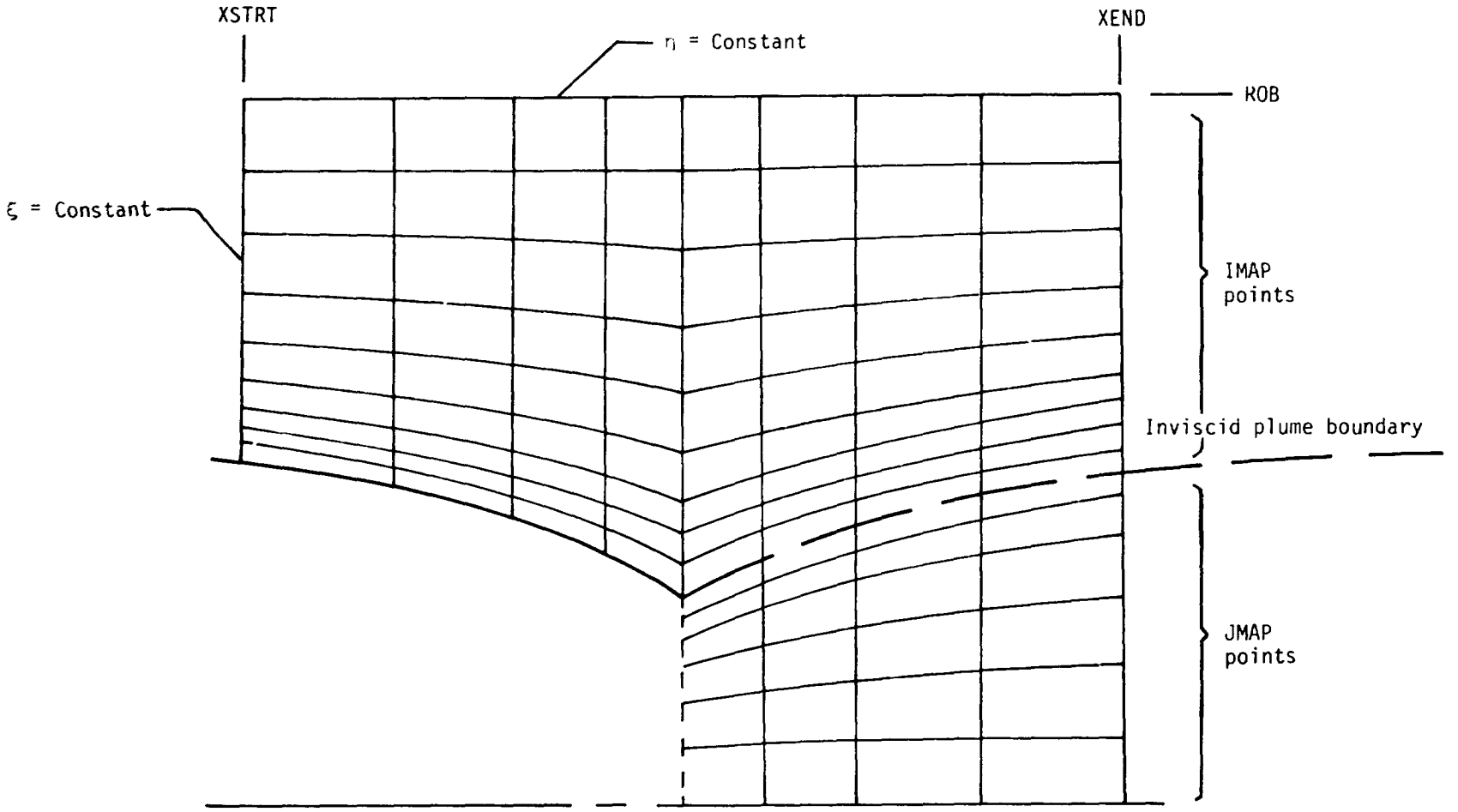

Figure 13.- Definition of flow-field output grid parameters.

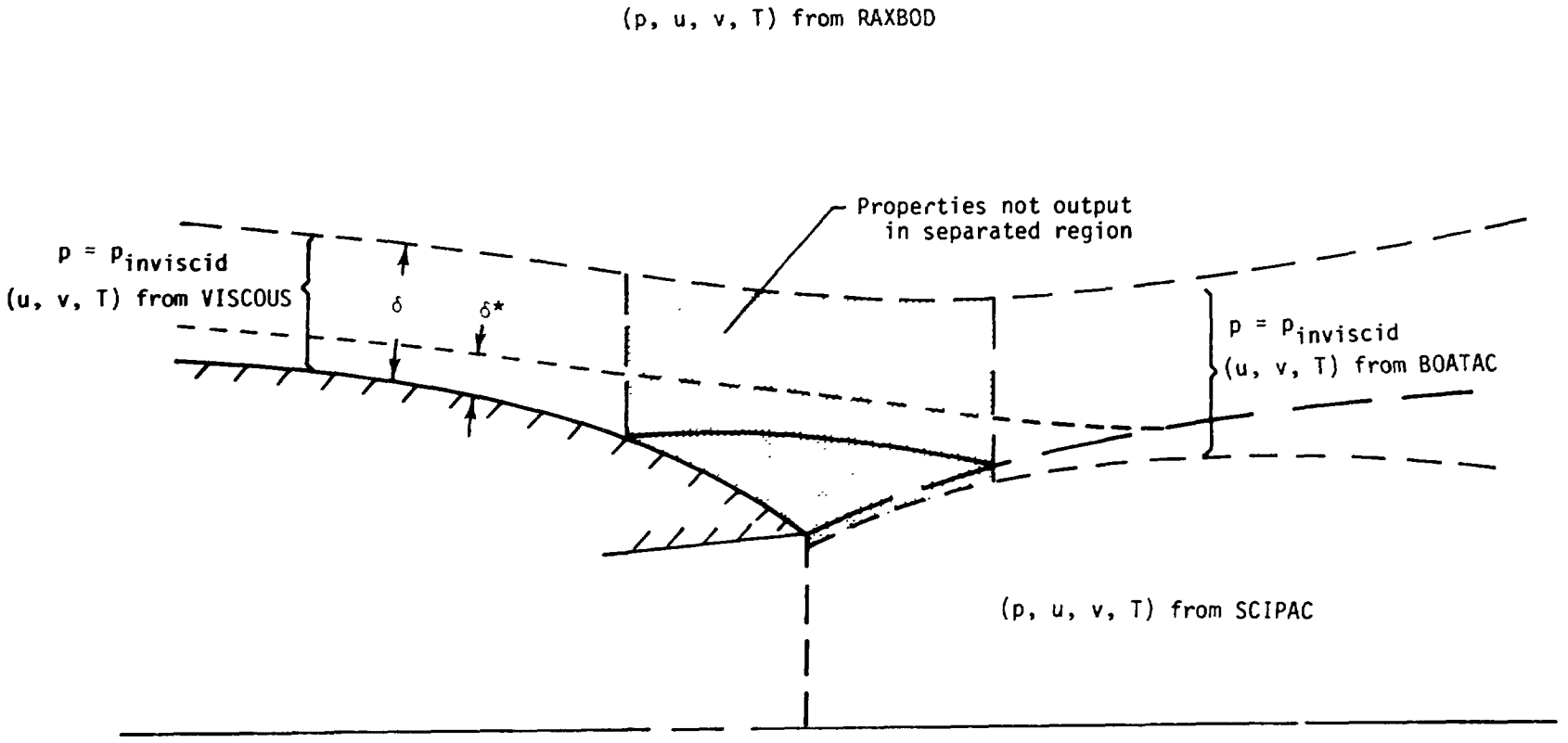

Figure 14.- Composite flow-field properties.